The effects of halothane gas anesthesia on the visual neuronal activities in the feline caudate nucleus

Diána Nyujtó

PhD Thesis

Szeged

2023

University of Szeged
Albert Szent-Györgyi Medical School
Doctoral School of Theoretical Medicine

The effects of halothane gas anesthesia on the visual neuronal activities in the feline caudate nucleus

PhD Thesis

Diána Nyujtó, MSc

Supervisor:
Dr. habil. Attila Nagy, MS, PhD

Szeged

2023

List of publications related to the subject of the thesis

I. Barkoczi B, Nagypal T, **Nyujtó D**, Katona X, Eordegh G, Bodosi B, Benedek G, Braunitzer G, Nagy A Background activity and visual responsiveness of caudate nucleus neurons in halothane anesthetized and in awake, behaving cats, Neuroscience 356 (2017) 182-192
IF: 3.382

II. **Nyujtó D**, Kiss A, Bodosi B, Eördögh G, Tót K, Kelemen A, Nagy A Visually evoked local field potential changes in the caudate nucleus are remarkably more frequent in awake, behaving cats than in anesthetized animals. Physiol Internat in Press (2023)
IF: 1.4

Other publications

I. Puszta A, Katona X, Bodosi B, Pertich Á, Nyujtó D, Braunitzer G, Nagy A Cortical Power-Density Changes of Different Frequency Bands in Visually Guided Associative Learning: A Human EEG-Study. Front Hum Neurosci. 12 (2018) 188
IF: 2.87

II. Puszta A, Pertich Á, Katona X, Bodosi B, Nyujtó D, Giricz Z, Eördegh G, Nagy A Power-spectra and cross-frequency coupling changes in visual and Audio-visual acquired equivalence learning. Sci Rep 9 (2019) 9444
IF: 3.998

III. Puszta A, Pertich Á, Giricz Z, Nyujtó D, Bodosi B, Eördegh G, Nagy A Predicting Stimulus Modality and Working Memory Load During Visual- and Audiovisual-Acquired Equivalence Learning. Front Hum Neurosci 8 (2020) 569142
IF: 3.169

IV. Eördegh G, Pertich Á, Tárnok Z, Nagy P, Bodosi B, Giricz Z, Hegedűs O, Merkl D, Nyujtó D, Oláh S, Őze A, Vidomusz R, Nagy A Impairment of visually guided associative learning in children with Tourette syndrome. PLoS One 15 (2020) e0234724.
IF: 3.24

Table of Contents

List of Abbreviations

ANOVA – Analysis of Variance

CN – caudate nucleus

CRT – Cathode Ray Tube

GABA – Gamma-Aminobutyric Acid

GPe, – external segment of the globus pallidus

GPi, – internal segment of the globus pallidus

HFN – High-Firing Neuron

ISI – Interspike Interval

LFP – Local Field Potential

MAC – Minimum Alveolar Anesthetic Concentration

MSN – Medium Spiny Neuron

PAN – Phasically Active Neuron

PropISI – Proportion of Interspike-Intervals

PSTH – Peristimulus Time Histogram

SNr, – substantia nigra pars reticulata

SNc, – substantia nigra pars compacta

STN – subthalamic nucleus

TAN – Tonically Active Neuron

1. Introduction

1.1 The caudate nucleus

As the primary input structure of the basal ganglia, the caudate nucleus (CN) receives projections from a large variety of cortical areas. Therefore, it is involved in various higher neurological functions (Parent & Hazrati, 1995). Because of this, the CN shows topographic organization and can be divided into three functionally different regions. The dorsolateral striatum receives inputs from the sensory and motor cortices and accordingly plays a role in sensorimotor functions by connecting the incoming visual stimuli with motor responses. The frontal and parietal associations send projections to the dorsomedial striatum.Therefore, it is responsible for integrating the associative information. Lastly, the ventral striatum is connected with limbic structures, such as the hippocampus and the amygdala, and it is involved in memory, learning, and emotion (Joel & Weiner, 1994, Yin & Knowlton, 2006, Graybiel, 2008, Humphries & Prescott, 2010, Yarom & Cohen, 2011). Figure 1 represents the three distinct pathways, the direct, indirect, and hyperdirect pathways of the basal ganglia, that shows how the information flows from the cortex through the basal ganglia. The CN contains neurons that are sensitive to different modalities of visual stimulation. The visual receptive field and the response characteristics of these neurons make them markedly sensitive to dynamic stimuli. Therefore, it is assumingly involved in the perception of self-motion in the visual environment (Figure 1.).

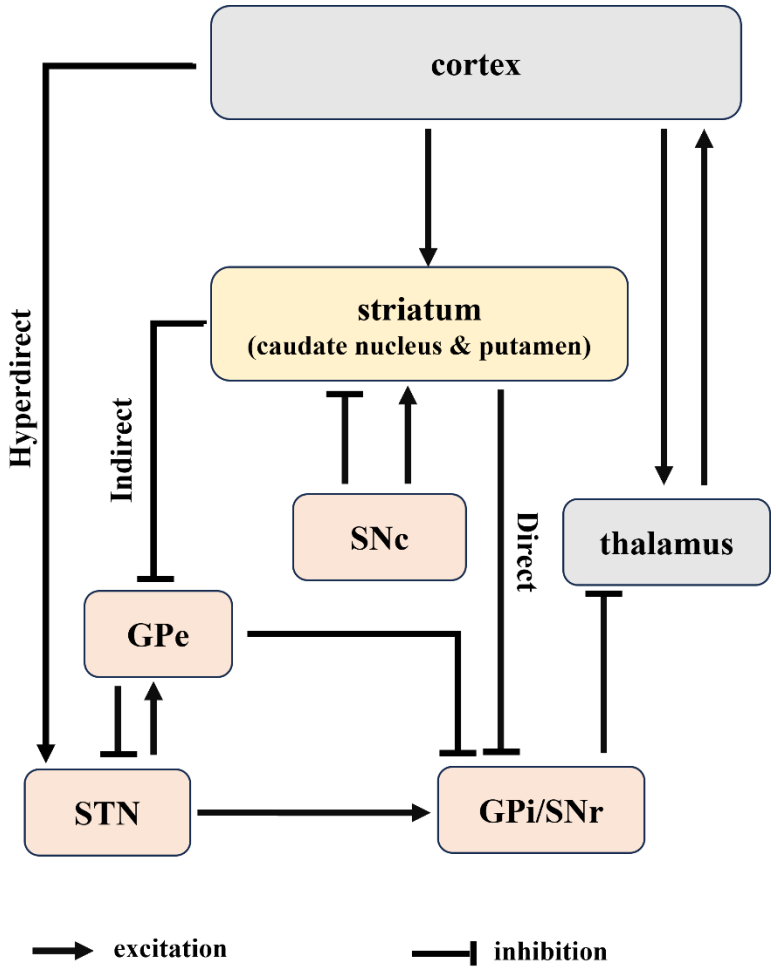

Figure 1. Schematic representation of the direct, indirect, and hyperdirect basal ganglia pathways. GPe, external segment of the globus pallidus; GPi, internal segment of the globus pallidus; SNr, substantia nigra pars reticulata; SNc, substantia nigra pars compacta; STN, subthalamic nucleus.

1.2 Neurons of the CN

In earlier studies, the striatal neurons were classified into two main neuronal groups according to their electrophysiological properties: phasically active neurons (PANs) and tonically active neurons (TANs) (Albe-Fessard *et al.*, 1960, Connor, 1970, Wilson & Groves, 1981, Kimura *et al.*, 1984, Kimura, 1986). It was only in the 1990s that new findings introduced a third group in the striatum: the high-firing neurons (HFN), which correspond most probably to the GABAergic interneurons, which can be further divided into several subcategories based on their expression of single markers (Kawaguchi, 1993, Kubota & Kawaguchi, 1994, Koos & Tepper, 1999, Munoz-Manchado *et al.*, 2018).

Most of the striatal neurons are the Medium Spiny Neurons (MSN) expressing D1 and D2 dopamine receptors. These neurons are the main contributors to the cortico-striatal and thalamocortical loops (Doig *et al.*, 2010, Chuhma *et al.*, 2011, Rothwell *et al.*, 2015), thus they have a crucial role in motor behavior and several other cognitive functions. The MSNs are comprised of 95-97% of the total number of neurons in the rodent striatum. This is much lower in higher vertebrates, especially in primates (75-80%), where the proportion of MSNs comprises 75-80% (Kemp & Powell, 1971, Wise *et al.*, 1996, Yarom & Cohen, 2011).

Besides the MSNs, the CN contains several interneuron types and comprises 3-5% of the rodent striatal neurons.This proportion in primates is much higher (20%). One of them is the GABAergic interneurons, which have at least three subtypes based on their neurochemical properties. Two groups express calcium-binding proteins: parvalbumin or calretinin. On the contrary, the third group expresses neuropeptide Y, somatostatin, nitric oxide synthase, and NADPH diaphorase.

The parvalbumin-expressing GABAergic interneurons can be characterized based on their electrophysiological properties. These neurons can be referred to as high-firing neurons (HFN) (Kawaguchi, 1993, Koos & Tepper, 1999, Berke, 2008, Tepper *et al.*, 2010, Galvan *et al.*, 2012, Chen *et al.*, 2019). These neurons have relatively high spontaneous firing rates that can be 10-30 Hz in behaving animals. As in many other brain regions, the striatal HFNs contribute to the fine modulation of spike timing of MSNs (Koos *et al.*, 2004) and can entrain to fast oscillations in the local field potential (LFP) (Berke, 2009).

The calretinin-expressing GABAergic interneurons are the least well-understood of the striatal neurons, and their electrophysiological properties have never been characterized (Ibanez-Sandoval *et al.*, 2010, Tepper *et al.*, 2010, Silberberg & Bolam, 2015). Garas et al. found that some of these striatal cell types show tonically active firing properties in vivo (Garas *et al.*, 2018).

The somatostatin/neuropeptide Y/nitric oxide synthase-expressing interneurons can be characterized by persistent and low threshold spiking activity (Partridge *et al.*, 2009, Beatty *et al.*, 2012). Recent studies have shown that by providing additional lateral inhibition to the MSNs, these interneurons are involved directly in the functional organization in the striatum. Plus, due to their inhibitory role in the dorsomedial striatum, they are believed to be involved in goal-directed learning (Holly *et al.*, 2019).

The other major interneuron type in the striatum contains the cholinergic interneurons and consist of about 1-3% of the total number of striatal neurons in rodents and ~2% in cats (Phelps *et al.*, 1985, Matamales *et al.*, 2016, Mallet *et al.*, 2019). Interestingly, the proportion is higher, around 10% in primates (Fino & Venance, 2011). It is generally agreed that in the striatum, these large aspiny interneurons correspond to the tonically active neurons (TANs) (Bolam *et al.*, 1984, Kimura *et al.*, 1984, Wilson *et al.*, 1990, Kawaguchi *et al.*, 1995, Bennett & Wilson, 1999, Tepper & Bolam, 2004, Tepper *et al.*, 2004, Berke, 2008, Inokawa *et al.*, 2010, Berke, 2011, Schulz *et al.*, 2011, Yarom & Cohen, 2011). Their periodically interrupted firing pattern allows them to have modulating effects on the striatal information processing, and they are thought to be involved in cue and reward-related functions (Kimura *et al.*, 1984, English *et al.*, 2011, Schulz & Reynolds, 2013). Furthermore, they observed different firing patterns in VS and DLS and therefore assumed to have different roles in each striatal region. TANs in the DLS are possibly involved in the control of movements. On the other hand, in the VS, TANs are more likely to participate in movement initiation, direction and expectation of movement ending (Yarom & Cohen, 2011).

1.3 Oscillation in the striatum

Several pieces of evidence from both animal in vivo recordings and human electrophysiology proved that neural oscillations play a major role in several cognitive functions, such as learning, memory, and sensory gating. Low-frequency signals (local field potentials (LFPs)) can reflect synaptic activity in the sum of EPSPs and IPSPs within a region (Logothetis *et al.*, 2002, Buzsaki *et al.*, 2012, Thorn & Graybiel, 2014). The visually evoked LFP changes in the striatum can carry information about the cortical and subcortical visual inputs. Therefore, the analysis of neural oscillations could show us important information about the impact of network inputs on striatal processing.

Low-frequency LFP oscillations can coordinate communication among brain regions (DeCoteau *et al.*, 2007, Tort *et al.*, 2008, Canolty & Knight, 2010, Fujisawa & Buzsaki, 2011, Thorn & Graybiel, 2014). Several studies have shown that theta-band (6-10 Hz) LFP rhythms occur in the dorsolateral striatum of rodents, and it is associated with the modulation of behavior-related information processes between the striatum and cortex or hippocampus (DeCoteau *et al.*, 2007, Lalla *et al.*, 2017). It has a major role in the organization of the encoding and retrieval of information in cortico-hippocampal circuits (DeCoteau *et al.*, 2007). It is

suggested that increased theta band LFP rhythms could be associated with the maintenance and the encoding of visual information during visual short-term memory (Gevins *et al.*, 1997, Hsieh *et al.*, 2011, Liebe *et al.*, 2012, Roberts *et al.*, 2013, Hsieh & Ranganath, 2014).

Increased cortical alpha activity is also demonstrated to be connected to visual and audio-visual processing (Worden *et al.*, 2000, Ergenoglu *et al.*, 2004, Schaefer *et al.*, 2011). Alpha-band LFP rhythms are shown to be associated with visual perception, such as target detection, and could be involved in the temporal resolution of perception (Samaha & Postle, 2015, VanRullen, 2016, Morrow *et al.*, 2023). The alpha activity could also be involved in sensory suppression. Another function that has been attributed to alpha activity is a mechanism of sensory suppression. Increased alpha-band activity in cortical areas could be responsible for modulating selective attention by gating information in the task-irrelevant brain areas (Michels *et al.*, 2008, Foxe & Snyder, 2011, Dou *et al.*, 2022).

Recent studies have proved that beta-band oscillations (15-30 Hz) are involved in the modulation of decision-making in the sensorimotor network by encoding categorical choices (Haegens *et al.*, 2011, Leventhal *et al.*, 2012, Spitzer & Haegens, 2017, Amemori *et al.*, 2018, Eisinger *et al.*, 2018). Primate studies have suggested that striatal beta activity could be involved in associative learning (Williams & Eskandar, 2006, Kim & Hikosaka, 2013, Santacruz *et al.*, 2017) and modulated during movement suppression (Courtemanche *et al.*, 2003). Normal beta band activity is also presumed to be an essential cortical outcome of the normal basal ganglia function during visual information processing (Puszta *et al.*, 2019).

Striatal gamma band oscillations (31-100 Hz) have a relevant role in synchronizing spiking activity in various brain regions, such as in the hippocampus (Harris *et al.*, 2003) and in olfactory structures (Laurent, 2002, Berke, 2009). Gamma oscillations could also play a role in cognitive processes, such as word learning, reading (Lanz *et al.*, 2013, Lee *et al.*, 2017, Puszta *et al.*, 2019), in memory processes (Howard *et al.*, 2003, van Vugt *et al.*, 2010, Guan *et al.*, 2022) and in behavior related modulation, such as reward approach and receipt (Berke, 2009, van der Meer & Redish, 2009, Malhotra *et al.*, 2015, Carmichael *et al.*, 2017) and reward anticipation (Cohen *et al.*, 2009, Donnelly *et al.*, 2014).

1.4 Effects of anesthesia on the neuronal activities

Earlier studies suggested that anesthetics only have a minor influence on visual responsiveness and background activity (Wurtz, 1969). However, the effects of anesthesia do not necessarily have the same effects on the different brain structures (Velly *et al.*, 2007). For example, it was shown that the thalamus was highly sensitive to various anesthetics.Whether it was gas anesthetics or propofol anesthesia, the neural activity was decreased significantly (Fiset *et al.*, 1999). It is also the case in the basal ganglia, which is extremely sensitive to anesthesia (Kaisti *et al.*, 2003, Franks & Zecharia, 2011). In the striatum, different anesthetics have different effects on neuronal activity. Only 1/3 of the neurons remained spontaneously active during nitric oxide/halothane anesthesia.On the other hand, the spontaneous activity was completely reduced when pentobarbital was used (Ben-Ari & Kelly, 1976). Based on this and our previous experiences, halothane has less influence on the neuronal activities in the CN compared to other gas anesthetics, although the effect of the anesthesia still cannot be entirely excluded.

To eliminate these confounding effects of anesthesia, it was necessary to turn towards the use of awake, behaving animal models in electrophysiological experiences. However, this raises many problems in visual electrophysiology because eye movement control is inevitable for several reasons. First, the spatial position of the visual stimulus has to be overlapped with the neuron's receptive field. Furthermore, visual response has to be separated from the oculomotor activity, i.e., from the saccadic responses. One possible solution to stabilize eye movements is to use anesthetics with muscle paralysis in animals. With the use of this model, the eye movement could be easily stabilized, and the procedure is relatively quick, as it does not require prior training of the animals. However, the main disadvantage is the anesthesia itself, because it can also influence neuronal activity, plus long-term data collection is not possible, thus increasing the number of animals sacrificed in these experiences. Due to these disadvantages, awake, behaving animals are often used in visual electrophysiological research. By using awake animals in visual electrophysiological experiments, we can eliminate these problems.However, it can be a challenging process, too. The main reason for this is that these experiments are preceded by a long-lasting training period in which the animal has to be trained to maintain fixation to be able to eliminate or at least reduce the effects of eye movements (Robinson, 1963, Fuchs & Robinson, 1966, Judge *et al.*, 1980).

A few years ago, our laboratory introduced an awake, behaving feline model that is suitable for visual electrophysiological recordings (Nagypal *et al.*, 2014). The advantages of this model are the extended recording time of up to 2 hours a day for years, continuous eye movement control

with an eye tracker method, where the eye movements were followed, hence it was possible to detect failed fixation. Although this model has many advantages, the preparation of the animals is difficult. To train a single cat to the fixation paradigm completely is a challenging process and may take up to several months.

2. Aims of the study

Based on these described earlier, the question arises whether the benefit of experiments performed in the CN of awake, behaving animals outweighs the hardness of the preparation of the animals for visual electrophysiological experiments. To address this question, single-cell activity and LFP were recorded in the CN during visual stimulation (static and dynamic stimulation) from anesthetized, paralyzed, and awake, behaving cats. The activity of CN neurons and their visual responses were analyzed, as well as the LFPs and visually evoked LFP changes and compared in the two feline models.

The specific aims of the present thesis are the following:

1. To analyze the background single-cell neuronal activities and the visual responsiveness of these units to static and dynamic stimulation recorded from the CN in behaving and anesthetized animals.
2. To analyze low-frequency signals (local field potentials (LFPs)) recorded from the CN in behaving and anesthetized animals.
3. Describe the LFP power changes during visual stimulation in behaving and anesthetized animals.
4. To draw a conclusion about the proposed suppressive effect of halothane anesthesia in the neuronal activities in the feline CN.

3. Materials and methods

All procedures were performed to minimize the number and the discomfort of the animals, and the experimental protocol was accepted by the Government Office based on the suggestion of the Ethical Committee for Animal Research of Albert Szent-Györgyi Medical and Pharmaceutical Centre at the University of Szeged (No.: XIV./518/2018 and XIV/1818/2021) and was conducted in full accordance with the Directive 2010/63/EU of the European Parliament and the Council on the Protection of Animals Used for Scientific Purposes and the guidelines of the Committee.

3.1 Acute experiments

The acute (halothane-anesthetized, paralyzed) experiments were performed on four domestic cats weighing 2.5-5 kg. The first experiments, where the single cell recordings were performed, were on two cats (a female and a male, ages 2 and 3 years, respectively). These recordings lasted for five days. In our latest anesthetized experiments, where the LFPs were recorded, two adult cats were used similarly. Both of them were male and aged 4 and 5 years. These recordings lasted for three days.

3.1.1 Animal preparation and surgery

The animals were first anesthetized with ketamine hydrochloride (Calypsol (Gedeon Richter), 30 mg/kg i.m.). To reduce salivation and bronchial secretion 0.2 ml 0.1% atropine sulphate was injected subcutaneously. The trachea and the femoral vein were cannulated, then the animals were placed in a stereotaxic frame. All wound edges and pressure points were treated regularly with local anesthetic (1% procaine hydrochloride). The cats were artificially ventilated with 1.2-1.6% halothane during surgery. The depth was monitored thoroughly during the experiments with the end-tidal anesthetic concentration and heart rate. The minimum alveolar anesthetic concentration (MAC) values calculated from the end-tidal halothane concentration were kept in a recommended range (Villeneuve & Casanova, 2003). The body temperature of the animal was maintained at around 37ºC by an electric heating blanket. The peak expired CO2 concentrations were monitored continuously with a capnometer (CapnomacUltima, Datex-Ohmeda, ICN) and were kept within the range of 3.8–4.2% by adjustment of the respiratory rate or volume. The O_2 saturation of the capillary blood was monitored by pulse oximetry. The

animals were immobilized with an initial 2 ml intravenous bolus of gallamine triethiodide (Flaxedil, 20 mg/kg, Sigma, St. Louis, MO, USA). Also, a mixture containing gallamine triethiodide (8 mg/kg/h), glucose (10 mg/kg/h), and dextran (50 mg/kg/h) in Ringer lactate solution was infused continuously at a rate of 4 ml/h during the whole experiment.

The craniotomy was performed with a dental drill to allow a vertical approach to the target structures. First, the dura mater was removed, and then the skull hole was covered with a 4% solution of 37 °C agar dissolved in Ringer's solution. The eye contralateral to the subcortical recording site was treated locally with atropine sulphate (one or two drops, 0.1%) and phenylephrine hydrochloride (one or two drops, 10%) to dilate the pupils, block accommodation, and retract the nictitating membranes. Inaddition, it was equipped with a +2 diopter contact lens.

3.1.2 Registration

The recordings took place in a dark and quiet room. Halothane anesthesia was reduced to 0.8-1.0% during the recording sessions to reduce its effects. Recordings were made between the Horsley-Clarke coordinates anterior 12-16 mm and lateral 4.5-6 mm at stereotaxic depths 12-16 mm.

In earlier acute experiments (going to be referring to these experiments as A experiments from further on) the extracellular recordings were performed with tungsten microelectrodes (A-M Systems, Inc., USA). The amplified neuronal signals were recorded at a 20 kHz sampling rate and stored for offline analysis (Datawave SciWorks, Version 5.0, DataWave Technologies Corporation, USA). The recording session lasted approximately 40 minutes, and between each registration, the position of the electrode was changed, and a 10-30 minute break was held.

On the contrary, in our latest acute experiments (going to bereferring to these experiments as B experiments from further on), the recordings were carried out with a 64-channel 2 shank (32 channel/shank, diameter: 300 μm/shank) platinum-iridium linear probe (Neuronelektród Ltd., Hungary). The distance between each channel was 50 μm. The electrical signals were amplified and digitalized with the Hinstra amplifying system (Hinstra Instruments Ltd., Hungary) and were recorded at a 20-28 kHz sampling rate and stored for offline analysis. One recording session lasted for 20 minutes, and between each registration, the electrode position was changed (200 μm upward or downward), and a 30 minute break was kept.

3.1.3 Visual stimulation paradigm

The visual stimulation was generated by a custom-made script in Matlab (MathWorks Inc., Natick, MA) using the Psychophysics Toolbox extension (Brainard, 1997, Pelli, 1997) in the A experiment, and a custom-made software in the B experiment. The stimulation in both experiments was presented on an 18-inch CRT monitor (refresh rate: 100 Hz) placed 57 cm in front of the cat. The visual stimulation consisted of three steps: first, a blank, black screen was presented to record background activity without visual stimulation (intertrial interval); next, a random dot pattern appeared (static stimulus) then the same white dots started to move randomly either toward the periphery or toward the center of the screen (dynamic stimulus, center-in and center-out). The lengths of these phases were the following: intertrial interval was 1500 ms in the A and 2000 ms in the B experiments, 1500 ms static stimulation, and 1500 ms dynamic stimulation. In the A experiments, the diameter of each white dot was 0.15°, and during the dynamic stimulus, the speed of the dots was 5°/sec. The stimulus sequence was repeated 500 times. In the B experiments, the size of each dot was 0.1°, and the speed of dot movement increased from 0 to 7°/sec toward the periphery. The stimulus sequence was repeated 100 times. In both cases, the stimulus, either with center-in or center-out, was presented in a random order.

3.2 Chronic experiments

In the chronic (awake, behaving) recordings two adult domestic cats were involved. Both cats were female and aged 1-4 years. The cats weighed between 2.5-3.5 kg. The training of these animals took 9 months, and the recording sessions were performed 4 to 5 days a week and took 30 minutes to 1 hour a day. Unfiltered electrical signals were recorded, which contained both low-frequency signals (LFPs) and high-frequency signals (spikes of the single cells).

3.2.1 Animal preparation and surgery

The preparation and the craniotomy were performed similarly to the previously described acute experiments, however, there were a few changes. First, an initial dose of ketamine hydrochloride was given i.m, then a subcutaneous injection of 0.2 ml 0.1% atropine sulphate and a preventive dose of antibiotic was given (1000 mg ceftriaxon, i.m., Rocephin 500 mg (Roche®)) preoperatively. After the femoral vein cannulation, the scleral search coil (Cooner wire, Owensmouth, CA, USA) was implanted into one eye to monitor the eye movements of

the cats during the recordings (Pigarev & Rodionova, 1998, Populin & Yin, 1998, Populin & Yin, 2002, Huxlin & Pasternak, 2004, Tollin *et al.*, 2005, Pigarev & Levichkina, 2011, Nagypal *et al.*, 2014). Then, we continued with the intubation of the trachea, and the cats were placed in the stereotaxic frame. Their body temperature was kept at 37^{o}C by a computer-driven, warm-water heating blanket. In contrast to the acute experiments, the anesthesia was maintained with 1.5% halothane in a 2:1 mixture of N_2O and oxygen and was continuously monitored throughout the surgery. Firstly, a stainless-steel head holder was implanted on the skull to fixate the head in the recording sessions. Then, the craniotomy was performed with a dental drill to allow a vertical approach to the target structures. The dura mater was preserved, and the skull hole was covered with agar. A re-closable recording chamber (20 mm in diameter) was cemented on the skull to avoid pollution and protect the microdrive system and the extracellular electrodes. Lastly, eight wire electrodes covered by a guiding tube were implanted above the CN according to the Horsley-Clarke coordinates anterior 12–14 mm, lateral 5–6.5 mm, at the stereotaxic depths between 13–19 mm. The electrodes were implanted in the brain with the help of an adjustable microdrive system, for the first cat a modified Harper-McGinty microdrive (McKown & Schadt, 2006), and a modified Korshunov microdrive for the second cat (Korshunov, 1995). On the first five postoperative days, ceftriaxone antibiotic was administered intramuscularly (Rocephine, 50 mg/kg). Nalbuphin (0.25 mg/kg) and non-steroidal anti-inflammatory drugs were administered until the seventh postoperative day.

3.2.2 Behavioural training

The training began with the adaptation to the laboratory environment which was formed by a feeding routine. The animals only received food (150-250 g/day) in the laboratory where the behavioural training and the experiments took place. During the weekends the animals received food in their home cage ad libitum. Water deprivation was not used.

The next few steps of our training were the suspension of the animals by a canvas harness, which leaves the head, legs, and tail free. At first, the cats were clothed carefully, then they were lifted manually only a few centimeters from the floor in the canvas harness, while they were being fed. When the animals got accustomed to being suspended this way, they were introduced to the experimental stand. In the following step, the head of the cat was fixed to the stereotaxic frame by the steel head holder. The stereotaxic frame was placed within an electromagnetic field, which is generated by metal coils, and installed into the wall of the experimental stand. Then the cats were introduced to the behavioral fixation paradigm. The

animals were trained to hold their eyes in the center of the monitor during recordings of neuronal activities to different kinds of visual stimulation. The initial size of the fixation acceptance window was 10^o around the center of the monitor, which was reduced to 5^o during the progress of the training. If the cats held fixation during the whole trial of the task, the animals received pulpy food as a reward through a plastic tube dosed by a computer-driven hydraulic pump. The behavioral training lasted approximately 1 to 2 hours per day, four to five times during a week. The training phases, and later the registrations took place in a dark and quiet laboratory room. The recordings started after the cats reached a stable 80% efficiency during the fixation task.

3.2.3 Visual fixation paradigm

The visual stimulation was generated by a custom-made script written in Matlab and using the Psychtoolbox ®. The stimuli were presented on an 18-inch CRT monitor (refresh rate: 100 Hz) and were placed 57 cm in front of the animal. In this case, the visual paradigm (one single trial) consisted of 5 steps: 1. Fixation: A green fixation point was projected on the center of the monitorto help maintain the fixation on the middle of the monitor during the relevant stimulus phases. The cats had to direct their gaze to the fixation point and keep fixating for 500 ms. 2. Standing stimulus: static random dot pattern appeared on the screen after the successful fixation phase for 1000ms. 3. Dynamic stimulus: the dots, similarly as described before, started to move either toward the periphery or the center of the screen, again, this was presented in a random order. The length of this phase was 1000ms. 4. Reward: If the cats could hold fixation during the whole single trial, they received a food reward, and the trial was considered a correct trial. If the cat broke fixation during any of the stimulation phases, the trial was aborted immediately, it was not accepted, and no reward was given. This phase was 500ms long and was part of the intertrial phase. 5. Intertrial interval: no stimulation was given, only a black screen was presented for 5000-10000ms to record background activity, and, the cat could eat the reward without muscle activity interfering with the recordings of the next trial. The size of the fixation point was 0.8^o in diameter, and the fixation window was 5^o in diameter. The size of the white dots during standing and dynamic stimuli was 0.1^o, and the speed of the dot movement was 0 to 7^o/sec.

3.2.4 Registration

The recordings took place in a dark, quiet laboratory room. The electrophysiological extracellular recordings were carried out with parylene-isolated platinum-iridium wire-

electrodes with a diameter of 25 μm for the first cat; and formvar insulated nickel-chrome wire-electrodes with a diameter of 50 μm for the second cat, with the sampling rate of 10 kHz. The recording of the eye movements, stimulus presentation, reward delivery, and data collection were controlled by a custom-made LabView software via a 16-channel National Instruments data acquisition card. Eye movements were monitored and recorded with a search coil system (DNI Instruments, Newark, DE, USA). At the end of each registration, the depth of the electrode was changed 125-250 μm downward or upward.

3.3 Data analysis

3.3.1 Spike sorting and neuron classification

To analyze the single-cell activities, the raw data was processed by Neuroscope, NDManager, KlustKwik software package (Harris *et al.*, 2000, Hazan *et al.*, 2006). The amplified neuronal activities first needed to be band-pass filtered between 300-3000Hz, then after the threshold was calculated, the program clustered automatically the extracted spike based on the principal company analysis. The final step was done manually in the Klusters software, where the proper discrimination of the simultaneously recorded neurons was confirmed by testing the autocorrelograms and overlaid spike shapes.

The neuron classification was done by using the background discharge rate, propISI>2sec, and the shape of the two autocorrelograms (±100 ms and ±1000 ms) (Schmitzer-Torbert & Redish, 2004, Barnes *et al.*, 2005, Schmitzer-Torbert *et al.*, 2005, Nagypal *et al.*, 2015). The background discharge rate was calculated from the intertrial intervals. PropISI>2sec is defined as the proportion of the summed interspike interval values over 2 sec divided by the total spike intervals. Based on these parameters, the striatal neurons could be separated into three main electrophysiological categories: phasically active neurons (PANs), high-firing neurons (HFNs), and tonically active neurons (TANs). PANs could be characterized by lower discharge rates (around 3 spikes/sec), peaky autocorrelogram, and the propISI>2sec is usually higher than 0.5. On the contrary, the HFNs have higher discharge rates than 5 spikes/sec, their autocorrelogram has a blunt peak, and the propISI>2sec is less than 0.5. TANs can be characterized by a discharge rate between 2-12 spikes/sec, propISI>2sec, and their autocorrelogram has a typical deep gap (Nagypal *et al.*, 2015) (see Figure 2.).

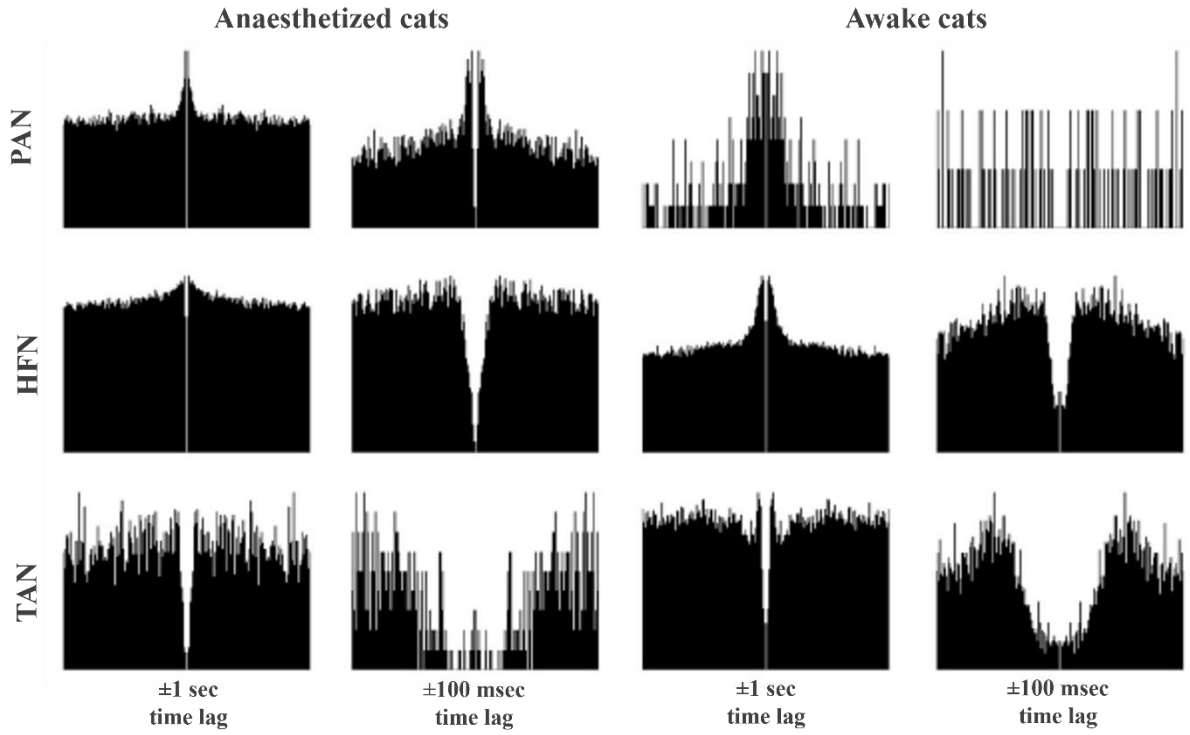

Figure 2. Representative autocorrelograms of the feline CN neurons. *The six panels on the left side show representative autocorrelograms from awake, behaving cats, while the six panels on the right side are from the anesthetized cats. Each of the autocorrelograms is at two different (1 sec and 100 msec) time resolutions. The neurons were categorized by their shape of autocorrelograms (at 100 msec and 1-sec resolutions), propISI >2sec, and background discharge rate. The three neuron types are phasically active neurons (PANs), tonically active neurons (TANs), and high-firing neurons (HFNs). PANs can usually be characterized by peaky autocorrelograms with low background discharge rates, TANs have a deep gap in their autocorrelogram, while HFNs are characterized by a blunt peak in*

3.3.2 Analysis of neuronal activities and visual responsiveness

All statistical analyses were performed in Matlab (MathWorks Inc., Version 8.3, Natick, MA) and STATISTICA for Windows (StatSoft Inc., Version 12.0, Tulsa, OK) softwares. First, peristimulus time histograms (PSTH) were made from the temporal distribution of the spikes for each single neuron. We used the Wilcoxon matched pair test to compare the firing rate during the static and dynamic stimuli to the background activity. If the firing rates were

significantly different ($p<0.05$) than the background activity, and the mean net change was at least 0.1-fold (10%), we considered the neuronal as a response. We included only those striatal neurons in the analysis whose background activities were at least 1 spike/sec i to exclude potential biases. We calculated the evoked activities by taking the average of all activities separately in the static and dynamic phases. Next, the evoked activities were compared to the 1 sec of the intertrial interval (background activity). We calculated both the gross and net activities.Therefore, we could gain information about the overall neuronal activity. In addition, we got the magnitude of visually evoked responses by calculating the ratio between the gross and net activities,. The net activities were calculated by taking the background activity from the gross activity, which was the total mean firing rate during the different visual stimulation phases. Normality was checked using the Shapiro-Wilk test, which showed that the studied variables were non-normal. Therefore, we used nonparametric statistical tests. We used the Mann-Whitney rank sum test to compare the background activities of the anesthetized and behaving cats at the population level.

3.3.3 Analysis of LFP activities

Matlab R2021a (The Mathworks, Natic, MA, USA) software was used for data analysis and statistical analysis of the power of the delta (1-3 Hz), theta (4–7 Hz), alpha (8–13 Hz), beta (14–30 Hz), and gamma (31–70 Hz) bands. Firstly, the recorded raw data went through a visual inspection to exclude those channels from further analysis that had high amplitude noise and/or bad signal-noise ratio. Then, the remaining channels were downsampled using a low pass filter and decimation to 500 Hz with the the Matlab *decimate* function. This was followed by the Fourier analysis, then the power spectrum was video-filtered by a ten-bin rectangle window (see Figure 3.). To be able to visualize the higher frequency bands commensurately, whitening compensation was used. For this, the calculations were carried out from the original raw data. The median filter (Matlab medfilt1) was applied next with the default parameters. During the visualization of the Fourier spectra the bins around 50 Hz were cut off.

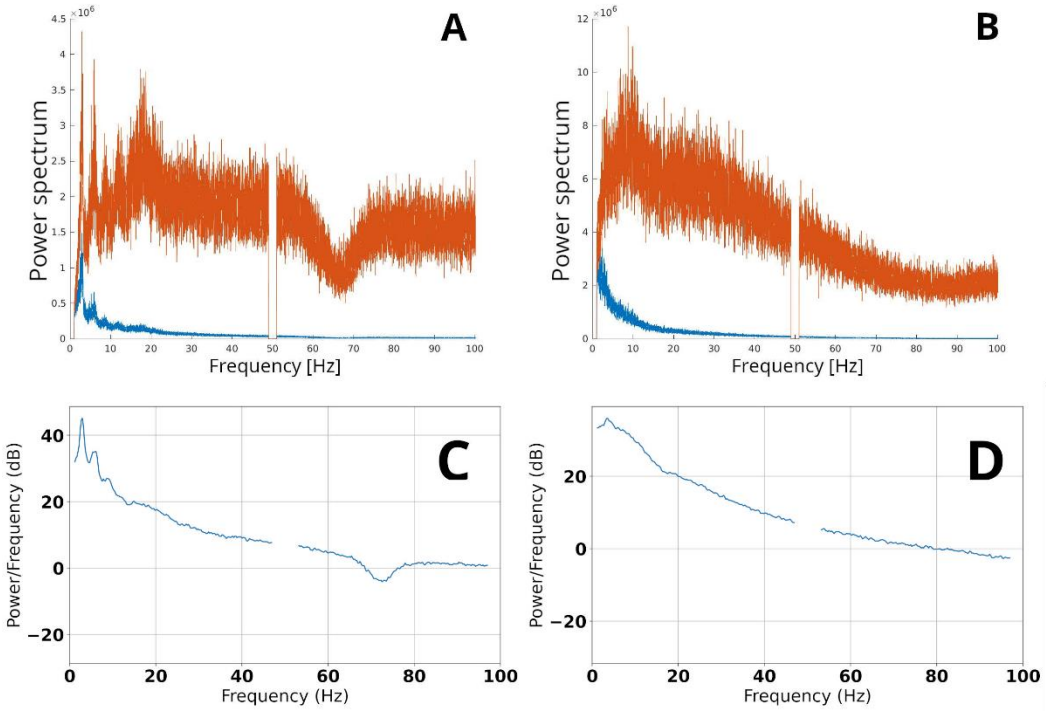

Figure 3. Spectral images of the LFP recordings. *Upper left image (A) shows the Fourier spectrum of a recorded signal from an awake cat. Image B shows the Fourier spectrum of a recorded signal from an anesthetized cat. The blue color represents the raw Fourier spectrum, whereas the orange color shows the whitened one. Image C and D represents the spectral power of the same recorded signals calculated with the Welch function.*

For the decimation of raw data the finite impulse response filter (FIR) decimation filter was used with a length of 20 ms. For every band, the center frequency was shifted to 0 Hz by multiplying the signal with a complex rotating vector. This step was followed by signal decimation to a lower sampling frequency with the Chebyshev infinite impulse filter (IIR). To reach the desired width of the band and hence meet the stability criteria of the filters, the filtering and decimating steps were repeated (see Figure 4.). Because the analysis of theta band requires a 25 Hz for the resulting stable filters, the last decimation was carried out for this sampling frequency, hence the time resolution of the power of signals was t=1/f=40. The higher frequency bands were then calculated and decimated with the same time resolution and sampling frequency. As a result, the absolute value of the signals represents the power of the signal for each 40 ms wide sample.

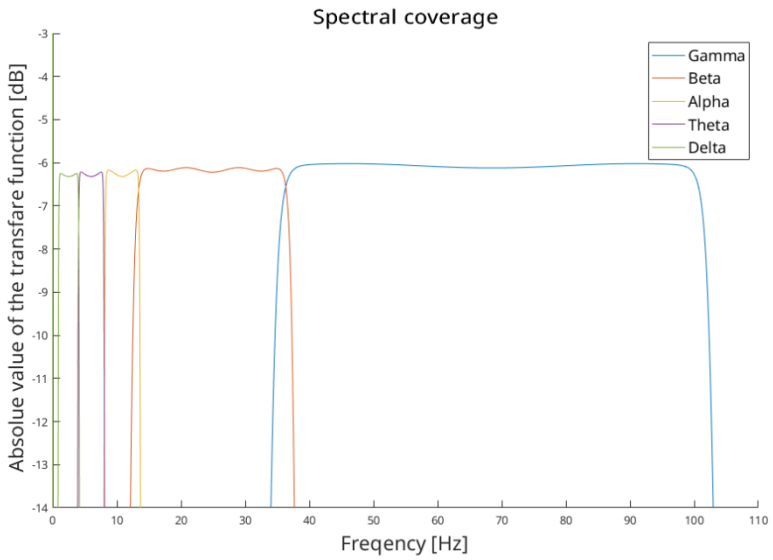

Figure 4. Spectral coverage of the applied band pass filters. *The different colors represent the characteristics of the filters in each frequency band: green-delta, purple-theta, yellow-alpha, orange-beta, and blue-gamma. Note the overlap between the frequency-based neighboring filters and their sharp filtering properties.*

3.3.4 Statistical analysis of LFP activities

320 ms periods (the average of eight 40 ms wide bins) were randomly selected from the background activity and the start of the stationary and dynamic stimulus from both the behaving and anesthetized LFP recordings. The powers of these periods in each frequency band from all trials were non-normally distributed (Shapiro-Wilk $p<0.05$) and then were compared with the Friedmann ANOVA test with Bonferroni correction. A significant difference ($p<0.05$) in the LFP recording means that at least one of the three conditions (background activity, response to static or dynamic stimulation) differs from one another. To check exactly which part of the stimulated activity (static, dynamic, or both) differs significantly from the background activity Wilcoxon matched pair test was used.

4. Results

4.1 Analysis of single neurons in the caudate nucleus (CN)

From the A anesthetized experiments 206 neurons were recorded altogether from the two cats (83 from the first and 123 from the second cat) in the CN. A total of 344 neurons (285 from the first and 59 from the second cat) were recorded in the CN from the two awake, behaving cats.

4.1.1 Background activity of CN neurons

The background activity of CN neurons was calculated from the intertrial intervals, which was significantly higher (Mann–Whitney U, $p < 0.001$) in awake, behaving cats compared to that of CN neurons recorded in anesthetized cats (Figure 1, see descriptive statistical data in Table 1). Due to the high prevalence of CN neurons exhibiting extremely low background activity, with a separate analysis those neurons whose background activity was below 1 spike/s were excluded. It was necessary to exclude potential biases in the analysis. It resulted in the exclusion of 135 neurons from the awake (39.2%) and 125 neurons from the anesthetized model (60.7%). Due to the exclusion, a significantly higher prevalence of CN neurons with background activities below 1 Hz could be observed in the anesthetized cats. A comparison of background activities exceeding 1 Hz demonstrated a significantly higher activity of CN neurons recorded from the behaving cats (Mann-Whitney U, $p < 0.001$).

	Awake cats		Anesthetized cats		
	N	Mean	N	Mean	
All neurons	344	5.19	206	1.58	Background activity
≥1 Hz	209	8.32	81	3.60	
HFNs	88	14.6	85	2.56	
PANs	219	1.39	73	0.14	
TANs	28	5.35	43	2.21	
≥1 Hz HFNs	88	14.6	56	3.64	
≥1 Hz PANs	85	3.03	0	-	
≥1 Hz TANs	28	5.35	25	3.49	
≥1 Hz ≥10% increase gross	51	12.86	3	3.23	Static stimulus
≥1 Hz ≥10% Increase net		4.33		0.47	
≥1 Hz ≥10% decrease gross	32	4.92	2	4.85	
≥1 Hz ≥10% decrease net		-2.37		-1.85	
≥1 Hz no change gross	126	10.22	76	3.58	
≥1 Hz no change net		1.73		0.03	
≥1 Hz ≥10% increase gross	22	14.11	0	-	Dynamic stimulus
≥1 Hz ≥10% Increase net		3.82		-	
≥1 Hz ≥10% decrease gross	3	5.86	10	2.78	
≥1 Hz ≥10% decrease net		-0.89		-0.68	
≥1 Hz no change gross	184	8.66	71	3.63	
≥1 Hz no change net		0.55		0.02	

Table 1. Descriptive statistics of background and visually evoked activities of CN neurons from awake, behaving, and anesthetized, paralyzed cats. *PAN – phasically active neuron, HFN – high firing neuron, TAN – tonically active neuron. ≥1Hz: CN neurons with a background activity over 1 Hz (1 spike/s); ≥10%: evoked responses with a change equal to or higher than 10% of the background activity; Increase, Decrease, No change: indicates the evoked visual responses changes; Gross: the averaged firing frequency during the entire stimulation session; Net: evoked gross activity subtracted from the background firing frequency; Background, Static, Dynamic: visual trial phases; N: sample size. Discharge rates are in spikes/s. The background activities, the visually evoked activities, and the number of visually responsive CN neurons were smaller in the case of anesthetized animals. Note that no PANs with a background activity higher than 1Hz were found in the anesthetized cats.*

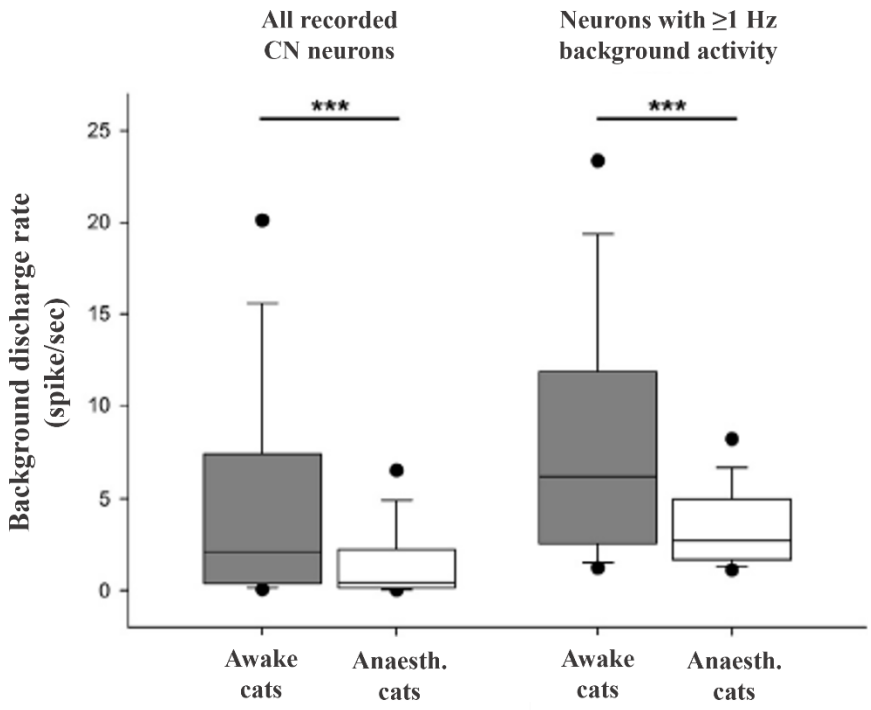

Figure 5. Background discharge activity in the CN of awake, behaving, and anesthetized, paralyzed cats. *The box plots show the background discharge rates of all analyzed CN neurons (left) and CN neurons that had a background discharge rate higher than 1 Hz (1 spike/sec)(Right). The gray boxes show the results from behaving cats, while the white boxes contain the results from anesthetized cats. The margins of the boxes indicate the 25th and 75th percentile, and the lines in the boxes mark the median. The error bars show the 90th and 10th percentiles and the dots indicate the 95th and 5th percentiles. All the differences we found between the background discharge rates of the two feline models appeared to be statistically significant (Mann-Whitney U, $p < 0.001$).*

4.1.2 Single-cell responses to static and dynamic visual stimulation in the CN

The stimulated activities (static and dynamic stimulus) were compared to the background activities. The proportion of neurons which showed responsiveness to static stimulation was greater in behaving cats (see descriptive statistics in Table 1.). Both gross and net activity increments during static stimulation were notably stronger in the behaving cats compared to the anesthetized animals (Table 1). Additionally, the magnitude of net activity decrements during static visual stimulation was more apparent in the behaving model. Similarly to the responsiveness to static stimulation, the proportion of neurons responsive to dynamic stimulation was higher in the behaving cats. During dynamic stimulation, the activity

increments were notable in the behaving cats. However, no such responses were seen in the anesthetized model at all.

The CN neurons can be categorized into three groups — phasically active neurons (PANs), high-firing neurons (HFNs), and tonically active neurons (TANs)— based on their discharge properties. Figure 6. shows the distribution of these CN neuron types recorded from the anesthetized and behaving feline model. The vast majority of the registered CN neurons in the awake, behaving cats were PANs (N = 219, 63.7%), with lesser HFNs (N=88, 25.6%) and TANs (N=28, 8.1%). On the contrary, in the anesthetized cats, the majority of the recorded neurons were HFNs (N=85, 41.3%) with fewer PANs (N=73, 35.4%) and even fewer TANs (N=43, 20.9%). Some recorded CN neurons could not be definitively categorized according to their discharge properties (awake, behaving cats: 9, 2.6%; anesthetized cats: 5, 20.4%).

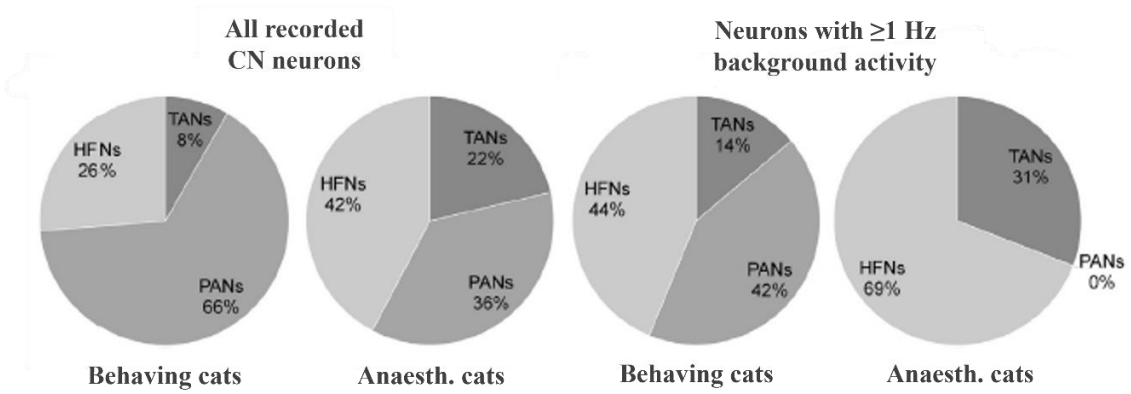

Figure 6. Distribution of the CN neuron types. *The pie charts represent the distribution of the neuron types (PANs – phasically active neurons, TAN – tonically active neurons, HFN – high-firing neurons) of the CN in the anesthetized and behaving cats. The two pie charts on the right side also indicate the distribution of neuron types but only with neurons that's background discharge rate is over 1 Hz (1 spike/sec). Note that halothane anesthesia decreased the neuronal activity in such a way that PANs with background activity over 1 Hz disappeared.*

In behaving cats, the background activities of each of these electrophysiological groups were significantly higher (Mann-Whitney U, $p<0.001$) compared to the anesthetized model (see Figure 7.). Due to their low background activity, 135 recorded CN neurons were excluded from further analysis in the awake, among them, only one neuron was uncategorized, while the rest

were all PANs (N=134). In the anesthetized model, 125 recorded CN units had to be excluded, and they displayed a more diverse distribution: PAN (N=73), HFN (N=29), TAN (N=18), and uncategorized (N=5). One of the most notable findings was that due to the applied 1 Hz cut-off criteria, in the anesthetized animals resulted in the exclusion of all PANs (see Figure 2). The background activities of both HFNs and TAN groups were significantly higher in the awake animals (Mann-Whitney U, $p<0.005$).

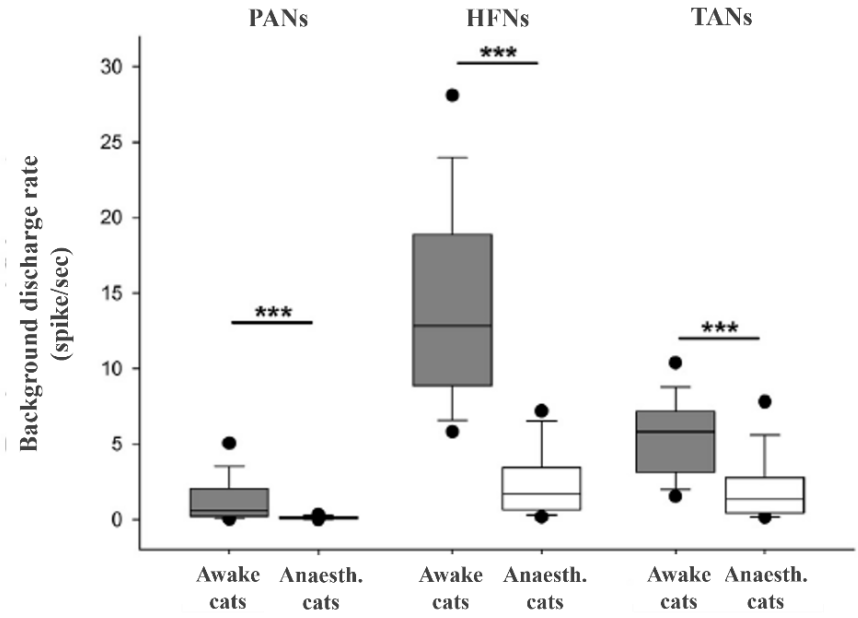

Figure 7. Background discharge activities of the different types of CN neurons, i.e. PANs, HFNs, and TANs in the awake, behaving, and anesthetized cats. *The percentile representation of the box plots is the same as in Figure 2. Similarly, the grey boxes indicate the results from the awake cats, and the white boxes from the anesthetized cats. Note that each neuron group has a significantly higher background discharge rate in the awake cats than in the anesthetized animals.*

4.2 Analysis of Local Field Potential changes elicited by visual stimulation in the CN

In the data analysis of LFPs, 226 LFP recordings were included from the awake, behaving cats and 960 LFPs from the anesthetized cats recorded in the B anesthetized experiments. All LFP recordings were analyzed separately. All these LFPs comprised a minimum of 80 trials, and the LFPs were analyzed across five different frequency bands, i.e. delta (1-3 Hz), theta (4-7 Hz), alpha (8-13 Hz), beta (14-30 Hz) and gamma frequency bands (31-70 Hz)).

4.2.1 Visually evoked LFP changes

Comparison of the response activities to the background activity with the Wilcoxon matched pair test indicated that 90% (N=207) of all registered LFPs from awake cats exhibited significant responses in at least one visual condition (static, dynamic) and one frequency band. It was notably less in the anesthetized cats, where only 63% (N=609) of the LFPs showed significant responses to visual stimulation (see descriptive statistical data in Table 2.).

	Awake cats *(N=226)*		Anesthetized cats *(N=960)*	
	N	%	N	%
Delta	80	35	168	17
Theta	98	43	178	19
Alpha	121	56	181	19
Beta	144	64	210	22
Gamma	53	23	220	23
All	204	90	609	63

Table 2. Descriptive statistics of visually evoked LFPs in the awake, behaving, and anesthetized cats. *In awake cats, LFPs with significant changes to visual stimulation showed a much higher proportion in all, but the gamma frequency band was much higher compared to the anesthetized animals.*

Figure 8. presents examples of visually evoked power changes in awake, behaving animals, while Figure 9. depicts such changes in anesthetized animals. In the awake, behaving animals, the percentage of visually evoked LFPs in the theta band was 43% (N=98), in alpha was 56 % (N=121), and 64 % (N=114) in the beta frequency band. On the contrary, in the anesthetized animals, the percentages were lower, in the theta band it was only 19% (N=178), 19% (N=181) in the alpha band, and 22% (N=210) in the beta frequency band. The percentage of LFPs with significant changes showed no difference in the gamma frequency band between the two models, it was consistent at 23% for both awake and anesthetized cats (N=34).

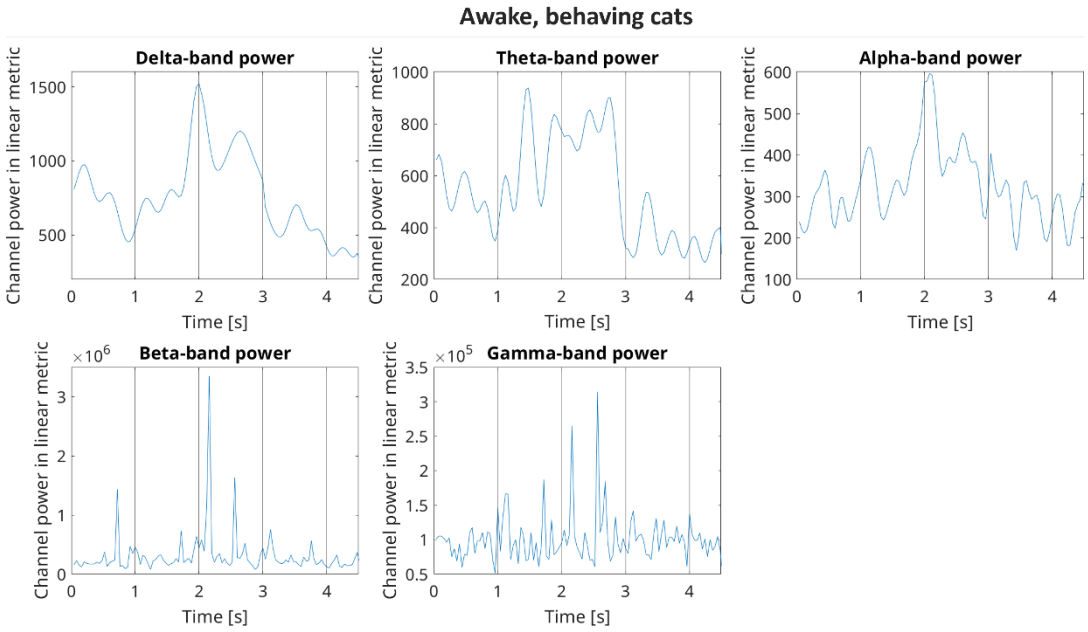

Figure 8. Visually evoked LFP changes in awake, behaving cats. *Cumulated power of the different frequency bands (delta to gamma) after the application of the spectral filter. The blue curve represents the mean activity of all trials. The vertical lines represent the borders between the different epochs of the visual paradigm (from left to right): background activity, fixation activity, response to static visual stimulus, response to dynamic visual stimulus, and reward. The abscissa shows the time relationship of the signals. The ordinate denotes the channel power in linear metrics.*

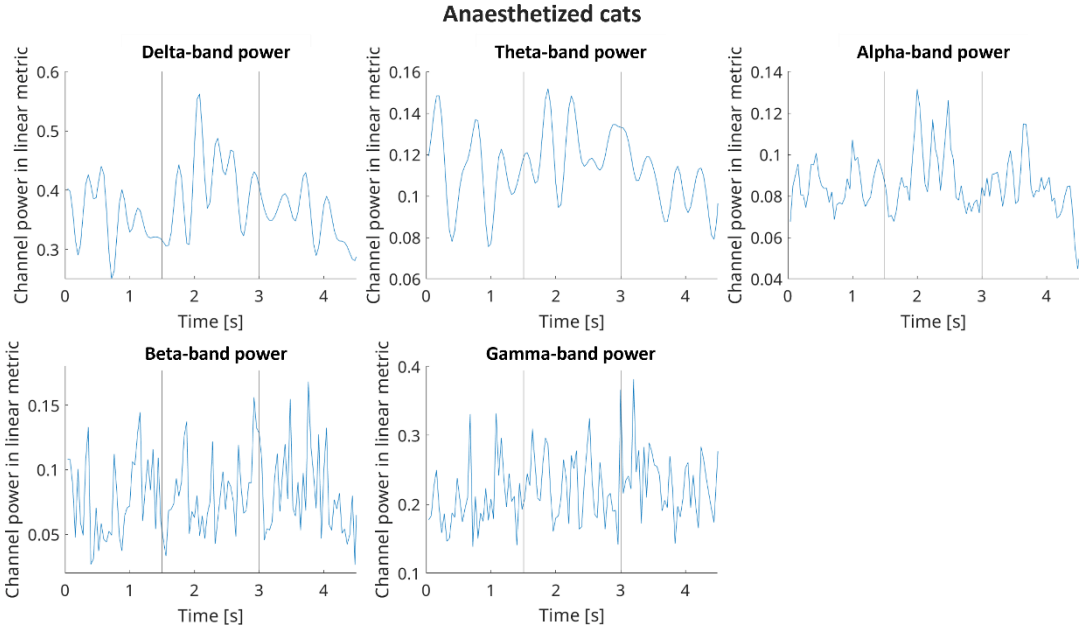

Figure 9. Visually evoked LFP changes in halothane anesthetized cats. *Cumulated power of the different frequency bands (delta to gamma) after the application of the spectral filter. The conventions are the same as in Figure 4.*

4.2.2. Visually evoked LFP changes during static and dynamic visual stimulation

The percentage of LFPs exhibiting a significant response during static visual stimulation was higher in awake, behaving cats (83%, N=187) compared to anesthetized cats (63%, N=602). Visually evoked LFP changes were observed at a higher percentage in nearly every frequency range in the behaving animals, except the theta band where the same percentages were seen (Wilcoxon matched pair test, see descriptive statistical data in Table 3.). The most notable differences were observed in the alpha and beta frequency bands. In the case of the alpha band, the percentage was 49% (N=110) in awake cats, contrasting with only 24% (N=228) in anesthetized cats. Similarly, in the beta band, the percentage of significant LFP changes was 49% (N=110) for behaving cats, in contrast to 23% (N=221) for anesthetized cats.

	Static stimulus				Dynamic stimulus			
	Awake cats *(N=226)*		Anesthetized cats *(N=960)*		Awake cats *(N=226)*		Anesthetized cats *(N=960)*	
	N	%	N	%	N	%	N	%
Delta	68	30	178	19	61	27	218	23
Theta	58	26	282	29	89	39	183	19
Alpha	110	49	228	24	76	34	147	15
Beta	110	49	221	23	69	31	203	21
Gamma	72	32	225	23	46	20	215	22
All	187	83	602	63	172	76	611	64

Table 3. Descriptive statistics of visually evoked LFP changes during static and dynamic visual stimulation. *A higher proportion of visually evoked LFPs during static stimulation is noticeable in the delta, alpha, beta, and gamma frequency ranges in behaving animals. The same trend is also evident in the theta, alpha, and beta frequency bands during dynamic visual stimulation.*

In the case of dynamic stimulation, in the behaving model, a slightly lower proportion of LFPs (76%, N=172) showed significant responsiveness compared to the impact of static stimulation, where the proportion was 83% (N=187). However, the percentages of LFPs responsive to static and dynamic stimulation were comparable in anesthetized animals, measuring at 63% (N=602) and 64% (N=611), respectively.

The same tendency was observed in the results of dynamic visual stimulation as in the case of static stimulation, i.e., the percentage of LFPs exhibiting significant responses was higher in awake, behaving cats (76%, N=172) than in their anesthetized counterparts (64%, N=611, Wilcoxon matched pair test, see descriptive statistical data in ***Table 2***). The differences in the proportion of significant visually evoked LFPs were more prominent in the case of the theta, alpha, and beta frequency bands. In the theta band, the percentage was 39% (N=89) in awake cats and only 19% (N=183) in anesthetized cats. In the alpha band, the percentage was 34% (N=76) in behaving animals, whereas it was 15% (N=147) in anesthetized cats. In the beta frequency band, the percentage of significant LFP changes was 31% (N=69) in behaving cats, whereas it was lower at 21% (N=37) in anesthetized cats.

5. Discussion

During the work leading to this thesis, we analyzed the visual response characteristics of CN neurons and low-frequency neuronal activities (local field potential, LFP) from the CN during visual stimulation. We assessed the effects of halothane anesthesia on single-cell activities and visually evoked LFPs of CN. To our knowledge, this is the first study which compares these neuronal activities recorded from the CN in two different animal models, in anesthetized, paralyzed, and awake, behaving cats. The presented results clearly demonstrate that the applied halothane anesthesia suppressed not only the background activity and visual responses of single cells but also the visually evoked LFP changes at a prominent level.

The domestic cat is a commonly used animal model in visual electrophysiology experiments. In the last few decades, animal research gradually shifted towards the use of awake, behaving animals instead of anesthetized and paralyzed animals. Both animal models have their advantages and disadvantages. The continuous control of eye movements in visual electrophysiological research is crucial to exclude the effects of unnecessary eye movements. In anesthetized, paralyzed animals, the eye movements are eliminated by muscle relaxants, thus making these animal models relatively easy to use for visual electrophysiological research. However, the applied anesthesia can impact neural activity. For example, the basal ganglia are heavily sensitive to different kinds of anesthetics (Kaisti *et al.*, 2003, Franks & Zecharia, 2011). Based on our previous experiences, halothane anesthesia influences the neuronal activities in the CN less compared to other gas anesthetics (i.e., isoflurane), however, we cannot exclude the effects of anesthesia completely. Prior behavioral and fixation training needs to be performed to use awake animal models in visual electrophysiology. Using this model, we can eliminate the disturbing effects of anesthesia, however, to properly train the animal for the fixation paradigm could last for several months or over a year. This naturally raised the question whether the benefit of experiments performed in the CN of awake, behaving animals is in balance with the hardness of the preparation of the animals for visual electrophysiological recordings.

Concerning the background discharge rates of the recorded CN neurons, the majority (60.7%) of the units had less than 1 Hz activity in the anesthetized cats. It was much lower in the case of the behaving cats, where the percentage was 39.2%. These CN neurons had to be excluded from further analysis though, because of their extremely low activities. Additionally, the activity changes during applied visual stimulation were weak in the case of anesthetized cats.

The maximal net response was 2.1 Hz in the anesthetized animals, which was higher in the behaving animals (maximal net response 19.5 Hz).

Besides the background activities, the visual responsiveness to static and dynamic visual stimulation of CN neurons was significantly reduced in the anesthetized animals. The increased neuronal discharge rate was obvious in the awake cats during visual stimulation.However, no such clear responses were seen in the anesthetized animals. The biggest differences were found in the largest neuronal population in the medium spiny neurons of the CN. It was absolutely amazing that we lost the entire medium spiny neuron group in the anesthetized animals because of the extremely low neuronal discharge rates.

We categorized neurons from the feline CN based on their electrophysiological properties in behaving cats as described in our previous study (Nagypal *et al.*, 2015). The base of the neuron-type categorization was its discharge properties, i.e. level of background discharge rate, propISI>2sec, and the shape of autocorrelograms (both in time resolution of 100ms and 1000 ms was considered) (Schmitzer-Torbert & Redish, 2004, Schmitzer-Torbert *et al.*, 2005, Schmitzer-Torbert & Redish, 2008, Nagypal *et al.*, 2015). Earlier studies suggest three types of CN neurons based on their electrophysiological properties: phasically active neurons (PANs), tonically active neurons (TANs), high-firing neurons (HFNs) (Schmitzer-Torbert & Redish, 2004, Schmitzer-Torbert & Redish, 2008, Kubota *et al.*, 2009, Gage *et al.*, 2010, Thorn *et al.*, 2010, Barnes *et al.*, 2011, Stalnaker *et al.*, 2012). We could observe these types of CN neurons in both (anesthetized and behaving) applied feline models. Although the neuronal activities and spike numbers differed in the two feline models, the shapes of the autocorrelograms of PANs, TANs, and HFNs remained the same. Thus, the temporal spiking characteristics of the CN neurons are likely to be similar in the two models. Some units could not be categorized into any of the categories mentioned above. The ratio of uncategorizable neurons (less than 3%) was also similar between the two models. A growing number of studies suggest that there is a robust coherence between the three electrophysiological (PAN, TAN, HFN) and the anatomical (medium spiny, cholinergic, and parvalbumin immunpositive GABAergic interneurons) groups of the CN neurons. Most probably, the PANs correspond to the medium spiny projection neurons, HFNs likely could be matched with the parvalbumin immunpositive GABAergic interneurons, and the TANs could be linked to the cholinergic interneurons (Kawaguchi, 1993, Wilson, 1993, Kawaguchi *et al.*, 1995, Mallet *et al.*, 2005, Berke, 2008, Tepper *et al.*, 2010, Yamada *et al.*, 2016, Tepper *et al.*, 2018, Hjorth *et al.*, 2020, Inokawa *et al.*, 2020, Nosaka & Wickens, 2022). Regarding the uncategorized neurons, these can be linked to one of the many interneuron types of the CN, such as neuropeptide Y, nitric oxide synthase (Vincent *et al.*, 1983,

Smith & Parent, 1986, Tepper *et al.*, 2018), calretinin immunpositive interneurons (Rymar *et al.*, 2004, Silberberg & Bolam, 2015, Garas *et al.*, 2018, Tepper *et al.*, 2018), etc. Our results are in line with earlier studies, which suggest that 77-97% of the striatal projection neurons in other species correspond to the GABAergic MSNs (Kemp & Powell, 1971, Luk & Sadikot, 2001). We found that the vast majority of the recorded CN units in our behaving feline model were PANs (64%). It should be mentioned here that PANs are often difficult to register (Lau & Glimcher, 2007) due to their extremely low background activity. It means that our registered 64% of PANs may be underestimation due to undersampling. As for the other two electrophysiological groups, the HFNs (25%) and TANs (8%) were much less frequent in our sample, which also corresponds to several prior studies (Phelps *et al.*, 1985, Luk & Sadikot, 2001). On the other hand, neuron type distribution in the anesthetized cats differed from the distribution we observed in the awake cats. Interestingly, the PAN was not the biggest group in this sample. It seems as if we have lost the majority of these neurons in the anesthetized animals. The largest population of the recorded CN neurons from the anesthetized feline model was HFN (41%). PANs were less represented in the anesthetized cats: only 35% of the CN neurons were classified in this neuron type. Even fewer neurons were found to be TANs (21%).

The difference between the anesthetized and behaving feline model is striking. Halothane anesthesia appears to have impacted the background activity to the extent that a valid analysis of PANs was impossible during anesthesia due to their extremely low background activity. In light of this finding, it is clear why these types of neurons are so difficult to detect in the anesthetized models. One of the most important findings of the present thesis work is that the PANs, which seem to correspond to the medium spiny projection neurons (the most frequent neuron group in the CN), were practically silent under anesthesia, and thus these neurons cannot be investigated in anesthetized, paralyzed cats without afferent stimulation. Not only the PANs were affected by halothane, but the activity of the HFNs and TANs was also strongly suppressed in the anesthetized cats.

The differences between the two feline models are also evident in the case of LFP changes during visual stimulation (dynamic and static stimulation). The vast majority (90%) of the LFPs recorded in behaving cats showed significant activity changes in at least one visual condition and one frequency band. Although, in the anesthetized cats, the visually evoked LFP changes were less frequent (only 61%). During static visual stimulation, the difference in power changes was more obvious (83% in the behaving cats and 63% in the anesthetized cats). During dynamic stimulation, this difference between the two models was less, but it was still evident (76% in the behaving cats and 64% in the anesthetized cats). These differences in the LFPs are also

remarkable but not as dramatic as the differences found and described in single-cell activities in the CN. In the awake, behaving model, the proportion of visually evoked LFP power changes was observed to be higher in all investigated frequency bands except gamma (delta, theta, alpha, beta) compared to the results found in the anesthetized cats. However, the difference is much more obvious in the case of static stimulation in the alpha and the beta frequency bands and concerning dynamic stimulation to the theta, the alpha, and the beta bands.

Similarly to previous human EEG studies, the increased theta activity might be a result of synchronized reactivation of information represented in the visual brain areas (Gevins *et al.*, 1997, Hsieh *et al.*, 2011, Liebe *et al.*, 2012, Roberts *et al.*, 2013, Hsieh & Ranganath, 2014). Studies suggested that elevated alpha activity likely corresponds to visual and audiovisual information processing (Worden *et al.*, 2000, Ergenoglu *et al.*, 2004, Schaefer *et al.*, 2011), and it is also believed to play a role in sensory suppression by information gating (Michels *et al.*, 2008, Foxe & Snyder, 2011). Normal beta band activity also seems to play an important role in visual information processing by modulating the outcome of the normal activity of the basal ganglia (Puszta et al., 2019). One possible answer to the differences seen between the two feline models could be novelty detection and the connected sensory gating because we included in our investigation the first 320 ms time window of both static and dynamic visual stimulation. Since the analysis addressed the first 320 ms time window of both static and dynamic stimulation, novelty detection and the connected sensory gating could be the task that shows these differences between the anesthetized, paralyzed, and awake, behaving animals (Nagy *et al.*, 2008, Benedek *et al.*, 2019).

Let's see the shortcomings of our results. Previous electrophysiological experiments, which addressed the visual information processing in the CN, applied simple dynamic geometric forms (spots, dots, bars) and drifting sinewave gratings (Pouderoux & Freton, 1979, Strecker & Jacobs, 1985, Nagy *et al.*, 2003, Nagy *et al.*, 2006, Nagy *et al.*, 2008, Gombkoto *et al.*, 2011). These types of visual stimuli are more adequate for the CN neurons than our random dot patterns and kinematograms that we used in the presented PhD thesis work. However, with this type of visual stimuli, the effects of spatiotemporal and direction preference can be minimized, and we could probably record more CN neurons with the applied stimuli. In our awake and behaving feline model, both eyes of the cats remained open during visual stimulation. On the other hand, in anesthetized experiments, only the contralateral eye of the cats was opened, while the other eye was covered. In anesthetized and paralyzed animals, it is crucial to prevent binocular inhibition that results from ocular misalignment during paralysis because this could

impact the magnitude of visual responses. However, it is unlikely that this factor alone would explain our observed difference. Furthermore, the difference we observed in the background activity is also against this explanation. The reason is that muscle tone, arousal, and goal-oriented movements could increase the activity of CN. Fixation also affects neuronal activity because it corresponds to attention at some level, and it is known to be modulating the activity of visually responsive brain areas (Rajkai *et al.*, 2008). Anesthesia likely can eliminate or at least reduce attention.Hence, it could also be an explanation for why the visual responsiveness was reduced in the anesthetized model. However, we believe that this could not create such obvious differences, which we found between the visual activity recorded in the anesthetized and paralyzed cats. To support this idea, only one-quarter of the recorded CN neurons showed significant activity changes during the fixation phase, and the vast majority of the neurons remained silent.

It is also worth mentioning that the anesthetized animals were cycloplegic, and the visus was corrected with appropriate lenses. The awake cats had normal pupils and lenses. The background luminance was the same for the two models, and the same CRT monitor was used, so these do not explain the observed difference.

An important limitation of our analysis of LFP changes is that the recording systems with different background noise levels differed between the behaving and anesthetized cats. Hence, we could not perform a valid comparison of the magnitude of the visual responses. Thus, we concentrated on whether the LFP changes were significant and to perform a descriptive statistic about the percentage of these visually-evoked LFP changes. Another limitation is that electrodes with different geometries were applied in the behaving (wire electrodes) and anesthetized (linear probe) experiments. It was found that the geometry of the electrodes could also influence the magnitude of the LFPs (Herreras, 2016). In order not to influence the number of significant LFP changes and thus the differences between the two feline models, the baseline power spectrum density of one channel was compared with the power spectrum density during visual stimulation of the same channel. 8-channel wire electrodes were used in the behaving experiments, and 64-channel linear probes in the anesthetized experiments, which explains the higher number of recorded LFPs from the anesthetized animals.

In summary, we consider the following as the most important achievements of this study: we found that there was a significant difference between single-cell neuronal activities recorded from the feline CN in an anesthetized and a behaving model. Halothane anesthesia with the applied muscle relaxant significantly decreased the number of visually responsive CN neurons and strongly reduced the net discharge rate changes to visual stimulation. Halothane suppressed

the single-cell activity so drastically that the analysis of the biggest neuronal population, the PANs (possibly corresponding to medium spiny neurons), was almost impossible in the anesthetized cats because of their extremely low activity. Similarly to the single-cell activities, we demonstrated that there were obvious differences between the visually evoked LFP changes in the CN of the two feline models. Anesthesia significantly suppressed the significant LFP power changes to visual stimulation (both static and dynamic stimulation). However, these differences in the LFPs are also remarkable but not as dramatic as the differences found and described in single-cell activities in the CN.

6. Summary

In visual electrophysiological experiments, both anesthetized, paralyzed, and awake, behaving animal models are widely used. It is well known that anesthesia influences neuronal activity which effect could be different between different brain areas. The goal of our presented work was to answer if neuronal activities (both single-cell and local field potential (LFP)) recorded from these two animal models are comparable or not. Because using the behaving animal model could be more difficult than the anesthetized model, it raises the question of whether the costs and benefits are in equilibrium.

To answer this question, we compared the background activity and visual responsiveness of CN neurons and the visually evoked LFPs recorded from the CN of two halothane-anesthetized (1.0%), paralyzed, and two awake, behaving cats during static and dynamic visual stimulation. The behaving animals were trained to perform a visual fixation task. Extracellular recordings were made from the CN during static and dynamic visual stimulation. Based on their electrophysiological properties, the recorded CN neurons were separated into three different classes: phasically active (PANs), high-firing (HFNs), and tonically active (TANs) neurons. The visually evoked LFPs were analyzed in the delta (1-3 Hz), theta (4–7 Hz), alpha (8–13 Hz), beta (14–30 Hz), and gamma (31–70 Hz) frequency bands.

Halothane anesthesia significantly decreased the background activity of all three neuron types of the CN. The suppressive effect of anesthesia was most prominent in the case of PANs. The background activity of the PANs was consequently under 1 Hz, which made it almost impossible to investigate these neuronal populations in anesthetized animals. Only weak visual responses were found in the CN neurons in the anesthetized cats, however, the visual responses were more obvious in the behaving cats. We also found remarkable differences between the visually evoked LFP power changes in the CN of the two feline models. However, these differences in the LFPs are also remarkable, but not as dramatic as the differences found and described in single-cell activities in the CN. The halothane anesthesia suppressed the LFP changes in the CN in each frequency range from delta to beta to both static and dynamic stimulation. These differences in power changes were more prominent in static visual stimulation, but still, remarkable differences were found in dynamic stimulation, too.

These results indicate that halothane anesthesia has an obvious suppressive effect on the cat CN. Based on the presented results we argue that the benefits of the awake animal models could balance or also outweigh the cost in the investigation of the visual properties of the CN. The work with awake and behaving animals in visual electrophysiology seems to be much more

difficult than the work with anesthetized animals, primarily due to the long-lasting training period of the behaving animals. However, the results from the awake, behaving animals are much more evident both in the single-cell activities and the LFPs, and the visually activity of the biggest neuronal population in the CN the PANs can be investigated exclusively in the behaving model.

7. Acknowledgments

First of all, I would like to express my deepest gratitude to Dr. Attila Nagy, for his invaluable guidance and unwavering support throughout the journey of helping me with my PhD work to writing this dissertation and helping me through difficult situations.

I would like to thank Professor Gábor Jancsó for giving me the chance to participate in the Neuroscience PhD program and to Professor Gyula Sáry for allowing me to do my research in the Department of Physiology.

I am also grateful to my fellow PhD students with whom I became friends over the years, namely Dr. Zsófia Giricz, Dr. András Puszta, Dr. Ákos Pertich and Dr. Attila Őze. I would not have had such beautiful years without you, the many shared experiences we had together will stay with me forever. And a special thanks goes to Dr. Balázs Barkóczi, for his help in my early years in laboratory work and his friendship.

I would like to extend my gratitude to Dr. Balázs Bodosi and Dr. Eördegh Gabriella for their continues support over the years of my PhD work and to Dr. András Kelemen for his help with the LFP analysis and statistics. I would also like to thank Ádám Kiss with his great help with the LFP analysis and preparing the article.

I am also grateful to Gabriella Dósai for her valuable laboratory assistance and Péter Liszli for his help in the technical part of the research. I would like to express my thanks to all my colleagues and friends in the Department of Physiology for their support and kindness they showed towards me, specially to Dr. Alexandra Büki, Dr. András Benyhe, Dr. Péter Kaposvári, Dr. Ágnes Fehér and Dr. Zoltán Lelkes.

The most significant acknowledgement is reserved for my parents, for their continuous love and support which they have provided me, that helped me achieve everything I have.

I am deeply grateful to my friends, who have always listened and encouraged me, namely Szabina Pap, Dr. Zita Timár, Andrea Steiger and Dr. Tamás Zarnócz, whom I can always count on and are the greatest friends one can ever ask for. A special thanks to Gréti Kozocsay, who is like a sister to me and who helped me through many difficult situations. And finally, I would like to thank everyone who inspired or helped me in any sort of way over the years.

The present PhD work was supported by the University of Szeged Grant SZTE-ÁOK-KKA Grant No. 2019/270-62-2 and SZTE SZAOK-KKA-SZGYA Grant no: 2023/5S479.

8. References

1. Albe-Fessard D, Rocha-Miranda C & Oswaldo-Cruz E (1960) [Activity evoked in the caudate nucleus of the cat in response to various types of afferent stimulation. II. Microphysiological study]. *Electroencephalogr Clin Neurophysiol* **12**: 649-661.
2. Amemori KI, Amemori S, Gibson DJ & Graybiel AM (2018) Striatal Microstimulation Induces Persistent and Repetitive Negative Decision-Making Predicted by Striatal Beta-Band Oscillation. *Neuron* **99**: 829-841 e826.
3. Barnes TD, Kubota Y, Hu D, Jin DZ & Graybiel AM (2005) Activity of striatal neurons reflects dynamic encoding and recoding of procedural memories. *Nature* **437**: 1158-1161.
4. Barnes TD, Mao JB, Hu D, Kubota Y, Dreyer AA, Stamoulis C, Brown EN & Graybiel AM (2011) Advance cueing produces enhanced action-boundary patterns of spike activity in the sensorimotor striatum. *J Neurophysiol* **105**: 1861-1878.
5. Beatty JA, Sullivan MA, Morikawa H & Wilson CJ (2012) Complex autonomous firing patterns of striatal low-threshold spike interneurons. *J Neurophysiol* **108**: 771-781.
6. Ben-Ari Y & Kelly JS (1976) Dopamine evoked inhibition of single cells of the feline putamen and basolateral amygdala. *J Physiol* **256**: 1-21.
7. Benedek G, Keri S, Nagy A, Braunitzer G & Norita M (2019) A multimodal pathway including the basal ganglia in the feline brain. *Physiol Int* **106**: 95-113.
8. Bennett BD & Wilson CJ (1999) Spontaneous activity of neostriatal cholinergic interneurons in vitro. *J Neurosci* **19**: 5586-5596.
9. Berke JD (2008) Uncoordinated firing rate changes of striatal fast-spiking interneurons during behavioral task performance. *J Neurosci* **28**: 10075-10080.
10. Berke JD (2009) Fast oscillations in cortical-striatal networks switch frequency following rewarding events and stimulant drugs. *Eur J Neurosci* **30**: 848-859.
11. Berke JD (2011) Functional properties of striatal fast-spiking interneurons. *Front Syst Neurosci* **5**: 45.
12. Bolam JP, Wainer BH & Smith AD (1984) Characterization of cholinergic neurons in the rat neostriatum. A combination of choline acetyltransferase immunocytochemistry, Golgi-impregnation and electron microscopy. *Neuroscience* **12**: 711-718.
13. Brainard DH (1997) The Psychophysics Toolbox. *Spat Vis* **10**: 433-436.

14. Buzsaki G, Anastassiou CA & Koch C (2012) The origin of extracellular fields and currents--EEG, ECoG, LFP and spikes. *Nat Rev Neurosci* **13**: 407-420.

15. Canolty RT & Knight RT (2010) The functional role of cross-frequency coupling. *Trends Cogn Sci* **14**: 506-515.

16. Carmichael JE, Gmaz JM & van der Meer MAA (2017) Gamma Oscillations in the Rat Ventral Striatum Originate in the Piriform Cortex. *J Neurosci* **37**: 7962-7974.

17. Chen X, Liu Z, Ma C, Ma L & Liu X (2019) Parvalbumin Interneurons Determine Emotional Valence Through Modulating Accumbal Output Pathways. *Front Behav Neurosci* **13**: 110.

18. Chuhma N, Tanaka KF, Hen R & Rayport S (2011) Functional connectome of the striatal medium spiny neuron. *J Neurosci* **31**: 1183-1192.

19. Cohen MX, Axmacher N, Lenartz D, Elger CE, Sturm V & Schlaepfer TE (2009) Good vibrations: cross-frequency coupling in the human nucleus accumbens during reward processing. *J Cogn Neurosci* **21**: 875-889.

20. Connor JD (1970) Caudate nucleus neurones: correlation of the effects of substantia nigra stimulaton with iontophoretic dopamine. *J Physiol* **208**: 691-703.

21. Courtemanche R, Fujii N & Graybiel AM (2003) Synchronous, focally modulated beta-band oscillations characterize local field potential activity in the striatum of awake behaving monkeys. *J Neurosci* **23**: 11741-11752.

22. DeCoteau WE, Thorn C, Gibson DJ, Courtemanche R, Mitra P, Kubota Y & Graybiel AM (2007) Oscillations of local field potentials in the rat dorsal striatum during spontaneous and instructed behaviors. *J Neurophysiol* **97**: 3800-3805.

23. DeCoteau WE, Thorn C, Gibson DJ, Courtemanche R, Mitra P, Kubota Y & Graybiel AM (2007) Learning-related coordination of striatal and hippocampal theta rhythms during acquisition of a procedural maze task. *Proc Natl Acad Sci U S A* **104**: 5644-5649.

24. Doig NM, Moss J & Bolam JP (2010) Cortical and thalamic innervation of direct and indirect pathway medium-sized spiny neurons in mouse striatum. *J Neurosci* **30**: 14610-14618.

25. Donnelly NA, Holtzman T, Rich PD, *et al.* (2014) Oscillatory activity in the medial prefrontal cortex and nucleus accumbens correlates with impulsivity and reward outcome. *PLoS One* **9**: e111300.

26. Dou W, Morrow A, Iemi L & Samaha J (2022) Pre-stimulus alpha-band phase gates early visual cortex responses. *Neuroimage* **253**: 119060.

27. Eisinger RS, Urdaneta ME, Foote KD, Okun MS & Gunduz A (2018) Non-motor Characterization of the Basal Ganglia: Evidence From Human and Non-human Primate Electrophysiology. *Front Neurosci* **12**: 385.

28. English DF, Ibanez-Sandoval O, Stark E, Tecuapetla F, Buzsaki G, Deisseroth K, Tepper JM & Koos T (2011) GABAergic circuits mediate the reinforcement-related signals of striatal cholinergic interneurons. *Nat Neurosci* **15**: 123-130.

29. Ergenoglu T, Demiralp T, Bayraktaroglu Z, Ergen M, Beydagi H & Uresin Y (2004) Alpha rhythm of the EEG modulates visual detection performance in humans. *Brain Res Cogn Brain Res* **20**: 376-383.

30. Fino E & Venance L (2011) Spike-timing dependent plasticity in striatal interneurons. *Neuropharmacology* **60**: 780-788.

31. Fiset P, Paus T, Daloze T, Plourde G, Meuret P, Bonhomme V, Hajj-Ali N, Backman SB & Evans AC (1999) Brain mechanisms of propofol-induced loss of consciousness in humans: a positron emission tomographic study. *J Neurosci* **19**: 5506-5513.

32. Foxe JJ & Snyder AC (2011) The Role of Alpha-Band Brain Oscillations as a Sensory Suppression Mechanism during Selective Attention. *Front Psychol* **2**: 154.

33. Franks NP & Zecharia AY (2011) Sleep and general anesthesia. *Can J Anaesth* **58**: 139-148.

34. Fuchs AF & Robinson DA (1966) A method for measuring horizontal and vertical eye movement chronically in the monkey. *J Appl Physiol* **21**: 1068-1070.

35. Fujisawa S & Buzsaki G (2011) A 4 Hz oscillation adaptively synchronizes prefrontal, VTA, and hippocampal activities. *Neuron* **72**: 153-165.

36. Gage GJ, Stoetzner CR, Wiltschko AB & Berke JD (2010) Selective activation of striatal fast-spiking interneurons during choice execution. *Neuron* **67**: 466-479.

37. Galvan A, Hu X, Smith Y & Wichmann T (2012) In vivo optogenetic control of striatal and thalamic neurons in non-human primates. *PLoS One* **7**: e50808.

38. Garas FN, Kormann E, Shah RS, Vinciati F, Smith Y, Magill PJ & Sharott A (2018) Structural and molecular heterogeneity of calretinin-expressing interneurons in the rodent and primate striatum. *J Comp Neurol* **526**: 877-898.

39. Gevins A, Smith ME, McEvoy L & Yu D (1997) High-resolution EEG mapping of cortical activation related to working memory: effects of task difficulty, type of processing, and practice. *Cereb Cortex* **7**: 374-385.

40. Gombkoto P, Rokszin A, Berenyi A, Braunitzer G, Utassy G, Benedek G & Nagy A (2011) Neuronal code of spatial visual information in the caudate nucleus. *Neuroscience* **182**: 225-231.

41. Graybiel AM (2008) Habits, rituals, and the evaluative brain. *Annu Rev Neurosci* **31**: 359-387.

42. Guan A, Wang S, Huang A, Qiu C, Li Y, Li X, Wang J, Wang Q & Deng B (2022) The role of gamma oscillations in central nervous system diseases: Mechanism and treatment. *Front Cell Neurosci* **16**: 962957.

43. Haegens S, Nacher V, Hernandez A, Luna R, Jensen O & Romo R (2011) Beta oscillations in the monkey sensorimotor network reflect somatosensory decision making. *Proc Natl Acad Sci U S A* **108**: 10708-10713.

44. Harris KD, Henze DA, Csicsvari J, Hirase H & Buzsaki G (2000) Accuracy of tetrode spike separation as determined by simultaneous intracellular and extracellular measurements. *J Neurophysiol* **84**: 401-414.

45. Harris KD, Csicsvari J, Hirase H, Dragoi G & Buzsaki G (2003) Organization of cell assemblies in the hippocampus. *Nature* **424**: 552-556.

46. Hazan L, Zugaro M & Buzsaki G (2006) Klusters, NeuroScope, NDManager: a free software suite for neurophysiological data processing and visualization. *J Neurosci Methods* **155**: 207-216.

47. Herreras O (2016) Local Field Potentials: Myths and Misunderstandings. *Front Neural Circuits* **10**: 101.

48. Hjorth JJJ, Kozlov A, Carannante I, *et al.* (2020) The microcircuits of striatum in silico. *Proc Natl Acad Sci U S A* **117**: 9554-9565.

49. Holly EN, Davatolhagh MF, Choi K, Alabi OO, Vargas Cifuentes L & Fuccillo MV (2019) Striatal Low-Threshold Spiking Interneurons Regulate Goal-Directed Learning. *Neuron* **103**: 92-101 e106.

50. Howard MW, Rizzuto DS, Caplan JB, Madsen JR, Lisman J, Aschenbrenner-Scheibe R, Schulze-Bonhage A & Kahana MJ (2003) Gamma oscillations correlate with working memory load in humans. *Cereb Cortex* **13**: 1369-1374.

51. Hsieh LT & Ranganath C (2014) Frontal midline theta oscillations during working memory maintenance and episodic encoding and retrieval. *Neuroimage* **85 Pt 2**: 721-729.

52. Hsieh LT, Ekstrom AD & Ranganath C (2011) Neural oscillations associated with item and temporal order maintenance in working memory. *J Neurosci* **31**: 10803-10810.

53. Humphries MD & Prescott TJ (2010) The ventral basal ganglia, a selection mechanism at the crossroads of space, strategy, and reward. *Prog Neurobiol* **90**: 385-417.

54. Huxlin KR & Pasternak T (2004) Training-induced recovery of visual motion perception after extrastriate cortical damage in the adult cat. *Cereb Cortex* **14**: 81-90.

55. Ibanez-Sandoval O, Tecuapetla F, Unal B, Shah F, Koos T & Tepper JM (2010) Electrophysiological and morphological characteristics and synaptic connectivity of tyrosine hydroxylase-expressing neurons in adult mouse striatum. *J Neurosci* **30**: 6999-7016.

56. Inokawa H, Matsumoto N, Kimura M & Yamada H (2020) Tonically Active Neurons in the Monkey Dorsal Striatum Signal Outcome Feedback during Trial-and-error Search Behavior. *Neuroscience* **446**: 271-284.

57. Inokawa H, Yamada H, Matsumoto N, Muranishi M & Kimura M (2010) Juxtacellular labeling of tonically active neurons and phasically active neurons in the rat striatum. *Neuroscience* **168**: 395-404.

58. Joel D & Weiner I (1994) The organization of the basal ganglia-thalamocortical circuits: open interconnected rather than closed segregated. *Neuroscience* **63**: 363-379.

59. Judge SJ, Richmond BJ & Chu FC (1980) Implantation of magnetic search coils for measurement of eye position: an improved method. *Vision Res* **20**: 535-538.

60. Kaisti KK, Langsjo JW, Aalto S, Oikonen V, Sipila H, Teras M, Hinkka S, Metsahonkala L & Scheinin H (2003) Effects of sevoflurane, propofol, and adjunct nitrous oxide on regional cerebral blood flow, oxygen consumption, and blood volume in humans. *Anesthesiology* **99**: 603-613.

61. Kawaguchi Y (1993) Physiological, morphological, and histochemical characterization of three classes of interneurons in rat neostriatum. *J Neurosci* **13**: 4908-4923.

62. Kawaguchi Y, Wilson CJ, Augood SJ & Emson PC (1995) Striatal interneurones: chemical, physiological and morphological characterization. *Trends Neurosci* **18**: 527-535.

63. Kemp JM & Powell TP (1971) The structure of the caudate nucleus of the cat: light and electron microscopy. *Philos Trans R Soc Lond B Biol Sci* **262**: 383-401.

64. Kim HF & Hikosaka O (2013) Distinct basal ganglia circuits controlling behaviors guided by flexible and stable values. *Neuron* **79**: 1001-1010.

65. Kimura M (1986) The role of primate putamen neurons in the association of sensory stimuli with movement. *Neurosci Res* **3**: 436-443.

66. Kimura M, Rajkowski J & Evarts E (1984) Tonically discharging putamen neurons exhibit set-dependent responses. *Proc Natl Acad Sci U S A* **81**: 4998-5001.

67. Koos T & Tepper JM (1999) Inhibitory control of neostriatal projection neurons by GABAergic interneurons. *Nat Neurosci* **2**: 467-472.

68. Koos T, Tepper JM & Wilson CJ (2004) Comparison of IPSCs evoked by spiny and fast-spiking neurons in the neostriatum. *J Neurosci* **24**: 7916-7922.

69. Korshunov VA (1995) Miniature microdrive for extracellular recording of neuronal activity in freely moving animals. *J Neurosci Methods* **57**: 77-80.

70. Kubota Y & Kawaguchi Y (1994) Three classes of GABAergic interneurons in neocortex and neostriatum. *Jpn J Physiol* **44 Suppl 2**: S145-148.

71. Kubota Y, Liu J, Hu D, DeCoteau WE, Eden UT, Smith AC & Graybiel AM (2009) Stable encoding of task structure coexists with flexible coding of task events in sensorimotor striatum. *J Neurophysiol* **102**: 2142-2160.

72. Lalla L, Rueda Orozco PE, Jurado-Parras MT, Brovelli A & Robbe D (2017) Local or Not Local: Investigating the Nature of Striatal Theta Oscillations in Behaving Rats. *eNeuro* **4**.

73. Lanz F, Moret V, Rouiller EM & Loquet G (2013) Multisensory Integration in Non-Human Primates during a Sensory-Motor Task. *Front Hum Neurosci* **7**: 799.

74. Lau B & Glimcher PW (2007) Action and outcome encoding in the primate caudate nucleus. *J Neurosci* **27**: 14502-14514.

75. Laurent G (2002) Olfactory network dynamics and the coding of multidimensional signals. *Nat Rev Neurosci* **3**: 884-895.

76. Lee H, Stirnberg R, Stocker T & Axmacher N (2017) Audiovisual integration supports face-name associative memory formation. *Cogn Neurosci* **8**: 177-192.

77. Leventhal DK, Gage GJ, Schmidt R, Pettibone JR, Case AC & Berke JD (2012) Basal ganglia beta oscillations accompany cue utilization. *Neuron* **73**: 523-536.

78. Liebe S, Hoerzer GM, Logothetis NK & Rainer G (2012) Theta coupling between V4 and prefrontal cortex predicts visual short-term memory performance. *Nat Neurosci* **15**: 456-462, S451-452.

79. Logothetis N, Merkle H, Augath M, Trinath T & Ugurbil K (2002) Ultra high-resolution fMRI in monkeys with implanted RF coils. *Neuron* **35**: 227-242.

80. Luk KC & Sadikot AF (2001) GABA promotes survival but not proliferation of parvalbumin-immunoreactive interneurons in rodent neostriatum: an in vivo study with stereology. *Neuroscience* **104**: 93-103.

81. Malhotra S, Cross RW, Zhang A & van der Meer MA (2015) Ventral striatal gamma oscillations are highly variable from trial to trial, and are dominated by behavioural state, and only weakly influenced by outcome value. *Eur J Neurosci* **42**: 2818-2832.

82. Mallet N, Le Moine C, Charpier S & Gonon F (2005) Feedforward inhibition of projection neurons by fast-spiking GABA interneurons in the rat striatum in vivo. *J Neurosci* **25**: 3857-3869.

83. Mallet N, Leblois A, Maurice N & Beurrier C (2019) Striatal Cholinergic Interneurons: How to Elucidate Their Function in Health and Disease. *Front Pharmacol* **10**: 1488.

84. Matamales M, Gotz J & Bertran-Gonzalez J (2016) Quantitative Imaging of Cholinergic Interneurons Reveals a Distinctive Spatial Organization and a Functional Gradient across the Mouse Striatum. *PLoS One* **11**: e0157682.

85. McKown MD & Schadt JC (2006) A modification of the Harper-McGinty microdrive for use in chronically prepared rabbits. *J Neurosci Methods* **153**: 239-242.

86. Michels L, Moazami-Goudarzi M, Jeanmonod D & Sarnthein J (2008) EEG alpha distinguishes between cuneal and precuneal activation in working memory. *Neuroimage* **40**: 1296-1310.

87. Morrow A, Dou W & Samaha J (2023) Individual alpha frequency appears unrelated to the latency of early visual responses. *Front Neurosci* **17**: 1118910.

88. Munoz-Manchado AB, Bengtsson Gonzales C, Zeisel A, *et al.* (2018) Diversity of Interneurons in the Dorsal Striatum Revealed by Single-Cell RNA Sequencing and PatchSeq. *Cell Rep* **24**: 2179-2190 e2177.

89. Nagy A, Eordegh G & Benedek G (2003) Extents of visual, auditory and bimodal receptive fields of single neurons in the feline visual associative cortex. *Acta Physiol Hung* **90**: 305-312.

90. Nagy A, Eordegh G, Paroczy Z, Markus Z & Benedek G (2006) Multisensory integration in the basal ganglia. *Eur J Neurosci* **24**: 917-924.

91. Nagy A, Paroczy Z, Markus Z, Berenyi A, Wypych M, Waleszczyk WJ & Benedek G (2008) Drifting grating stimulation reveals particular activation properties of visual neurons in the caudate nucleus. *Eur J Neurosci* **27**: 1801-1808.

92. Nagypal T, Gombkoto P, Barkoczi B, Benedek G & Nagy A (2015) Activity of Caudate Nucleus Neurons in a Visual Fixation Paradigm in Behaving Cats. *PLoS One* **10**: e0142526.

93. Nagypal T, Gombkoto P, Utassy G, Averkin RG, Benedek G & Nagy A (2014) A new, behaving, head restrained, eye movement-controlled feline model for chronic visual electrophysiological recordings. *J Neurosci Methods* **221**: 1-7.

94. Nosaka D & Wickens JR (2022) Striatal Cholinergic Signaling in Time and Space. *Molecules* **27**.

95. Parent A & Hazrati LN (1995) Functional anatomy of the basal ganglia. I. The cortico-basal ganglia-thalamo-cortical loop. *Brain Res Brain Res Rev* **20**: 91-127.

96. Partridge JG, Janssen MJ, Chou DY, Abe K, Zukowska Z & Vicini S (2009) Excitatory and inhibitory synapses in neuropeptide Y-expressing striatal interneurons. *J Neurophysiol* **102**: 3038-3045.

97. Pelli DG (1997) The VideoToolbox software for visual psychophysics: transforming numbers into movies. *Spat Vis* **10**: 437-442.

98. Phelps PE, Houser CR & Vaughn JE (1985) Immunocytochemical localization of choline acetyltransferase within the rat neostriatum: a correlated light and electron microscopic study of cholinergic neurons and synapses. *J Comp Neurol* **238**: 286-307.

99. Pigarev IN & Rodionova EI (1998) Two visual areas located in the middle suprasylvian gyrus (cytoarchitectonic field 7) of the cat's cortex. *Neuroscience* **85**: 717-732.

100. Pigarev IN & Levichkina EV (2011) Distance modulated neuronal activity in the cortical visual areas of cats. *Exp Brain Res* **214**: 105-111.

101. Populin LC & Yin TC (1998) Behavioral studies of sound localization in the cat. *J Neurosci* **18**: 2147-2160.

102. Populin LC & Yin TC (2002) Bimodal interactions in the superior colliculus of the behaving cat. *J Neurosci* **22**: 2826-2834.

103. Pouderoux G & Freton E (1979) Patterns of unit responses to visual stimuli in the cat caudate nucleus under chloralose anesthesia. *Neurosci Lett* **11**: 53-58.

104. Puszta A, Pertich A, Katona X, Bodosi B, Nyujto D, Giricz Z, Eordegh G & Nagy A (2019) Power-spectra and cross-frequency coupling changes in visual and Audio-visual acquired equivalence learning. *Sci Rep* **9**: 9444.

105. Rajkai C, Lakatos P, Chen CM, Pincze Z, Karmos G & Schroeder CE (2008) Transient cortical excitation at the onset of visual fixation. *Cereb Cortex* **18**: 200-209.

106. Roberts BM, Hsieh LT & Ranganath C (2013) Oscillatory activity during maintenance of spatial and temporal information in working memory. *Neuropsychologia* **51**: 349-357.

107. Robinson DA (1963) A Method of Measuring Eye Movement Using a Scleral Search Coil in a Magnetic Field. *IEEE Trans Biomed Eng* **10**: 137-145.

108. Rothwell PE, Hayton SJ, Sun GL, Fuccillo MV, Lim BK & Malenka RC (2015) Input- and Output-Specific Regulation of Serial Order Performance by Corticostriatal Circuits. *Neuron* **88**: 345-356.

109. Rymar VV, Sasseville R, Luk KC & Sadikot AF (2004) Neurogenesis and stereological morphometry of calretinin-immunoreactive GABAergic interneurons of the neostriatum. *J Comp Neurol* **469**: 325-339.

110. Samaha J & Postle BR (2015) The Speed of Alpha-Band Oscillations Predicts the Temporal Resolution of Visual Perception. *Curr Biol* **25**: 2985-2990.

111. Santacruz SR, Rich EL, Wallis JD & Carmena JM (2017) Caudate Microstimulation Increases Value of Specific Choices. *Curr Biol* **27**: 3375-3383 e3373.

112. Schaefer RS, Vlek RJ & Desain P (2011) Music perception and imagery in EEG: alpha band effects of task and stimulus. *Int J Psychophysiol* **82**: 254-259.

113. Schmitzer-Torbert N & Redish AD (2004) Neuronal activity in the rodent dorsal striatum in sequential navigation: separation of spatial and reward responses on the multiple T task. *J Neurophysiol* **91**: 2259-2272.

114. Schmitzer-Torbert N, Jackson J, Henze D, Harris K & Redish AD (2005) Quantitative measures of cluster quality for use in extracellular recordings. *Neuroscience* **131**: 1-11.

115. Schmitzer-Torbert NC & Redish AD (2008) Task-dependent encoding of space and events by striatal neurons is dependent on neural subtype. *Neuroscience* **153**: 349-360.

116. Schulz JM & Reynolds JN (2013) Pause and rebound: sensory control of cholinergic signaling in the striatum. *Trends Neurosci* **36**: 41-50.

117. Schulz JM, Oswald MJ & Reynolds JN (2011) Visual-induced excitation leads to firing pauses in striatal cholinergic interneurons. *J Neurosci* **31**: 11133-11143.

118. Silberberg G & Bolam JP (2015) Local and afferent synaptic pathways in the striatal microcircuitry. *Curr Opin Neurobiol* **33**: 182-187.

119. Smith Y & Parent A (1986) Neuropeptide Y-immunoreactive neurons in the striatum of cat and monkey: morphological characteristics, intrinsic organization and co-localization with somatostatin. *Brain Res* **372**: 241-252.

120. Spitzer B & Haegens S (2017) Beyond the Status Quo: A Role for Beta Oscillations in Endogenous Content (Re)Activation. *eNeuro* **4**.

121. Stalnaker TA, Calhoon GG, Ogawa M, Roesch MR & Schoenbaum G (2012) Reward prediction error signaling in posterior dorsomedial striatum is action specific. *J Neurosci* **32**: 10296-10305.

122. Strecker RE & Jacobs BL (1985) Substantia nigra dopaminergic unit activity in behaving cats: effect of arousal on spontaneous discharge and sensory evoked activity. *Brain Res* **361**: 339-350.

123. Tepper JM & Bolam JP (2004) Functional diversity and specificity of neostriatal interneurons. *Curr Opin Neurobiol* **14**: 685-692.

124. Tepper JM, Koos T & Wilson CJ (2004) GABAergic microcircuits in the neostriatum. *Trends Neurosci* **27**: 662-669.

125. Tepper JM, Tecuapetla F, Koos T & Ibanez-Sandoval O (2010) Heterogeneity and diversity of striatal GABAergic interneurons. *Front Neuroanat* **4**: 150.

126. Tepper JM, Koos T, Ibanez-Sandoval O, Tecuapetla F, Faust TW & Assous M (2018) Heterogeneity and Diversity of Striatal GABAergic Interneurons: Update 2018. *Front Neuroanat* **12**: 91.

127. Thorn CA & Graybiel AM (2014) Differential entrainment and learning-related dynamics of spike and local field potential activity in the sensorimotor and associative striatum. *J Neurosci* **34**: 2845-2859.

128. Thorn CA, Atallah H, Howe M & Graybiel AM (2010) Differential dynamics of activity changes in dorsolateral and dorsomedial striatal loops during learning. *Neuron* **66**: 781-795.

129. Tollin DJ, Populin LC, Moore JM, Ruhland JL & Yin TC (2005) Sound-localization performance in the cat: the effect of restraining the head. *J Neurophysiol* **93**: 1223-1234.

130. Tort AB, Kramer MA, Thorn C, Gibson DJ, Kubota Y, Graybiel AM & Kopell NJ (2008) Dynamic cross-frequency couplings of local field potential oscillations in rat striatum and hippocampus during performance of a T-maze task. *Proc Natl Acad Sci U S A* **105**: 20517-20522.

131. van der Meer MA & Redish AD (2009) Low and High Gamma Oscillations in Rat Ventral Striatum have Distinct Relationships to Behavior, Reward, and Spiking Activity on a Learned Spatial Decision Task. *Front Integr Neurosci* **3**: 9.

132. van Vugt MK, Schulze-Bonhage A, Litt B, Brandt A & Kahana MJ (2010) Hippocampal gamma oscillations increase with memory load. *J Neurosci* **30**: 2694-2699.

133. VanRullen R (2016) Perceptual Cycles. *Trends Cogn Sci* **20**: 723-735.

134. Velly LJ, Rey MF, Bruder NJ, Gouvitsos FA, Witjas T, Regis JM, Peragut JC & Gouin FM (2007) Differential dynamic of action on cortical and subcortical structures of anesthetic agents during induction of anesthesia. *Anesthesiology* **107**: 202-212.

135. Villeneuve MY & Casanova C (2003) On the use of isoflurane versus halothane in the study of visual response properties of single cells in the primary visual cortex. *J Neurosci Methods* **129**: 19-31.

136. Vincent SR, Staines WA & Fibiger HC (1983) Histochemical demonstration of separate populations of somatostatin and cholinergic neurons in the rat striatum. *Neurosci Lett* **35**: 111-114.

137. Williams ZM & Eskandar EN (2006) Selective enhancement of associative learning by microstimulation of the anterior caudate. *Nat Neurosci* **9**: 562-568.

138. Wilson CJ (1993) The generation of natural firing patterns in neostriatal neurons. *Prog Brain Res* **99**: 277-297.

139. Wilson CJ & Groves PM (1981) Spontaneous firing patterns of identified spiny neurons in the rat neostriatum. *Brain Res* **220**: 67-80.

140. Wilson CJ, Chang HT & Kitai ST (1990) Firing patterns and synaptic potentials of identified giant aspiny interneurons in the rat neostriatum. *J Neurosci* **10**: 508-519.

141. Wise SP, Murray EA & Gerfen CR (1996) The frontal cortex-basal ganglia system in primates. *Crit Rev Neurobiol* **10**: 317-356.

142. Worden MS, Foxe JJ, Wang N & Simpson GV (2000) Anticipatory biasing of visuospatial attention indexed by retinotopically specific alpha-band electroencephalography increases over occipital cortex. *J Neurosci* **20**: RC63.

143. Wurtz RH (1969) Visual receptive fields of striate cortex neurons in awake monkeys. *J Neurophysiol* **32**: 727-742.

144. Yamada K, Takahashi S, Karube F, Fujiyama F, Kobayashi K, Nishi A & Momiyama T (2016) Neuronal circuits and physiological roles of the basal ganglia in terms of transmitters, receptors and related disorders. *J Physiol Sci* **66**: 435-446.

145. Yarom O & Cohen D (2011) Putative cholinergic interneurons in the ventral and dorsal regions of the striatum have distinct roles in a two choice alternative association task. *Front Syst Neurosci* **5**: 36.

146. Yin HH & Knowlton BJ (2006) The role of the basal ganglia in habit formation. *Nat Rev Neurosci* **7**: 464-476.

Co-author certification

I, myself as a corresponding author of the following publication(s) declare that the authors have no conflict of interest, and Diána Nyujtó Ph.D. candidate had significant contribution to the jointly published research(es). The results discussed in her thesis were not used and not intended to be used in any other qualification process for obtaining a PhD degree.

06.12.2023

..... **.....**

Date **Corr. Author**

The publication relevant to the applicant's thesis:

Barkoczi B, Nagypal T, Nyujto D, Katona X, Eordegh G, Bodosi B, Benedek G, Braunitzer G, Nagy A. Background activity and visual responsiveness of caudate nucleus neurons in halothane anesthetized and in awake, behaving cats, Neuroscience 356 (2017) 182-192

I. Barkoczi B, Nagypal T, **Nyujtó D**, Katona X, Eordegh G, Bodosi B, Benedek G, Braunitzer G, Nagy A Background activity and visual responsiveness of caudate nucleus neurons in halothane anesthetized and in awake, behaving cats, Neuroscience 356 (2017) 182-192
IF: 3.382

Neuroscience 356 (2017) 182–192

BACKGROUND ACTIVITY AND VISUAL RESPONSIVENESS OF CAUDATE NUCLEUS NEURONS IN HALOTHANE ANESTHETIZED AND IN AWAKE, BEHAVING CATS

BALÁZS BARKÓCZI, TAMÁS NAGYPÁL, DIÁNA NYUJTÓ, XÉNIA KATONA, GABRIELLA EÖRDEGH, BALÁZS BODOSI, GYÖRGY BENEDEK, GÁBOR BRAUNITZER AND ATTILA NAGY*

Department of Physiology, Faculty of Medicine, University of Szeged, Dóm tér 10, Szeged H-6720, Hungary

Abstract—This study focuses on the important question whether brain activity recorded from anesthetized, paralyzed animals is comparable to that recorded from awake, behaving ones. We compared neuronal activity recorded from the caudate nucleus (CN) of two halothane-anesthetized, paralyzed and two awake, behaving cats. In both models, extracellular recordings were made from the CN during static and dynamic visual stimulation. The anesthesia was maintained during the recordings by a gaseous mixture of air and halothane (1.0%). The behaving animals were trained to perform a visual fixation task. Based on their electrophysiological properties, the recorded CN neurons were separated into three different classes: phasically active (PANs), high firing (HFNs), and tonically active (TANs) neurons. Halothane anesthesia significantly decreased the background activity of the CN neurons in all three classes. The anesthesia had the most remarkable suppressive effect on PANs, where the background activity was consistently under 1 spike/s. The analysis of these responses was almost impossible due to the extremely low activity. The evoked responses during both static and dynamic visual stimulation were obvious in the behaving cats. On the other hand, only weak visual responses were found in some neurons of halothane anesthetized cats. These results show that halothane gas anesthesia has a marked suppressive effect on the feline CN. We suggest that for the purposes of the visual and related multisensory/sensorimotor electrophysiological exploration of the CN, behaving animal models are preferable over anesthetized ones.

Key words: caudate nucleus, visual stimulation, halothane anesthetized cats, behaving cats, neuron classification.

INTRODUCTION

The caudate nucleus (CN), one of the input structures of the basal ganglia, is strongly involved in sensorimotor functions through cortical and subcortical sensorimotor loops in the mammalian brain (McHaffie et al., 2005). Not surprisingly, the CN neurons are sensitive to both static and dynamic visual stimuli (Rolls et al., 1983; Strecker et al., 1985; Hikosaka et al., 1989; Chudler et al., 1995; Nagy et al., 2003; Nagy et al., 2008; Gombkoto et al., 2011; Rokszin et al., 2011; Vicente et al., 2012; Nagypal et al., 2015). Thus, the CN seems to belong to those brain structures that have to capacity to sample and evaluate a wide variety of changes in the visual environment.

The domestic cat is a classical mammalian model organism in visual neurophysiology and neuroanatomy. An aspect common to all visual electrophysiological experiments is the need to control for eye movements. This is critical, on the one hand because the spatial position of the visual stimulus has to overlap with the receptive field of the investigated neuron and, on the other hand, visual responses need to be separated from oculomotor activity. The latter is of particular importance here because neurons in the ascending tectofugal visual system, which relay visual information to the CN, also exhibit oculomotor activity (Hikosaka et al., 2000; Munoz and Fecteau, 2002). There are two possible ways to control for the effects of eye movements. The first is to use anesthetized and paralyzed animals, and the second is to train behaving animals to restrict eye movements. Anesthesia, combined with muscle paralysis is a very effective way of stabilizing the eye and thus the location of retinal stimulation. However, this does not allow long-term data collection, and it increases the number of animals that have to be sacrificed. In addition, the anesthetics can influence the neural activity. Although earlier findings suggested that anesthesia and paralysis have only a minor effect on the background activity, visual responsiveness and receptive field structure of cortical neurons (Wurtz, 1969), anesthetics do not necessarily have the same effect in the cortex as in the deeper brain structures (Velly et al., 2007). Furthermore, it has been reported that the basal ganglia are extremely sensitive to anesthesia (Kaisti et al., 2003; Franks and Zecharia, 2011). In an early work in halothane-anesthetized cats, only a small proportion of CN cells were found to show spontaneous activity (Ben-Ari and Kelly, 1976). In an effort to reduce the number of sacrificed animals, and also to eliminate the potentially confounding effects of anes-

*Corresponding author. Address: Department of Physiology, University of Szeged, Dóm tér 10., POB 427, H-6720 Szeged, Hungary. Fax: +36-62-545842.
E-mail address: nagy.attila.1@med.u-szeged.hu (A. Nagy).

Abbreviations: CN, caudate nucleus; HFN, high firing neuron; ISI, interspike interval; MAC, minimum alveolar anesthetic concentration; PAN, phasically active neuron; propISI > 2 sec, the ratio of the interspike intervals longer than 2 s; PSTH, peristimulus time histogram; SD, standard deviation; TAN, tonically active neuron.

http://dx.doi.org/10.1016/j.neuroscience.2017.05.028
0306-4522/

thetics, electrophysiology has gradually turned toward the use of awake, behaving animals in the last few decades. This tendency has been less marked in visual electrophysiology, because of the long training periods. In such a training period, the animals learn to keep fixation so that the effects of the eye movements can be eliminated, or at least reduced to the minimum (Robinson, 1963; Fuchs and Robinson, 1966; Judge et al., 1980). In our experience, the training and preparation of a single cat is often a challenging process that may take up to 9 months (Nagypal et al., 2014). This naturally raises the question as to whether the costs and benefits are in equilibrium. Assessing the effects of halothane on neural activity in the CN is important not only for the interpretation and re-evaluation of already existing results, but also for weighing the costs and benefits of utilizing awake, behaving animals in future studies.

EXPERIMENTAL PROCEDURES

Two awake, behaving and another two halothane-anesthetized, paralyzed, adult domestic cats were used for the experiments, each weighing between 2.5 and 4 kg. Both cats in the chronic (behaving) model were female, and recordings were made between the ages of one and four years. One animal in the anesthetized model was a female and the other was a male, aged two and three years, respectively. Experiments carried out with the anesthetized model lasted for five days.

All experimental procedures were carried out to minimize the number and the discomfort of animals involved, and followed the European Communities Council Directive of 24 November 1986 (86 609 EEC) and the US National Research Council's Guide to the care and Use of Laboratory Animals (National Research Council (U.S.). Committee for the Update of the Guide for the Care and Use of Laboratory Animals et al., 2011). The experimental protocol was approved by the Ethics Committee for Animal Research at the University of Szeged.

Animal preparation and surgery

All animals were initially anesthetized with ketamine hydrochloride (Calypsol (Gedeon Richter), 30 mg/kg i.m.). To reduce salivation and bronchial secretion, a subcutaneous injection of 0.2 ml 0.1% atropine sulfate was administered preoperatively. All wound edges and pressure points were treated generously with local anesthetic (1%, procaine hydrochloride). During the whole surgery for both experimental models, and during the recording sessions of anesthetized animals a tracheal tube was used for the delivery of gas anesthetics. The anesthetized animals were artificially ventilated with 1.6% halothane during surgery, which was reduced to 1.0% during the recording sessions. In the animals prepared for the awake recordings, the anesthesia was maintained by 1.0% isoflurane. The depth of the anesthesia was monitored by continuously checking the end-tidal anesthetic concentration and heart rate. The minimum alveolar anesthetic concentration (MAC) values calculated from the end-tidal anesthetic readings were kept in the range recommended by Villeneuve and Casanova (Villeneuve and Casanova, 2003). The end-tidal halothane and isoflurane concentration, MAC values and the peak expired CO_2 concentrations were monitored with a capnometer (Capnomac Ultima, Datex-Ohmeda, ICN). The peak expired CO_2 concentration was kept within the range 3.8–4.2% by the adjustment of the respiratory rate or volume via the ventilator and trachea-tube system, while the MAC values were set by the adjustment of the gas anesthetic evaporation rate. The body temperature of the animal was maintained at 37 °C by a computer-controlled, warm water heating blanket. Craniotomy was performed with a dental drill to allow a vertical approach to the target structures.

In the case of the anesthetized animals, both the femoral vein and the trachea were cannulated, and the animals were placed in a stereotaxic headholder. Throughout the surgery the anesthesia was continued with halothane (1.6%) in air. The animals were immobilized with an initial 2-ml intravenous bolus of gallamine triethiodide (Flaxedil, 20 mg/kg), and artificial ventilation was introduced. The dura mater was preserved, and the skull hole was covered with a 4% solution of 38 °C agar dissolved in Ringer's solution. During the recording sessions, a mixture containing gallamine triethiodide (8 mg/kg/h), glucose (10 mg/kg/h) and dextran (50 mg/kg/h) in Ringer lactate solution was infused systemically and continuously at a rate of 4 ml/h. The eye contralateral to the cortical recording site was treated locally with atropine sulfate (1–2 drops, 0.1%) and phenylephrine hydrochloride (1–2 drops, 10%) to dilate the pupils and block accommodation and to retract the nictitating membranes, respectively. In addition, a +2 diopter contact lens was applied. The ipsilateral eye was covered during the recordings with an opaque gauze pad. In order to minimize the effects of anesthesia during the recordings, the halothane concentration was reduced to 1.0%. Recordings were performed between the Horsley-Clarke coordinates anterior 12–16 and lateral 4–6.5 mm, at stereotaxic depths between 13 and 19 mm. The recordings were performed with tungsten microelectrodes (A-M Systems, Inc., USA) with an impedance of 2–4 MΩ.

The surgical preparation of the cats for the behaving experiments started with the insertion of a cannula in the femoral vein and continued with the intubation of the trachea. Then the animals were placed in a stereotaxic headholder. Throughout the surgery, the anesthesia was maintained with 1.6% halothane in a 2:1 mixture of N_2O and oxygen. Surgical procedures were carried out under aseptic conditions. Before the surgical procedure, a preventive dose of antibiotic was given (1000 mg ceftriaxon, i.m., Rocephin 500 mg (Roche)). A reclosable plastic recording chamber (20 mm in diameter) was installed on the skull to protect the microdrive system and extracellular electrodes from damage and pollution. Following this, eight parylene

isolated platinum-iridium wire-electrodes (diameter: 25 μm) were implanted in the CN in the first cat and eight formvar insulated Nickel-Chrome wire-electrodes (diameter: 50 μm) in the CN of the second cat. In the case of the first cat an adjustable microdrive system was applied (a modified Harper-McGinty microdrive, see McKown and Schadt (McKown and Schadt, 2006), and a modified Korshunov microdrive was used for the second animal, see Korshunov, (Korshunov, 1995). The implantation of the electrodes was done according to the Horsley-Clarke coordinates (anterior 12–14 mm, lateral 5–6.5 mm at stereotaxic depths between 13–19 mm). In order to monitor the eye movements of the animals, a scleral search coil was implanted into one eye. Although this method was originally developed for primates (Robinson, 1963; Fuchs and Robinson, 1966; Judge et al., 1980), it was later adapted to cats (Pigarev and Rodionova, 1998; Populin and Yin, 1998, 2002; Huxlin and Pasternak, 2004; Tollin et al., 2005; Pigarev and Levichkina, 2011). The scleral coils were made of insulated medical stainless steel hook-up wire (Cooner wire, Owensmouth, CA, USA). The coil was looped 3 times at a diameter of 22 mm.

Additionally, a stainless steel headholder was cemented to the skull for head fixation purposes. On the first five postoperative days, ceftriaxone antibiotic was administered intramuscularly (Rocephine, 50 mg/kg). Nalbuphin (0,25 mg/kg) and 40 ml Ringer's lactate solution were administered until the seventh postoperative day.

Behavioral training of the awake, behaving animals before the recordings

The detailed description of the implantation and the behavioral training of the animals can be found in our recent methodological paper (Nagypal et al., 2014). Therefore we give only a brief summary here. The duration of the behavioral training before the start of the recordings was a maximum of 9 months, including 3 months of pre- surgery training and 6 months of post-surgery training in each cat. The experimental animals were selected with care, and then they were adapted to the laboratory environment. Animals with intact vision and hearing were selected for the experiments. Outstanding teachability, cooperative behavior and easy adaptation to the laboratory environment were also eligibility criteria. Food deprivation was used on weekdays, and the animals received food only in the laboratory (150–250 g/day). During the weekends, the animals had access to food in their home cage *ad libitum*. Water was always available *ad libitum* in the animals' home cage. The cats were carefully wrapped in a canvas harness, which leaves the head, tail and legs free, and were suspended in the experimental stand. In the following step, the head of the suspended cat was fixed to the stereotaxic frame by the implanted steel headholder. Electromagnetic field was generated by metal coils installed into the wall of the experimental stand in order to record eye movements. The next step of the behavioral training focused on the control of the eye movements. A green fixation point was presented in the center of the CRT monitor, in a square acceptance window of variable size. The size of the fixation point was 0.8 deg in diameter. At the beginning of the training session, the gaze of the animal was directed at the middle of the CRT monitor. During the fixation training, the fixation time was gradually increased from 100 ms to 1500 ms. The size of the initial fixation window was 10 × 10 deg. During the training period, it was reduced to 5 × 5 deg in 2.5 deg steps. If the cat held fixation within the acceptance window for a pre-set fixation time, it was rewarded with pulpy food. Sessions (either training or recording) lasted 1 to 2 h a day, four to five times a week. Neither eye was covered during the recording sessions.

Visual stimulation

For the experiments conducted with anesthetized animals, stationary random dot patterns and random dot kinematograms were generated with a custom made script in Matlab (MathWorks Inc., Natick, MA), using the Psychophysics Toolbox extension (Brainard, 1997; Pelli, 1997), and presented on an 18-inch computer monitor (refresh rate: 100 Hz) placed 57 cm in front of the animal. The steady-state luminance of the stationary dots was 10 cd/m^2, while the background luminance was 2 cd/m^2. The dynamic stimuli contained 200 white dots, which moved at 5 deg/s. The extension of the stimulation screen was 40.5 deg by 30.5 deg. The diameter of each dot was 0.15 deg in diameter. In the stimulation protocol, a single trial consisted of three parts: first, a blank, black screen was presented to obtain background activity without visual stimulation; then a random dot pattern (static stimulus) was presented; finally, the same dots started to move (dynamic stimulus) in random directions at a speed of 5 deg/s. The lengths of these phases were as follows: 1500-ms intertrial interval with black screen, 1500-ms static stimulation, 1500-ms dynamic stimulation. The stimulus sequence was repeated 500 times, thus the duration of a recording period was approximately 40 min recorded from the same electrode position.

Similarly, in the experiments with behaving cats two sorts of visual stimuli were applied: first a static random dot pattern (static), which was followed by a center in or center out flow field (dynamic) stimulus. For visual stimulation and the presentation of the fixation point a standard 18- inch CRT monitor (refresh rate: 100 Hz) was placed in front of the animal, at a distance of 57 cm. The size of the stimulation screen was 40.5 deg by 30.5 deg. The size of each dot in both the static and the dynamic stimuli was 0.1 deg in diameter. The steady-state luminance of the stationary dots was 10 cd/m^2, while the background luminance was 2 cd/m^2. The speed of the dots in the flow field increased from 0 to 7 deg/s toward the periphery of the stimulation screen. The stimuli were generated using a custom made script prepared in the Psychophysics Toolbox of Matlab. During the recordings, the effect of the eye movements on the neuronal activity had to be controlled for, so the cats were trained to perform fixation during the stimulation. For this, a fixation point was presented in the center of the CRT monitor. The size of the fixation point was 0.8 deg in diameter. The animal had to look at

the fixation point and keep its gaze within a square fixation acceptance window during the trials of the visual fixation task. The size of the acceptance window was 5 × 5 deg. Any single trial consisted of four parts. The first part was the intertrial interval itself (black screen) in order to record the background activity. It was followed by a fixation phase, in which only the green fixation dot was presented on the monitor. In the last two phases, beside the fixation point static, and later dynamic visual stimulation was presented. The lengths of the epochs were as follows: 5000–10,000-ms black screen (intertrial interval), 500–1000-ms fixation phase with a green fixation point presented alone on the monitor, 200–1000-ms static and 1000-ms dynamic visual stimulation. If the cat managed to maintain fixation throughout all the stimulation phases of a single trial, the trial was accepted. To minimize the influence of eye movements on neuronal activity, the trial was aborted immediately if the animal failed to fixate (i.e. the gaze of the animal moved out of the acceptance window). Such trials were not accepted, neither was reward given to the animals in these cases.

Recording and data analysis

Amplified neuronal activities from the anesthetized cats were recorded at 20-kHz sampling rate and stored for off-line analysis (Datawave SciWorks, Version 5.0, DataWave Technologies Corporation, USA). In the case of behaving cats, eye movements were monitored and recorded with a search coil system (DNI Instruments, Newark, DE, USA). The recording of the eye movements, stimulus presentation, reward delivery, and data collection were coordinated by a custom made software via a 16 channels National Instruments data acquisition card.

The first step of the data analysis was spike sorting. The channels were band-pass filtered (300 to 3000 Hz), an amplitude threshold was calculated, and the extracted spikes were clustered automatically based on principal component analysis in NeuroScope, NDManager, KlustaKwik and Klusters, under manual control (Harris et al., 2000; Hazan et al., 2006). The proper discrimination of simultaneously recorded neurons (i.e. spike waveforms) was confirmed by the autocorrelogram of spike-trains and overlaid spike shapes. The dip of the autocorrelograms at 0 timelag indicated that the spike separation was proper. The clusterisation was followed by a neuron-type characterization based on the shape of the autocorrelogram (time resolutions 100 ms and 1000 ms), the level of background discharge rate and propISI > 2sec, defined as the proportion of the summed values over 2 s divided by the total session time (Schmitzer-Torbert and Redish, 2008; Nagypal et al., 2015). Based on these three parameters, the neurons were divided in three groups: phasically active neurons (PANs), high firing neurons (HFNs) and tonically active neurons (TANs), (Nagypal et al., 2015). From the temporal distribution of the action potentials, peristimulus time histograms (PSTHs) were created. The background discharge rate of each neuron was calculated from their activity in the intertrial intervals. Firing rates during static and dynamic stimulation were compared to the background activity with the Wilcoxon matched pairs test. We considered the neuronal activity as a response if it was significantly different ($p < 0.05$) from the mean background activity and if the mean net change was at least 0.1-fold (10%) compared to the background activity. This latter criterion was added to correct for an excessive experimentwise error rate in the statistical testing and try to avoid false positive responses.

To eliminate potential distortions due to the high prevalence of CN neurons with extremely low background activities, the visual responses of only those CN neurons were included in the analysis whose background activity was at least 1 spike/s. A question that may arise is why we compared the visual responses to the background activities and not to the fixation activities in behaving cats. One explanation of this is that there was no fixation phase in the stimulation protocol of anesthetized cats at all. The other is the low amount of fixation sensitive units in our neuronal population. Of the 209 CN neurons with background activity higher than 1 Hz, only 53 (25%) showed significantly different activity from the background during the fixation phase of the paradigm.

Activities were calculated separately for the different stimulation phases. The evoked activities were calculated by averaging all activities in a given stimulation phase. The last 1 s of the intertrial intervals was considered as background activity, against which the evoked activities were compared. Gross activities show the total mean firing rate during the different stages of stimulation (static or dynamic). The net discharge rates were calculated by subtracting the background activity from the gross activity. The presentation of both gross and net activities is necessary because gross activities provide information about the overall activity of the neurons and the ratio between the gross and net activities demonstrates magnitude of visually evoked responses.

As the Shapiro–Wilk test indicated that the distribution of the studied variables was non-normal, nonparametric statistical tests were used. The background activities recorded from anesthetized and behaving cats were compared at the population level with the Mann–Whitney rank sum test. All statistical analyses were performed in Matlab (MathWorks Inc., Version 8.3, Natick, MA) and STATISTICA for Windows (StatSoft Inc., Version 12.0, Tulsa, OK) softwares.

RESULTS

Altogether 206 neurons were recorded from the CN of the two anesthetized cats (83 from the first and 123 from the second cat). Three hundred and forty-four neurons were recorded from the CN of the two awake, behaving cats (285 from the first and 59 from the second cat). For the purposes of the analysis, the recorded trials were divided into three epochs: static visual stimulation, dynamic visual stimulation and intertrial interval without any visual stimulation. Background activity was calculated from the intertrial intervals and the stimulated

Table 1. Descriptive statistics of background and visually evoked activities of CN neurons from awake, behaving and anesthetized animals

	Awake						Anesthetized						
	N	Mean	Median	SD	Min	Max	N	Mean	Median	SD	Min	Max	
All	344	5.19	2.13	6.87	0.01	37.91	206	1.58	0.45	2.29	0.01	13.86	Background
≥1 Hz	209	8.32	6.21	7.27	1.02	37.91	81	3.60	2.75	2.56	1.04	13.86	
HFNs	88	14.60	12.87	6.96	4.67	37.91	85	2.56	1.70	2.53	0.10	13.86	
PANs	219	1.39	0.60	1.89	0.01	15.42	73	0.14	0.11	0.12	0.01	0.78	
TANs	28	5.35	5.82	2.53	1.26	10.61	43	2.21	1.37	2.57	0.13	13.14	
≥1 Hz HFNs	88	14.60	12.87	6.96	4.67	37.91	56	3.64	3.10	2.50	1.04	13.86	
≥1 Hz PANs	85	3.03	2.44	2.17	1.02	15.42	0	–	–	–	–	–	
≥1 Hz TANs	28	5.35	5.82	2.53	1.26	10.61	25	3.49	2.63	2.72	1.04	13.14	
≥1 Hz ≥10% Increase Gross	51	12.86	8.15	12.17	1.46	43.86	3	3.23	2.03	2.88	1.15	6.51	Static
≥1 Hz ≥10% Increase Net		4.33	2.60	4.73	0.34	19.52		0.47	0.46	0.37	0.11	0.85	
≥1 Hz ≥10% Decrease Gross	32	4.92	3.69	4.96	0.52	21.52	2	4.85	4.85	1.91	3.50	6.20	
≥1 Hz ≥10% Decrease Net		−2.37	−1.09	3.24	−15.91	−0.20		−1.85	−1.85	0.37	−2.11	−1.59	
≥1 Hz No change Gross	126	10.22	8.11	7.89	1.00	41.37	76	3.58	2.77	2.60	1.05	14.23	
≥1 Hz No change Net		1.73	0.99	2.86	−3.20	13.38		0.03	0.01	0.16	−0.32	1.09	
≥1 Hz ≥10% Increase Gross	22	14.11	12.10	10.98	1.52	33.32	0	–	–	–	–	–	Dynamic
≥1 Hz ≥10% Increase Net		3.82	2.53	3.66	0.48	13.53		–	–	–	–	–	
≥1 Hz ≥10% Decrease Gross	3	5.86	4.85	4.86	1.58	11.15	10	2.78	2.06	1.88	1.06	6.93	
≥1 Hz ≥10% Decrease Net		−0.89	−0.96	0.40	−1.26	−0.45		−0.68	−0.44	0.50	−1.62	−0.26	
≥1 Hz No change Gross	184	8.66	6.13	7.86	0.70	44.61	71	3.63	2.90	2.58	1.03	13.20	
≥1 Hz No change Net		0.55	0.27	1.46	−2.65	8.05		0.02	0.03	0.17	−0.73	0.46	

Not only the background activities, but the evoked responses and the number of visually responsive CN neurons were smaller in case of anesthetized animals. PAN – phasically active neuron, HFN – high firing neuron, TAN – tonically active neuron. The most noteworthy finding is that no PANs with a background activity higher than 1Hz were detected in the group of anesthetized animals. There was also no such neuron in the anesthetized recordings, evoked response of which increased more than 10% during dynamic visual stimulation. All: all neurons; ≥1Hz: neurons with a background activity equal to or higher than 1 spike/s; ≥10%: evoked responses with a change equal to or higher than 10 percent of the background activity; Increase, Decrease, No change: indicates how the evoked responses changed upon stimulation; Gross, Net: gross and net activities. Gross activity is the averaged firing frequency during the entire stimulation session, while net activity is calculated by subtracting the evoked gross activity from the background firing frequency; Background, Static, Dynamic: trial phases; N: sample size. Discharge rates are in spikes/s.

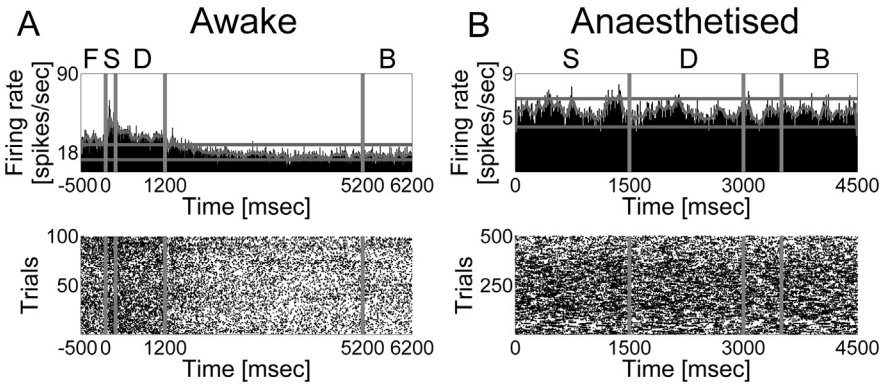

Fig. 1. Peristimulus time histograms and raster plots from awake (A) and anesthetized (B) models. Each panel of the figure contains a PSTH (top) and a raster plot (bottom) to represent the activity of a neuron. Vertical gray lines denote the boundaries between the different phases of the stimulation protocol. In the case of behaving cats the paradigm contained the following phases: fixation phase (F; −500 to 0 ms), static visual stimulation (S; 0 to 200 ms), dynamic visual stimulation (D; 200 to 1200 ms), reward phase and the following intertrial interval (from 1200 ms to 6200 ms). Background firing rate was calculated from the last second of intertrial interval (B; 5200 to 6200 ms). In the case of anesthetized cats the stimulation protocol contained the following phases: static visual stimulation (S; 0 to 1500 ms), dynamic visual stimulation (D; 1500 to 3000 ms), intertrial interval (3000 to 4500 ms). The last second of PSTH corresponds to the background discharge rate (B; 3500 to 4500 ms). Trial sessions are also highlighted with capital letters on the top of the PSTH graphs. The abscissa denotes the time in milliseconds. The ordinate denotes the number of trials (bottom) and the activity of the neuron in spikes per seconds (top). The lower value on the ordinate of PSTHs indicates the average background discharge rate during the whole recording, while the continuous gray curve is a smoothed curve of the activity, and the horizontal gray lines indicate ±2 SD of the average background discharge rate. Note that the scale of the ordinate on Part A is much wider than on Part B thus the activities recorded from behaving cat are much higher than those recorded from the anesthetized animals.

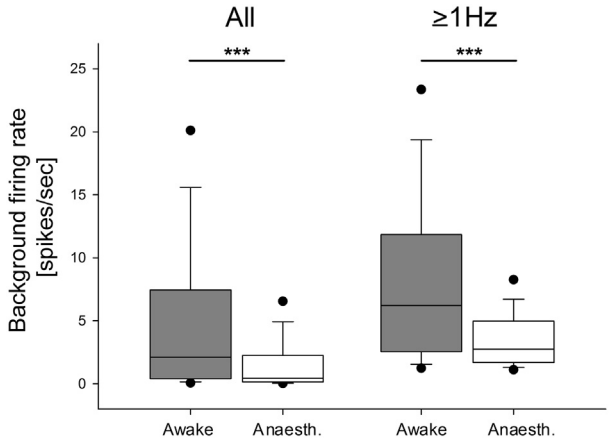

Fig. 2. Neuronal activity in the CN of awake and anesthetized cats. The box plots on the left side show the background discharge rates of all of the analyzed CN neurons (All). The two box plots on the right show the background activities of neurons with a discharge rate higher than 1 spike/s (≥1 Hz). The gray boxes show the results from behaving cats while the white boxes contains the results from anesthetized cats. The lower margin of the boxes indicates the 25th percentile, the line within the boxes marks the median, and the upper margin of the box indicates the 75th percentile. Whiskers (error bars) above and below the box indicate the 90th and 10th percentiles. The outliers (dots) represent the 95th and 5th percentiles. All of the presented differences are statistically significant ($p < 0.001$).

activities were compared to this activity. The summary of the detailed descriptive statistics of background and visually evoked activities of CN neurons from awake, behaving and anesthetized animals can be seen in Table 1.

Fig. 1 shows the peristimulus time histograms and raster plots of two CN neurons. The first neuron was recorded from an awake (Part A) and the second (Part B) from an anesthetized cat. Not only the background activity, but the evoked gross activities are higher in case of a neuron recorded from behaving animal.

Background activities

The background activity of the CN neurons from awake, behaving animals is significantly higher (Mann–Whitney U, $p < 0.001$) than that of the CN neurons recorded from anesthetized cats (Fig. 2 All; see descriptive statistical data in Table 1). To eliminate potential distortions due to the high prevalence of CN neurons with extremely low background activity, a separate analysis was performed after the exclusion of neurons with a background activity under 1 spike/s. In this way, 135 neurons from the awake (39.2%) and 125 neurons (60.7%) from the anesthetized model were excluded. The remarkably higher prevalence of background activities under 1 Hz in the anesthetized model were obvious already at this point. The comparison of the background activities higher than 1 Hz (Fig. 2 >1 Hz neurons) revealed significantly higher activity of CN neurons recorded from the behaving model (Mann–Whitney U, $p < 0.001$; see descriptive statistical data in Table 1).

Responses to static visual stimulation

The proportion of neurons responsive to static stimulation was much higher in the behaving cats. The gross and net activity increments during static stimulation were notably stronger in the awake, behaving animals than in the anesthetized ones (see descriptive statistical data in Table 1).

The magnitude of the net decrements in activity during static visual stimulation were also more obvious in the behaving model (see descriptive statistical data in Table 1).

Responses to dynamic visual stimulation

Similarly to the responsiveness to static stimulation, the proportion of neurons responsive to dynamic stimulation was higher in the behaving cats. Activity increments were evident in the behaving animals (see descriptive statistical data in Table 1), however, no such responses were observed in the anesthetized animals at all. The

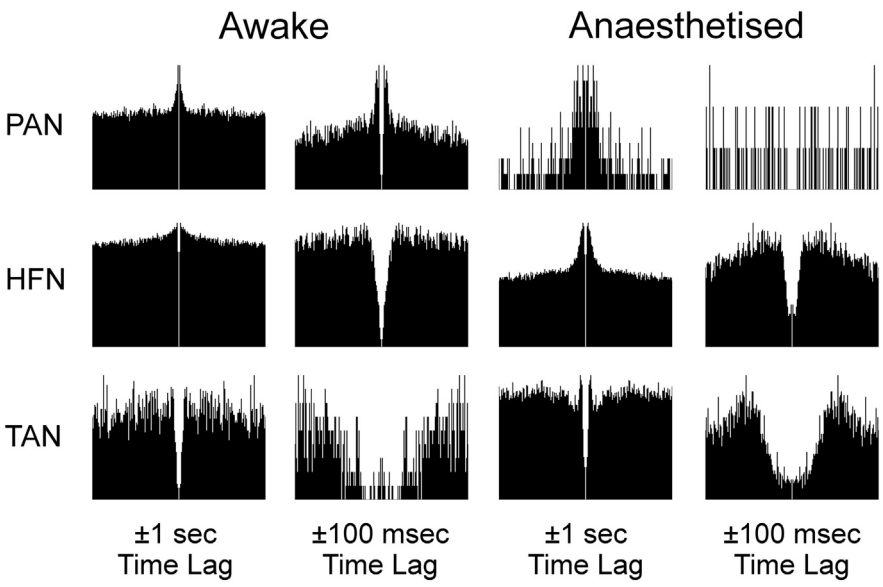

Fig. 3. Representative autocorrelograms of the CN neurons. CN neurons were classified on the basis of the shape of their autocorrelograms (at 100 ms and 1 s time resolutions), propISI > 2sec and the background discharge rate in three big groups as follows: PAN – phasically active neuron, HFN – high firing neuron, TAN – tonically active neuron. Neurons belonging to each group have characteristic autocorrelogram. PANs are usually characterized by peaky autocorrelogram and low background discharge rates, HFNs have autocorrelograms with a blunt peak and TANs are characterized by a deep gap in the autocorrelogram. The six representative autocorrelograms on the left side are from awake animals, while the six illustrative panels on the right side are from anesthetized ones, each of them at two different time resolutions.

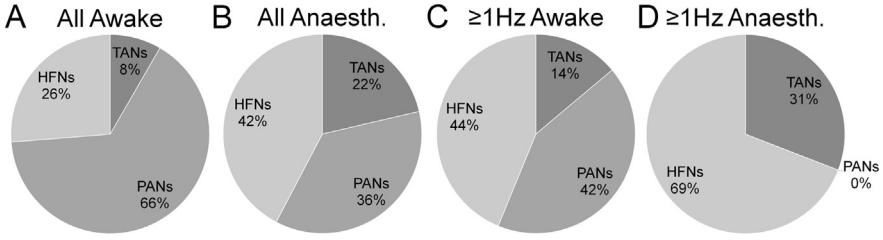

Fig. 4. Pie charts of the distribution of neuron types. Pie charts demonstrate the distribution of neuron types (PAN, HFN and TAN) in the CN in awake (A) and in anesthetized cats (B). The PAN, HFN, TAN labels indicate the different neuronal types, as follows PAN – phasically active neuron, HFN – high firing neuron, TAN – tonically active neuron. Panels C and D characterize the same distribution of CN neurons with a background discharge rate over 1 Hz. Note that PANs with a background activity over 1 spike/s disappeared during halothane anesthesia.

magnitude of the net decrements in activity during dynamic visual stimulation did not seem to differ by paradigm. It must be mentioned, though, that the sample sizes were quite low (see descriptive statistical data in Table 1).

Electrophysiological groups in the CN – Phasically active neurons are silent in anesthesia

Based on their discharge properties (see Recording and Data Analysis) we could classify the recorded CN neurons in three groups (Fig. 3): phasically active neurons (PANs), high firing neurons (HFNs), tonically active neurons (TANs).

In the CN of the awake, behaving animals the vast majority of the cells were PANs (N = 219, 63.7%). Much smaller numbers of HFNs (N = 88, 25.6%) and TANs (N = 28, 8.1%) were found. Surprisingly, in the anesthetized animals the HFN group was the most numerous (N = 85, 41.3%). Fewer PANs (N = 73, 35.4%) and even fewer TANs (N = 43, 20.9%) were found (Fig. 4 A, B). A few of the recorded CN neurons could not be categorized this way. This uncategorized group contained 9 units (2.6%) from the awake and 5 units (2.4%) from anesthetized animals.

Fig. 5 shows the background activities of the different neuron groups in behaving and anesthetized cats. Note that these activities were much lower in all groups recorded from anesthetized cats (see descriptive statistical data in Table 1). The statistical analysis revealed that background activities of all groups were significantly higher in the awake, behaving animals (Mann–Whitney U, $p < 0.001$).

Of the 135 neurons excluded from the analysis in the awake model because of their low background activity, only one was an uncategorized unit, and the others were all PANs (N = 134). On the other hand, the 125 units, which were excluded in the anesthetized model, showed a more varied distribution: PAN (N = 73); uncategorized (N = 5); HFN (N = 29); TAN (N = 18). The prevalence of the neurons belonging to the different electrophysiological groups after the exclusion of the above units can be seen in Fig. 4C, D. It is clear that in the anesthetized model, all PANs were excluded by applying the 1 Hz cut-off criterion. The statistical analysis revealed that the background activities of the HFN and TAN groups were significantly higher in the awake, behaving animals (Mann–Whitney U, $p < 0.005$).

DISCUSSION

To our knowledge this is the first study, which compares the neuronal activities recorded from the CN in two different animal models in anesthetized, paralyzed and in awake, behaving cats. Our results clearly demonstrated that halothane anesthesia could considerably suppress the background activity and visual responses in the CN of the feline brain.

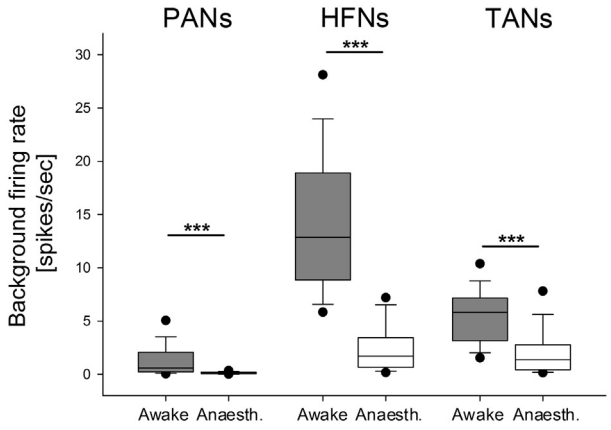

Fig. 5. Background activities of all PANs, HFNs and TANs in behaving and anesthetized cats. The background discharge rates of PANs, HFNs and TANs. The conventions are the same as in Fig. 2. Note that the background activities of each electrophysiological group were significantly higher in the behaving model ($p < 0.001$).

In the case of background discharge rates, the majority (60.7%) of the recorded CN units showed less than 1 Hz activity in the anesthetized model. This percentage was much lower in the behaving cats (39.2%). Because of the low activities, we had to exclude these units from the further analysis. Moreover, the activity changes upon the different kinds of visual stimulation were in most cases very weak in the anesthetized animals. The maximal net response was 2.1 Hz in the anesthetized animals, while it was much higher in the awake, behaving model (maximal net response 19.5 Hz). These results throw light on why it is so difficult to find any kind of activity in the CN of the anesthetized cats, not to mention proper visual responses. It is also important to see that earlier studies used simple dynamic geometric forms (spots, dots, bars) and drifting sinewave gratings (Pouderoux and Freton, 1979; Strecker et al., 1985; Nagy et al., 2003; Nagy et al., 2006; Nagy et al., 2008; Gombkoto et al., 2011), which are even more adequate visual stimuli for the CN neurons than our random dot patterns and kinematograms in the present study. According to the literature, a noteworthy proportion of the CN neurons show direction preference and spatio-temporal selectivity, however, multielectrode recordings allow the recording of several neurons simultaneously, including neurons with preference for different directions and spatio-temporal properties. The most remarkable advantage of the stimuli applied in the present study is that the effects of spatio-temporal and direction preference are minimized. Beyond the lack of halothane anesthesia and immobilization, our behaving model differed from anesthetized models also in a third way: both eyes of the animal were open during stimulation. In anesthetized models during visual stimulation the contralateral eye was opened, while the other eye was covered. Monocular stimulation is essential in anesthetized/paralyzed animal models in order to prevent binocular inhibition that results from ocular misalignment during paralysis. This monocular-binocular difference could influence the magnitude of visual responses, but such a strong difference as seen in this study is not likely to stem from this factor only. Furthermore, the difference in the background discharge rates is against this explanation. Muscle tone, arousal and goal-oriented movements can also increase the activity of the CN but these cannot be only the explanation for the stronger responsiveness of the CN neurons in the behaving model.

Fixation can also influence the neuronal activities in the central nervous system. Fixation can be considered to reflect at least some level of attention, and attention is known to influence the activity of the visually responsive parts of the mammalian brain (Rajkai et al., 2008). If we assume that anesthetics can reduce or eliminate attention, this lack of attention may be the reason for the reduction of visual responsiveness in the anesthetized cats. However, it is not likely to lead to such a strong difference as seen in this study. As stated earlier, the large majority of the analyzed CN units were not active during fixation – only one quarter of them showed significant activity changes in the fixation phase of the paradigm. It is also known that the superior colliculi, which comprise the main subcortical source of visual input to the basal ganglia, can also be suppressed during fixation (Sumner et al., 2006). The superior colliculi project to the lateral posterior-pulvinar and the lateral medial-suprageniculate nuclei complex of the thalamus, which are assumed to be the main subcortical visual inputs to the CN. While these thalamic inputs are predominantly excitatory (Hoshino et al., 1997; Hoshino et al., 2000; Hoshino et al., 2009) the lack of excitatory inputs during fixation cannot explain the increased activity in the CN in behaving animals.

In the intertrial intervals, where background discharge rates were measured, there was no fixation task, that is, the animals were allowed to perform eye movements. In these cases, because of the lack of fixation, the effects of the eye movements on the neuronal activities could also be observed. In our previous study we found no or only very weak correlation between the neuronal activities and the normalized amplitude of the eye movements in the CN. This suggests that the activity of the CN neurons in the intertrial intervals is not affected significantly by activity changes due to eye movements (Nagypal et al., 2015).

It is noteworthy to mention that the anesthetized cats were cycloplegic and the awake ones had normal pupils and lenses but in the case of anesthetized cats the visus was corrected with appropriate lenses. As the background luminance was the same for the two models and the same CRT monitor was used, these do not explain the observed difference either.

In our previous study, we managed to categorize neurons from the feline CN based on their electrophysiological properties in behaving cats (Nagypal et al., 2015). This categorization was adapted in the present study to the CN neurons recorded from anesthetized cats. Although the neuronal activities and the number of spikes are quite different in the two models, the shapes of the autocorrelograms of PANs, TANs and HFNs are basically the same, which suggests that the temporal spiking characteristics of the CN neurons are

very similar in the two models. Similarly to earlier findings (Schmitzer-Torbert and Redish, 2004; Schmitzer-Torbert and Redish, 2008; Kubota et al., 2009; Gage et al., 2010; Thorn et al., 2010; Barnes et al., 2011; Stalnaker et al., 2012), PANs, TANs and HFNs were found in both models. The ratio of uncategorizable neurons (under 3%) was also similar. Earlier studies suggested a strong correspondence between the three biggest anatomical (medium spiny, cholinergic and parvalbumin immunopositive GABAergic interneurons) and electrophysiological (PAN, TAN, HFN) groups of the CN neurons. Most probably the PAN neurons correspond to the medium spiny projection neurons, HFNs to the parvalbumin immunopositive GABAergic interneurons and the TANs to the cholinergic interneurons (Kawaguchi, 1993; Wilson, 1993; Kawaguchi et al., 1995; Mallet et al., 2005; Tepper et al., 2010). In line with the results of earlier studies in other species, the majority of the recorded CN units in the behaving model were PANs in our sample (64%). In other species, 77–97% of the striatal projection neurons belong to this presumably GABAergic cluster (Kemp and Powell, 1971; Luk and Sadikot, 2001). Similarly to earlier results, HFNs (25%) and TANs (8%) were much less prevalent in our sample (Phelps et al., 1985; Luk and Sadikot, 2001). It must be noted that PANs are often difficult to detect because of their extremely low background activity (Lau and Glimcher, 2007), which means that the sixty-four percent finding may be an underestimation due to undersampling, which, in turn, can also have an effect on the estimations of the two other groups. In contrast to these, the highest amount (41%) of the recorded CN neurons from anesthetized feline model was classified as HFN. Fewer neurons were in the PAN (35%) group and even fewer in the TAN (21%) group.

The difference between the anesthetized and behaving feline model is striking. Halothane seems to reduce the background activity of PANs so strongly that it makes a valid analysis impossible. Knowing that, it is clear why these cells are so difficult to detect and record in anesthetized models. We argue that the most important finding of the present study is that the PANs, which seem to correspond to the medium spiny projection neurons (the most prevalent neuron type in the CN), are almost silent under anesthesia, and thus these neurons cannot be investigated in anesthetized, paralyzed cats without any afferent stimulation. Furthermore, the activity of the HFNs and TANs was also strongly suppressed in the anesthetized cats, in contrast to the behaving model. In the light of these findings, it has also become clear that the neurons we reported in an earlier study of ours (Nagy et al., 2003) could not be of the medium spiny type – a question we could not agree on at that time.

To summarize our findings, we demonstrated marked and significant differences between the neuronal activities recorded from the feline CN in an anesthetized and a behaving model. The halothane gas anesthesia and the immobilization significantly suppressed the neuronal activity and the number of visually responsive neurons in the CN. Our results also show that the analysis of PANs (most probably these are the medium spiny projection CN neurons, the dominant neuronal population in the CN) is almost impossible in the anesthetized model because of their extremely low activity. It is clear that to work with behaving cats in visual electrophysiology is much more difficult than to work with anesthetized cats, mostly because of the lengthy preparatory period. However, based on the presented results we suggest that the benefits outweigh the costs, and if PANs are studied, a behaving model can almost be considered a *sine qua non* of success.

AUTHOR CONTRIBUTIONS

AN, GYB and GE designed the study; BBa, TN, DN, GE and XK performed the assessment and documented the findings; BBa, BBo, TN, DN and XK analyzed the data; AN, GB and BBa organized the study and wrote the manuscript.

Acknowledgements—The authors thank to Siposné Gabriella Dósai-Molnár, Rozalinda Pose and László Rácz for the technical assistance and to Robert Averkin for the microdrives and the wire electrodes. The authors declare no competing financial interests. This work was supported by Hungarian Brain Research Program Grant KTIA_13_NAP-A-I/15. XK was supported by the ÚNKP-16-2 New National Excellence Program of the Ministry of Human Capacities, Hungary.

REFERENCES

Barnes TD, Mao JB, Hu D, Kubota Y, Dreyer AA, Stamoulis C, Brown EN, Graybiel AM (2011) Advance cueing produces enhanced action-boundary patterns of spike activity in the sensorimotor striatum. J Neurophysiol 105:1861–1878.

Ben-Ari Y, Kelly JS (1976) Dopamine evoked inhibition of single cells of the feline putamen and basolateral amygdala. J Physiol 256:1–21.

Brainard DH (1997) The Psychophysics Toolbox. Spat Vis 10:433–436.

Chudler EH, Sugiyama K, Dong WK (1995) Multisensory convergence and integration in the neostriatum and globus pallidus of the rat. Brain Res 674:33–45.

Franks NP, Zecharia AY (2011) Sleep and general anesthesia. Can J Anaesth 58:139–148.

Fuchs AF, Robinson DA (1966) A method for measuring horizontal and vertical eye movement chronically in the monkey. J Appl Physiol 21:1068–1070.

Gage GJ, Stoetzner CR, Wiltschko AB, Berke JD (2010) Selective activation of striatal fast-spiking interneurons during choice execution. Neuron 67:466–479.

Gombkoto P, Rokszin A, Berenyi A, Braunitzer G, Utassy G, Benedek G, Nagy A (2011) Neuronal code of spatial visual information in the caudate nucleus. Neuroscience 182:225–231.

Harris KD, Henze DA, Csicsvari J, Hirase H, Buzsaki G (2000) Accuracy of tetrode spike separation as determined by simultaneous intracellular and extracellular measurements. J Neurophysiol 84:401–414.

Hazan L, Zugaro M, Buzsaki G (2006) Klusters, NeuroScope, NDManager: a free software suite for neurophysiological data processing and visualization. J Neurosci Methods 155:207–216.

Hikosaka O, Sakamoto M, Usui S (1989) Functional properties of monkey caudate neurons. II. Visual and auditory responses. J Neurophysiol 61:799–813.

Hikosaka O, Takikawa Y, Kawagoe R (2000) Role of the basal ganglia in the control of purposive saccadic eye movements. Physiol Rev 80:953–978.

Hoshino K, Eordegh G, Nagy A, Benedek G, Norita M (2009) Overlap of nigrothalamic terminals and thalamostriatal neurons in the feline lateralis medialis-suprageniculate nucleus. Acta Physiol Hung 96:203–211.

Hoshino K, Hicks TP, Hirano S, Norita M (2000) Ultrastructural organization of transmitters in the cat lateralis medialis-suprageniculate nucleus of the thalamus: an immunohistochemical study. J Comp Neurol 419:257–270.

Hoshino K, Hicks TP, Meguro R, Hirano S, Kase M, Norita M (1997) Cholinergic innervation of the lateralis medialis-suprageniculate nuclear complex (LM-Sg) of the cat's thalamus: a double labeling immunohistochemical study. Brain Res 747:151–155.

Huxlin KR, Pasternak T (2004) Training-induced recovery of visual motion perception after extrastriate cortical damage in the adult cat. Cereb Cortex 14:81–90.

Judge SJ, Richmond BJ, Chu FC (1980) Implantation of magnetic search coils for measurement of eye position: an improved method. Vision Res 20:535–538.

Kaisti KK, Langsjo JW, Aalto S, Oikonen V, Sipila H, Teras M, Hinkka S, Metsahonkala L, Scheinin H (2003) Effects of sevoflurane, propofol, and adjunct nitrous oxide on regional cerebral blood flow, oxygen consumption, and blood volume in humans. Anesthesiology 99:603–613.

Kawaguchi Y (1993) Physiological, morphological, and histochemical characterization of three classes of interneurons in rat neostriatum. J Neurosci 13:4908–4923.

Kawaguchi Y, Wilson CJ, Augood SJ, Emson PC (1995) Striatal interneurones: chemical, physiological and morphological characterization. Trends Neurosci 18:527–535.

Kemp JM, Powell TP (1971) The structure of the caudate nucleus of the cat: light and electron microscopy. Philos Trans R Soc Lond B Biol Sci 262:383–401.

Korshunov VA (1995) Miniature microdrive for extracellular recording of neuronal activity in freely moving animals. J Neurosci Methods 57:77–80.

Kubota Y, Liu J, Hu D, DeCoteau WE, Eden UT, Smith AC, Graybiel AM (2009) Stable encoding of task structure coexists with flexible coding of task events in sensorimotor striatum. J Neurophysiol 102:2142–2160.

Lau B, Glimcher PW (2007) Action and outcome encoding in the primate caudate nucleus. J Neurosci 27:14502–14514.

Luk KC, Sadikot AF (2001) GABA promotes survival but not proliferation of parvalbumin-immunoreactive interneurons in rodent neostriatum: an in vivo study with stereology. Neuroscience 104:93–103.

Mallet N, Le Moine C, Charpier S, Gonon F (2005) Feedforward inhibition of projection neurons by fast-spiking GABA interneurons in the rat striatum in vivo. J Neurosci 25:3857–3869.

McHaffie JG, Stanford TR, Stein BE, Coizet V, Redgrave P (2005) Subcortical loops through the basal ganglia. Trends Neurosci 28:401–407.

McKown MD, Schadt JC (2006) A modification of the Harper-McGinty microdrive for use in chronically prepared rabbits. J Neurosci Methods 153:239–242.

Munoz DP, Fecteau JH (2002) Vying for dominance: dynamic interactions control visual fixation and saccadic initiation in the superior colliculus. Prog Brain Res 140:3–19.

Nagy A, Eordegh G, Norita M, Benedek G (2003) Visual receptive field properties of neurons in the caudate nucleus. Eur J Neurosci 18:449–452.

Nagy A, Eordegh G, Paroczy Z, Markus Z, Benedek G (2006) Multisensory integration in the basal ganglia. Eur J Neurosci 24:917–924.

Nagy A, Paroczy Z, Markus Z, Berenyi A, Wypych M, Waleszczyk WJ, Benedek G (2008) Drifting grating stimulation reveals particular activation properties of visual neurons in the caudate nucleus. Eur J Neurosci 27:1801–1808.

Nagypal T, Gombkoto P, Barkoczi B, Benedek G, Nagy A (2015) Activity of caudate nucleus neurons in a visual fixation paradigm in behaving cats. PLoS One 10:e0142526.

Nagypal T, Gombkoto P, Utassy G, Averkin RG, Benedek G, Nagy A (2014) A new, behaving, head restrained, eye movement-controlled feline model for chronic visual electrophysiological recordings. J Neurosci Methods 221:1–7.

National Research Council (U.S.) (2011) Committee for the Update of the Guide for the Care and Use of Laboratory Animals., Institute for Laboratory Animal Research (U.S.), National Academies Press (U.S.) (2011) Guide for the care and use of laboratory animals. Washington, D.C.: National Academies Press. p. 220.

Pelli DG (1997) The VideoToolbox software for visual psychophysics: transforming numbers into movies. Spat Vis 10:437–442.

Phelps PE, Houser CR, Vaughn JE (1985) Immunocytochemical localization of choline acetyltransferase within the rat neostriatum: a correlated light and electron microscopic study of cholinergic neurons and synapses. J Comp Neurol 238:286–307.

Pigarev IN, Levichkina EV (2011) Distance modulated neuronal activity in the cortical visual areas of cats. Exp Brain Res 214:105–111.

Pigarev IN, Rodionova EI (1998) Two visual areas located in the middle suprasylvian gyrus (cytoarchitectonic field 7) of the cat's cortex. Neuroscience 85:717–732.

Populin LC, Yin TC (1998) Behavioral studies of sound localization in the cat. J Neurosci 18:2147–2160.

Populin LC, Yin TC (2002) Bimodal interactions in the superior colliculus of the behaving cat. J Neurosci 22:2826–2834.

Pouderoux G, Freton E (1979) Patterns of unit responses to visual stimuli in the cat caudate nucleus under chloralose anesthesia. Neurosci Lett 11:53–58.

Rajkai C, Lakatos P, Chen CM, Pincze Z, Karmos G, Schroeder CE (2008) Transient cortical excitation at the onset of visual fixation. Cereb Cortex 18:200–209.

Robinson DA (1963) A method of measuring eye movement using a scleral search coil in a magnetic field. IEEE Trans Biomed Eng 10:137–145.

Rokszin A, Gombkoto P, Berenyi A, Markus Z, Braunitzer G, Benedek G, Nagy A (2011) Visual stimulation synchronizes or desynchronizes the activity of neuron pairs between the caudate nucleus and the posterior thalamus. Brain Res 1418:52–63.

Rolls ET, Thorpe SJ, Maddison SP (1983) Responses of striatal neurons in the behaving monkey. 1. Head of the caudate nucleus. Behav Brain Res 7:179–210.

Schmitzer-Torbert N, Redish AD (2004) Neuronal activity in the rodent dorsal striatum in sequential navigation: separation of spatial and reward responses on the multiple T task. J Neurophysiol 91:2259–2272.

Schmitzer-Torbert NC, Redish AD (2008) Task-dependent encoding of space and events by striatal neurons is dependent on neural subtype. Neuroscience 153:349–360.

Stalnaker TA, Calhoon GG, Ogawa M, Roesch MR, Schoenbaum G (2012) Reward prediction error signaling in posterior dorsomedial striatum is action specific. J Neurosci 32:10296–10305.

Strecker RE, Steinfels GF, Abercrombie ED, Jacobs BL (1985) Caudate unit activity in freely moving cats: effects of phasic auditory and visual stimuli. Brain Res 329:350–353.

Sumner P, Nachev P, Castor-Perry S, Isenman H, Kennard C (2006) Which visual pathways cause fixation-related inhibition? J Neurophysiol 95:1527–1536.

Tepper JM, Tecuapetla F, Koos T, Ibanez-Sandoval O (2010) Heterogeneity and diversity of striatal GABAergic interneurons. Front Neuroanat 4:150.

Thorn CA, Atallah H, Howe M, Graybiel AM (2010) Differential dynamics of activity changes in dorsolateral and dorsomedial striatal loops during learning. Neuron 66:781–795.

Tollin DJ, Populin LC, Moore JM, Ruhland JL, Yin TC (2005) Sound-localization performance in the cat: the effect of restraining the head. J Neurophysiol 93:1223–1234.

Velly LJ, Rey MF, Bruder NJ, Gouvitsos FA, Witjas T, Regis JM, Peragut JC, Gouin FM (2007) Differential dynamic of action on cortical and subcortical structures of anesthetic agents during induction of anesthesia. Anesthesiology 107:202–212.

Vicente AF, Bermudez MA, Romero Mdel C, Perez R, Gonzalez F (2012) Putamen neurons process both sensory and motor information during a complex task. Brain Res 1466:70–81.
Villeneuve MY, Casanova C (2003) On the use of isoflurane versus halothane in the study of visual response properties of single cells in the primary visual cortex. J Neurosci Methods 129:19–31.
Wilson CJ (1993) The generation of natural firing patterns in neostriatal neurons. Prog Brain Res 99:277–297.
Wurtz RH (1969) Visual receptive fields of striate cortex neurons in awake monkeys. J Neurophysiol 32:727–742.

(Received 21 December 2016, Accepted 15 May 2017)
(Available online 22 May 2017)

I. Nyujtó D, Kiss A, Bodosi B, Eördögh G, Tót K, Kelemen A, Nagy A Visually evoked local field potential changes in the caudate nucleus are remarkably more frequent in awake, behaving cats than in anesthetized animals. Physiol Internat in Press (2023)
IF: 1.4

Visually evoked local field potential changes in the caudate nucleus are remarkably more frequent in awake, behaving cats than in anaesthetized animals

Diána Nyujtó[1], Ádám Kiss[1], Balázs Bodosi[1], Gabriella Eördegh[2], Kálmán Tót[1], András Kelemen[3], Attila Nagy[1*]

[1] Department of Physiology, Faculty of Medicine, University of Szeged, Szeged, Hungary

[2] Faculty of Health Sciences and Social Studies, University of Szeged, Szeged, Hungary

[3]Department of Applied Informatics, University of Szeged, Szeged, Hungary

*** Corresponding author**:

Attila Nagy, associate professor

H-6720 Szeged, Dóm tér 10.

E-mail: nagy.attila.1@med.u-szeged.hu

Tel: +36 62 545869

Fax: +3662545842

Abstract

Previous results show that halothane gas anaesthesia has a suppressive effect on the visually evoked single-cell activities in the feline caudate nucleus (CN). In this study, we asked whether the low-frequency neuronal signals, the local field potentials (LFP) are also suppressed in the CN of anaesthetized animals.

To answer this question, we compared the LFPs recorded from the CN of two halothane-anaesthetized (1.0%), paralyzed, and two awake, behaving cats during static and dynamic visual stimulation. The behaving animals were trained to perform a visual fixation task.

Our results denoted a lower proportion of significant power changes to visual stimulation in the CN of the anesthetized cats in each frequency range (from delta to beta) of the LFPs, except gamma. These differences in power changes were more obvious in static visual stimulation, but still, remarkable differences were found in dynamic stimulation, too. The largest differences were found in the alpha and beta frequency bands for static stimulation. Concerning dynamic stimulation, the differences were the biggest in the theta, alpha and beta bands.

Similar to the single-cell activities, remarkable differences were found between the visually evoked LFP changes in the CN of the anaesthetized, paralyzed and awake, behaving cats. The halothane gas anaesthesia and the immobilization suppressed the significant LFP power alterations in the CN to both static and dynamic stimulation. These results suggest the priority of the application of behaving animals even in the analysis of the visually evoked low-frequency electric signals, the LFPs recorded from the CN.

Keywords

visual; local field potential; power spectrum analysis, halothane anaesthetized cat; behaving cat

Introduction

Beside the prominent role of the caudate nucleus (CN) in motor processes, it is also involved in sensory information processing through cortical and subcortical loops in the mammalian brain [1, 2]. The primary source of the visual inputs to the basal ganglia is the ascending tectofugal visual system, which sends the information from the superior colliculus through the posterior thalamus to the CN. The CN also receives visual cortical inputs from the anterior ectosylvian cortex (Rokszin et al., 2010). These inputs are responsible for the specific visual properties of the CN. Previous studies denoted that the CN neurons are sensitive to static and dynamic visual stimuli, too [3-12]. The particular spatial and temporal visual properties of the CN neurons, i.e., preferences for low spatial and high temporal frequencies and narrow spatiotemporal spectral tuning [8, 13] suggest the contribution of these neurons to motion and novelty detection. Thus, the CN seems to belong to those brain structures that have the capacity to sample and evaluate a wide variety of changes in the visual environment.

The control of eye movements is obligatory in visual electrophysiological experiments because of various reasons. First of all, the spatial position of the visual stimulus has to overlap with the receptive field of the investigated neuron. Additionally, several visually active brain structures possess visuomotor activity, such as saccadic responses [14, 15]. Therefore, the researchers must eliminate the effect of eye movements on neuronal activities. Acute, anaesthetized, paralyzed, and awake, behaving animals are often used in visual electrophysiological research. Both models have their own advantages and disadvantages. The work in acute animals seems to be easier because there is no long behavioural training to restrict eye movement prior to the electrophysiological recordings [12, 16]. On the other hand, this increases the number of animals sacrificed, and the anaesthetics can also influence the activity of the brain. The deep brain sensorimotor structures, i.e., the cerebellum and the basal ganglia, are extremely sensitive to anaesthesia [17, 18]. Single-cell activity analysis revealed

significant differences between the neuronal activities recorded from the feline CN in anaesthetized and behaving cats. The anaesthesia and the immobilization significantly suppressed the neuronal activity and the visual responsiveness of the CN. Furthermore, it was almost impossible to analyse phasically active neurons, the dominant neuronal population of the CN, due to the low neuronal activities. [19]. These results suggest the necessity of the behaving animals if the activity of the single CN cell is the focus of the research. The training and preparation of cats is often a challenging process that may last up to 9 months [16, 19]. Beside single cell activities, the low-frequency signals (local field potentials = LFPs) can also carry information from the visual environment. The visually evoked LFP changes can give information about the sum of the cortical and subcortical visual inputs in the CN. The question raises whether the LFP activities and the visually evoked LFP changes are suppressed similarly in the anaesthetized animals as the single-cell activities. To address these questions, we compared the LFPs recorded from the CN in halothane anaesthetized, paralyzed, artificially ventilated and awake, behaving cats. An earlier study denoted that the median of visual onset response latencies was 100 ms in the CN (the range was 20-200 ms, Rokszin et al. 2011). Additionally, the CN is involved in novelty detection and the detection of changes in the visual environment [2, 8]. We have focused on the alterations in different frequency bands (theta, alpha, beta, and gamma) of the LFPs in the first 320 ms time after the appearance of the static visual stimulus, and in the first 320 ms after the starting of the movement of the dynamic visual stimulus.

Materials and methods

We recorded from the CN of two halothane anaesthetized, paralyzed, and two awake, behaving adult, domestic cats that weighed between 2.5 and 5 kg. The acute recordings lasted for 3 days. The recording sessions of the behaving cats lasted 30 minutes to 1 hour per day, four to five times a week.

All procedures were performed to minimize the number and the discomfort of the animals, and the experimental protocol was accepted by the Government Office based on the suggestion of the Ethical Committee for Animal Research of Albert Szent-Györgyi Medical and Pharmaceutical Centre at the University of Szeged (No.: XIV./518/2018 and XIV/1818/2021) and was conducted in full accordance with the Directive 2010/63/EU of the European Parliament and the Council on the Protection of Animals Used for Scientific Purposes and the guidelines of the Committee.

Surgical procedure of the anaesthetized animals

The animals were initially anaesthetized with ketamine hydrochloride (Calypsol (Gedeon Richter LTD), 30 mg/kg i.m.). A subcutaneous injection of 0.2 ml 0.1% atropine sulphate was administered preoperatively to reduce salivation and bronchial secretion. All wound edges and pressure points were treated regularly with a local anesthetic (1% procaine hydrochloride). The trachea and the femoral vein were cannulated, and then the animals were placed in a stereotaxic frame. The cats were artificially ventilated with 1.2-1.6% halothane during surgery, which was reduced to 0.8-1.0% during the recording sessions to minimize the effects of anesthesia. The depth of the anesthesia was monitored continuously with the end-tidal anesthetic concentration and heart rate. The minimal alveolar anesthetic concentration (MAC) values calculated from the end-tidal halothane concentration were kept in a recommended range [20]. The end-tidal halothane concentration, MAC values and the peak

expired CO_2 concentrations were monitored with a capnometer (CapnomacUltima, Datex-Ohmeda, ICN). The O_2 saturation of the capillary blood was monitored by pulse oximetry. The peak expired CO_2 concentration was kept within the range of 3.8–4.2% by adjustment of the respiratory rate or volume. The animals were immobilized with an initial 2 ml intravenous bolus of gallamine triethiodide (Flaxedil, 20 mg/kg, Sigma, St. Louis, MO, USA). During the whole experiment, a mixture containing gallamine triethiodide (8 mg/kg/h), glucose (10 mg/kg/h) and dextran (50 mg/kg/h) in Ringer lactate solution was infused continuously at a rate of 4 ml/h. The body temperature of the cats was maintained at 37 $^{\circ}$C by an electric heating blanket. Craniotomy was performed with a dental drill to allow a vertical approach to the target structures. The dura mater was removed, and the skull hole was covered with a 4% solution of 37 °C agar dissolved in Ringer's solution. The eye contralateral to the subcortical recording site was treated locally with atropine sulphate (one or two drops, 0.1%) and phenylephrine hydrochloride (one or two drops, 10%) to dilate the pupils, block accommodation and retract the nictitating membranes, and was equipped with a +2 diopter contact lens. During the recordings, the ipsilateral eye was covered.

Visual paradigm and recording in anaesthetized animals

The recording sessions took place in a dark, quiet room where the background luminance was 2 cd/m^2. Vertical penetrations made within the Horsley-Clarke coordinates anterior 14 mm and lateral 4-5 mm, at a stereotaxic depth of 10-15.3 mm. The extracellular electrophysiological recordings were carried out with a 64-channel 2 shank (32 channel/shank, diameter: 300 μm/shank) platinum-iridium linear probe (Neuronelektród Ltd., Hungary). The vertical distance between each channel was 50 μm. The reference electrode was a 125 micrometer tungsten electrode which was inserted in the white matter in the position of anterior 7 and lateral 8 according to the Horsley-Clarke coordinates. The electrical signals were amplified and digi-

talized with Intan rhd 2132 chips and Hinstra Dedas data acquisition system (Hinstra Instruments Ltd., Hungary). Amplified neuronal activities were recorded at a 20 kHz sampling rate and stored for offline analysis. The stimulus presentation was controlled by a custom-made software and was presented on an 18-inch CRT monitor (refresh rate: 100 Hz) 57 cm in front of the animal. A single trial (one repetition of the whole stimulation protocol) consisted of 3 epochs (phases): first a blank, black screen was presented to obtain background activity without visual stimulation for 2000 ms; then a random dot pattern appeared on the screen for 1500 ms as a stationary stimulus; that was followed by the dynamic stimulus, where the same white dots started to move randomly either toward the periphery (center-out flow field) or toward the center (center-in flow field) of the screen. The dynamic stimulus also lasted 1500 ms. The size of each dot was 0.1° in diameter in both the static and the dynamic stimulus. The speed of dot movement increased from 0 to 7°/sec toward the periphery. One recording session lasted 15 minutes, where 50 trials were presented from for each of the center in and center out conditions in a pseudo-random order. Between the recordings, the electrode position was changed (200 μm downward), and a 30-minute break was kept before the next recording.

Surgical procedure in case of awake, behaving animals

The preparation before the surgery was carried out the same way as with the anaesthetized animals. First, the cats were initially anaesthetized with ketamine hydrochloride (Calypsol (Gedeon Richter®), 30 mg/kg i.m), then a subcutaneous injection of 0.2 ml 0.1% atropine sulphate was administered. In addition, a preventive dose of antibiotic (1000 mg ceftriaxon, i.m., Rocephin 500 mg (Roche®)) was given preoperatively. The surgical preparation started with the cannulation of the femoral vein, then continued with the implantation of a scleral search coil (Cooner wire, Owensmouth, CA, USA) into one eye to monitor the eye movements of the cats during the recordings [16, 21-26]. After the intubation of the trachea,

the cats were placed in a stereotaxic frame. All pressure points and wounds were treated with local anesthetic (1% procaine hydrochloride). During the surgery, the anesthesia was maintained with 1.5% halothane in a 2:1 mixture of N_2O and oxygen. The depth of the anesthesia was monitored by continuously checking the end-tidal halothane concentration, MAC values, the peak expired CO_2 concentrations and the O_2 saturation. Firstly, a stainless steel head-holder was installed on the skull to fixate the head during the recordings. After this, the craniotomy was performed with a dental drill; the dura mater was preserved, and the skull hole was covered with a 4% solution of 38 $^{\circ}$C agar dissolved in Ringer's solution. Then a reclosable plastic recording chamber (20 mm in diameter) was cemented on the skull to avoid any contamination and to protect the microdrive system and the extracellular electrodes. Following this, eight wire electrodes covered by a guiding tube were implanted above the CN according to the Horsley-Clarke coordinates anterior 12–14 mm, lateral 4–6.5 mm. Recordings were performed at the stereotaxic depths between 10–16 mm. The electrodes were implanted in the brain with the help of an adjustable microdrive system [27, 28].

On the first five postoperative days, ceftriaxone antibiotic was administered intramuscularly (Rocephine, 50 mg/kg). Nalbuphin (0.25 mg/kg) and non-steroidal anti-inflammatory drugs were administered until the seventh postoperative day.

Behavioural training of awake, behaving cats

The detailed description of the training process and the recordings can be found in our previous studies [12, 16, 19]. The cats were suspended in the experimental stand by a canvas harness. The cats were trained to perform the behavioural fixation paradigm while their heads were fixed to the stereotaxic frame. The stereotaxic frame with the animal was placed within an electromagnetic field, which is generated by metal coils installed into the wall of the experimental stand. During the fixation training, the fixation time was gradually increased

from 100 ms to 2500 ms. Square fixation windows were used. The size of the initial fixation window was ±10° for both cats. During the training period, it was reduced to ±2.5° in ±2.5° steps. The animals were trained to hold their eyes in the center of the monitor during recordings of neuronal activities to different kinds of visual stimulation. The behavioral training lasted 9-12 months approximately 1 to 2 hours per day, four to five times a week. The training phases and later the recordings took place in a dark, quiet laboratory room.

Visual paradigm and recordings in case of awake, behaving cats

The electrophysiological extracellular recordings were carried out with perylene isolated platinum-iridium wire-electrodes with a diameter of 25 μm for the first cat; and formvar insulated nickel-chrome wire-electrodes with a diameter of 50 μm for the second cat. Each recording electrode contained 8 wires and one wire contained one recording channel. The reference electrode was positioned in the white matter in anterior 3 and lateral 8 according to the Horsley-Clarke coordinates. The recording of the eye movements, stimulus presentation, reward delivery, and data collection were controlled by a custom-made LabView software via a 16-channel National Instruments data acquisition card. The sampling rate was 10 kHz. Eye movements were monitored and recorded with a search coil system (DNI Instruments, Newark, DE, USA). A standard 17-inch CRT monitor (refresh rate: 100 Hz) was placed in front of the animal at a viewing distance of 57 cm for the visual stimulation. The fixation point and the visual stimuli were generated by a custom-made script written in Matlab and using the Psychophysics Toolbox® (Bartinard 1997). A fixation point was projected on the center of the monitor to help maintain the fixation on the middle of the monitor during the relevant stimulus phases. The size of the fixation point was 0.8° in diameter, the fixation window was 5° in diameter (5° x 5° square). In the case of the behaving, awake animals, a trial (one repetition of the whole stimulation protocol) consisted of 5 epochs (phases). First, a

green fixation point was presented in the center of the monitor. The cats had to direct their gaze to the fixation point and keep fixating for 500 ms. The visual stimulation task started immediately after the successful fixation phase. It means that the cat held his eye in the above described ±2.5° fixation window. This was similar to the stimulation used in the anaesthetized experiments: a static random dot pattern appeared first, which was followed by a dynamic center-in or center-out flow field stimulation in random order. The duration of both the static and the dynamic stimuli was 1000 ms. If the cats managed to fixate throughout all the stimulation phases of a single trial, they received a food reward, and it was considered a correct trial. If the cats broke fixation during any of the stimulation phases, the trial was aborted immediately, it was not accepted, and no reward was given. Between two trials, there was a random 5000-10000 ms long intertrial interval (reward was given at the beginning of this time range), where no stimuli appeared, only a black screen. This phase was long enough so that the cat could eat the reward without muscle activity interfering with the recordings of the next trial. One recording session lasted 30-45 minutes. The number of successful trials, where the animal could hold the fixation during the whole stimulation protocol, were analyzed. These varied between 80 and 200 in each recording.

Data analysis

For the data analysis and the statistical analysis, Matlab R2021a software (The Mathworks, Natic, MA, USA) was used. During the analysis, the power of the delta (1-3 Hz), theta (4–7 Hz), alpha (8–13 Hz), beta (14–30 Hz), and gamma (31–70 Hz) bands were calculated.

The first step was the visual inspection of the recorded raw data (Figure 1). Channels with high amplitude noise and/or bad signal-noise ratio were excluded from further analysis. After the subtraction of these channels, the downsampling of the remaining channels was performed for further mathematical analysis. It was done by applying a low pass filter and decimation to

500 Hz for the raw data using the Matlab *decimate* function. After the downsampling of the original dataset, Fourier analysis was performed. The power spectrum was then video-filtered (smoothed) by a ten-bin rectangle window. A whitening compensation was used to visualize higher frequency bands more equally, however, the calculations were made from the original raw data. After the whitening, a median filter (Matlab medfilt1) was also used with the default parameters. During the visualization of the Fourier spectra, the bins near 50 Hz were cut off.

Figure 1 is somewhere here

Filtering and power calculation

The raw data of each channel was decimated to 500 Hz by the Matlab *decimate* function. The decimation filter was an finite impulse response filter (FIR) one, and its length was chosen to 20 ms, not to alias brain events through each other.

For each band, a digital superheterodyne test receiver was implemented. The center frequency of every band was shifted to 0 Hz by multiplying the signal with a complex rotating vector. After this step, a Chebyshev infinite impulse response filter (IIR) filter was used, and the signal was decimated to a lower sampling frequency. The filtering and decimating steps were repeated in order to reach the desired width of the band, and fulfil the stability criteria of the filters (Figure 2). The final decimation was done for 25 Hz. For the theta signal (the lowest interesting frequency band in this study), the resulting stable filters require a 25 Hz sampling frequency. Calculating the power of signals hence shows t=1/f=40 ms time resolution. The higher frequency band was also summated and decimated with the same time resolution and sampling frequency. Having the 25 Hz complex signal for each band, the absolute value of these signals represents the power of the signal for each 40 ms wide sample.

Figure 2 is somewhere here

Statistical analysis

The powers of a randomly selected 320 ms period (the average of eight 40 ms wide bins (samples described above) from the background activity and 320 ms periods (the average of eight 40 ms wide samples described above) immediately after the appearance of the stationary stimulus and the start of the dynamic stimulus were calculated in each trial and each frequency band, both in the behaving and the anaesthetized LFP recordings. The powers of these 320 ms periods in each frequency band from all trials were non-normally distributed (Shapiro-Wilk $p<0.05$). Thus, they were compared with the Friedmann ANOVA test with Bonferroni correction both in the behaving and anaesthetized LFP recordings. If this test denoted a significant difference ($p<0.05$) in one LFP recording, it would indicate that at least one of the three conditions (background activity, response to static or dynamic stimulation) differs from the others. In this case, the Wilcoxon matched pair test was used for a pairwise comparison as a post hoc analysis to check which part of the stimulated activity (static, dynamic, or both) differs significantly from the background activity the different frequency bands. The significant differences from the background activity were considered in the present study as dynamic and static visual responses in the CN.

Results

Altogether 226 local field potential (LFP) recordings from awake, behaving cats and 960 LFP recordings from anaesthetized cats were involved in the data analysis. Each LFP recording (which contained at least 80 trials) was analysed separately. The LFPs were analysed in five different frequency bands (delta (1-3 Hz), theta (4–7 Hz), alpha (8–13 Hz), beta (14–30 Hz), and gamma (31–70 Hz)).

The summary of the detailed descriptive statistics can be seen in Table 1. Comparing the response activity during visual stimuli to the background activity, Wilcoxon matched pair test revealed that 90% (N=207) of all registered LFPs from awake, and only 63% (N=609) from the anaesthetized cats showed significant responses at least in one visual condition (static, dynamic) and one frequency band. Figure 3 denotes examples of the visually evoked power changes in the awake, behaving, and Figure 4 in anaesthetized animals.

Figures 3 and 4 are somewhere here

The percentage of LFPs that showed significant changes to static and/or dynamic stimulation in theta, alpha and beta frequency bands was higher in awake, behaving cats. In the theta band, the percentage was 43% (N=98) in awake and only 19% (N=178) in anaesthetized cats. In the alpha band, the percentage was 56% (N=121) in awake and 19% (N=181) in anaesthetized cats. In the beta frequency band, the percentage of the significant LFPs was 64% (N=114) in awake and 22% (N=210) in anaesthetized cats. In the gamma frequency band, the percentage of the significant LFP changes was 23% in both (N=34) the awake and the anaesthetized cats (**Table 1**).

Table 1 somewhere here

Responses to static visual stimulation

The proportion of LFPs that showed significant response during static visual stimulation was much higher in awake, behaving cats (83%, N=122) than in anaesthetized cats (63%, N=177). A higher percentage of visually evoked LFP changes can be observed in almost each frequency range in the behaving animals. The only exception is the theta band where the same percentages were found (Wilcoxon match paired test, see descriptive statistical data in **Table 2**). These differences are the most obvious in the alpha and the beta frequency bands. In the case of the alpha band, the percentage was 49% (N=110) in awake and only 24% (N=228) in anaesthetized cats. In the case of the beta band the percentage of the significant LFP changes was 49% (N=110) in behaving cats, and it was only 23% (N=221) in anaesthetized cats.

Table 2 somewhere here

Responses to dynamic visual stimulation

In comparison to the effect of the static stimulation (83%, N=187) a bit lower amount of the analysed LFPs showed significant changes to dynamic stimulation (76%, N=172) in behaving cats. However, the percentage of the responsive LFPs to static and dynamic stimulation were similar in the anaesthetized animals, 63% (N=602) and 64% (N=611), respectively.

Similarly, to the static visual stimulation, the proportion of LFPs that showed significant responses during dynamic visual stimulation was higher in awake, behaving cats (76%,

N=172) than in anaesthetized ones (64%, N=611, Wilcoxon match paired test, see descriptive statistical data in **Table 2**). These differences are the most notable in the theta, alpha and the beta frequency bands. In the case of the theta band, the percentage was 39% (N=89) in awake, and only 19% (N=183) in anaesthetized cats. In the alpha band the percentage was 34% (N=76) in the behaving animals and 15% in the anaesthetized cats. The percentage of the significant LFP changes was 31% (N=69) in behaving, and it was lower 21% (N=37) in anaesthetized cats in the beta frequency band.

Discussion

To our knowledge, this is the first descriptive study that compares the low-frequency neuronal activities (local field potentials, LFPs) recorded from the CN during visual stimulation in anaesthetized, paralyzed, and awake, behaving cats. In line with the findings of our previous study on the single cell activities [19], the present results clearly demonstrated that the applied halothane anesthesia indeed suppresses the visually evoked LFP changes at a remarkable level. Thus, lower proportion of significant power changes was detected to visual stimulation in the anaesthetized animals in each frequency range (from delta to gamma) of the LFPs.

In visual electrophysiological experiments, both anaesthetized, paralyzed, and awake, behaving models are commonly used. Both have their advantages and disadvantages. The control of eye movements in visual electrophysiology is critical. The spatial position of the visual stimulus must overlap with the receptive field of the investigated neuron, and oculomotor activity can also be found in some extrastriate visual structures [14, 15]. If one would like to eliminate these disturbing factors, there are two possibilities. In anaesthetized and paralyzed animal models, eye movements are inhibited through muscle relaxants. However, the applied anesthetics and muscle relaxants can influence the activity of the central nervous system. It is also assumed that this effect is not the same as in the cortex or the deeper brain structures [29]. The basal ganglia are strongly sensitive to different kinds of anesthesia [17, 18]. In the case of the single-cell activities in the CN, the anesthesia influences the timing of the action potential and the discharge rates significantly [19]. Beside these high-frequency signals, the LFPs could also be influenced. Based on our previous experiences that the halothane influences the neuronal activities less in the CN than other gas anesthetics (i.e., isoflurane), although we cannot exclude the effect of the anesthesia from the results in

anaesthetized animals. The big advantage of the application of this anaesthetized animal is the quick application of it without any training of the animals. The second solution for the elimination of the effect of eye movements on neuronal activities is the application of eye movement controlled fixating behaving animals. The disadvantage of the experiments with behaving animals is the long-lasting behavioral and fixation training, which could last for 9-12 months before the start of the electrophysiological recordings. However, there is no disturbing effect of anesthetics in this case.

The question raises whether the benefit of experiments performed in the CN of awake, behaving animals is in balance with the hardness of the preparation of the animals for visual electrophysiological recordings. The results of the visual information processing in the CN revealed that both the background activities and the neuronal responses to static and dynamic visual stimulation were strongly reduced in the anaesthetized animals. The most drastic differences can be seen in the biggest neuronal population in the medium spiny neurons of the caudate body [19]. Concerning the significant changes in LFP in response to visual stimulation, the differences between the two models are also obvious. The vast majority (90%) of the LFPs recorded in behaving cats showed significant responses at least in one visual condition (static, dynamic) and one frequency band. On the other hand, it was a smaller proportion of the LFPs (61%) in anaesthetized cats. These differences in power changes were the stronger concerning static visual stimulation (83% vs 63%). Less, but still obvious differences were found to dynamic stimulation, too (76% vs 64%). The higher proportion of the evoked LFP responses were detectable in both static and dynamic stimulation in each investigated frequency band from the lower delta to the highest gamma band. However, the biggest differences were concerning static stimulation in the alpha and the beta frequency bands and concerning dynamic stimulation to the theta, the alpha and the beta bands.

Similar to human EEG results, the increased theta activity could arise from the coordinated reactivation of information represented in visual areas [30-34]. The elevated cortical alpha activity is also connected to visual and audio-visual processing [35-37]. Another function that has been attributed to alpha activity is a mechanism of sensory suppression, thus functionally gating information in the task-irrelevant brain areas [38, 39]. It is also assumed that the normal beta activity is a necessary cortical outcome of the normal action of the basal ganglia in visual information processing (Puszta et al., 2019). Since the analysis addressed the first 320 ms time window of both static and dynamic stimulation, novelty detection and the connected sensory gating could be the task that shows these differences between the anaesthetized, paralyzed, and awake, behaving animals [2, 8].

Beyond the lack of halothane anesthesia and immobilization, our behaving model differed from anaesthetized models also in a third way: both eyes of the animal were open during stimulation (in anaesthetized cats, recordings are made only from one eye, while the other eye is covered, [40]). This monocular-binocular difference could influence the magnitude of visual responses, but such strong difference, as seen in this study, is not likely to stem from this factor only [41-43]. It is noteworthy to mention that the anaesthetized cats were cycloplegic, and the awake ones had normal pupils and lenses, but in the case of anaesthetized cats the visus was corrected with appropriate lenses. As the background luminance was the same for the two models and the same CRT monitor was used, these do not explain the observed difference either. An important shortcoming of the study is that the recordings from behaving and anaesthetized cats were performed with different recording systems with different background noise levels. Thus, the direct comparison of the magnitude of the visual responses was not possible in this study. Therefore, we could only concentrate on whether the changes were significant or not and we could give the presented a descriptive statistic about the percentage of these visually-evoked changes. Another limitation is that

electrodes with different geometries were applied in the behaving (wire electrodes) and anaesthetized (linear probe) experiments. It is known that the geometry of the electrodes could influence the magnitude of the recorded LFPs (Herreras 2016). But if we compare the baseline power spectrum density of one channel with the power spectrum density during visual stimulation of the same channel, it will not influence the number of significant changes and the differences between the two models. The different electrodes, 8-channel wire electrodes in the behaving experiments, and 64-channel linear probes in the anaesthetized experiments, explain the higher number of recorded LFPs from the anaesthetized animals.

To summarize our findings, we demonstrated similarly to the single cell activities [19], marked differences between the visually evoked LFP changes in the CN of the anaesthetized, paralyzed, and awake, behaving cats. The halothane gas anesthesia and the immobilization significantly suppressed the significant LFP power alterations to both static and dynamic stimulation. Although the work with behaving cats in visual electrophysiology is much more difficult, we argue that the benefits outweigh the costs, and we suggest the application of the behaving animal model even in the analysis of the low-frequency electric signals, the LFPs.

Acknowledgements

The authors thank to Siposné Gabriella Dósai-Molnár and László Rácz for the technical assistance and to Robert Averkin for the microdrives and the wire electrodes. This work was supported by a grant from SZTE ÁOK-KKA Grant No. 2019/270-62-2.

Author contributions

DNy, GE, and AN designed the study; DNy, GE, KT, NA and BB performed the assessment and documented the findings; ÁK, AK and NA analysed the data; DNy, ÁK, AK, BB and NA organized the study and wrote the manuscript.

Competing interest

The author(s) declare no competing interests (both financial and non-financial).

References

[1] J.G. McHaffie, T.R. Stanford, B.E. Stein, V. Coizet, P. Redgrave, Subcortical loops through the basal ganglia, Trends Neurosci 28 (2005) 401-407.

[2] G. Benedek, S. Keri, A. Nagy, G. Braunitzer, M. Norita, A multimodal pathway including the basal ganglia in the feline brain, Physiol Int 106 (2019) 95-113.

[3] R.E. Strecker, B.L. Jacobs, Substantia nigra dopaminergic unit activity in behaving cats: effect of arousal on spontaneous discharge and sensory evoked activity, Brain Res 361 (1985) 339-350.

[4] E.T. Rolls, S.J. Thorpe, S.P. Maddison, Responses of striatal neurons in the behaving monkey. 1. Head of the caudate nucleus, Behav Brain Res 7 (1983) 179-210.

[5] O. Hikosaka, M. Sakamoto, S. Usui, Functional properties of monkey caudate neurons. II. Visual and auditory responses, J Neurophysiol 61 (1989) 799-813.

[6] E.H. Chudler, K. Sugiyama, W.K. Dong, Multisensory convergence and integration in the neostriatum and globus pallidus of the rat, Brain Res 674 (1995) 33-45.

[7] A. Nagy, G. Eordegh, G. Benedek, Extents of visual, auditory and bimodal receptive fields of single neurons in the feline visual associative cortex, Acta Physiol Hung 90 (2003) 305-312.

[8] A. Nagy, Z. Paroczy, Z. Markus, A. Berenyi, M. Wypych, W.J. Waleszczyk, G. Benedek, Drifting grating stimulation reveals particular activation properties of visual neurons in the caudate nucleus, Eur J Neurosci 27 (2008) 1801-1808.

[9] P. Gombkoto, A. Rokszin, A. Berenyi, G. Braunitzer, G. Utassy, G. Benedek, A. Nagy, Neuronal code of spatial visual information in the caudate nucleus, Neuroscience 182 (2011) 225-231.

[10] A. Rokszin, P. Gombkoto, A. Berenyi, Z. Markus, G. Braunitzer, G. Benedek, A. Nagy, Visual stimulation synchronizes or desynchronizes the activity of neuron pairs between the caudate nucleus and the posterior thalamus, Brain Res 1418 (2011) 52-63.

[11] A.F. Vicente, M.A. Bermudez, C. Romero Mdel, R. Perez, F. Gonzalez, Putamen neurons process both sensory and motor information during a complex task, Brain Res 1466 (2012) 70-81.

[12] T. Nagypal, P. Gombkoto, B. Barkoczi, G. Benedek, A. Nagy, Activity of Caudate Nucleus Neurons in a Visual Fixation Paradigm in Behaving Cats, PLoS One 10 (2015) e0142526.

[13] A. Nagy, A. Berenyi, M. Wypych, W.J. Waleszczyk, G. Benedek, Spectral receptive field properties of visually active neurons in the caudate nucleus, Neurosci Lett 480 (2010) 148-153.

[14] O. Hikosaka, Y. Takikawa, R. Kawagoe, Role of the basal ganglia in the control of purposive saccadic eye movements, Physiol Rev 80 (2000) 953-978.

[15] D.P. Munoz, J.H. Fecteau, Vying for dominance: dynamic interactions control visual fixation and saccadic initiation in the superior colliculus, Prog Brain Res 140 (2002) 3-19.

[16] T. Nagypal, P. Gombkoto, G. Utassy, R.G. Averkin, G. Benedek, A. Nagy, A new, behaving, head restrained, eye movement-controlled feline model for chronic visual electrophysiological recordings, J Neurosci Methods 221 (2014) 1-7.

[17] N.P. Franks, A.Y. Zecharia, Sleep and general anesthesia, Can J Anaesth 58 (2011) 139-148.

[18] K.K. Kaisti, J.W. Langsjo, S. Aalto, V. Oikonen, H. Sipila, M. Teras, S. Hinkka, L. Metsahonkala, H. Scheinin, Effects of sevoflurane, propofol, and adjunct nitrous oxide on regional cerebral blood flow, oxygen consumption, and blood volume in humans, Anesthesiology 99 (2003) 603-613.

[19] B. Barkoczi, T. Nagypal, D. Nyujto, X. Katona, G. Eordegh, B. Bodosi, G. Benedek, G. Braunitzer, A. Nagy, Background activity and visual responsiveness of caudate nucleus neurons in halothane anesthetized and in awake, behaving cats, Neuroscience 356 (2017) 182-192.
[20] M.Y. Villeneuve, C. Casanova, On the use of isoflurane versus halothane in the study of visual response properties of single cells in the primary visual cortex, J Neurosci Methods 129 (2003) 19-31.
[21] K.R. Huxlin, T. Pasternak, Training-induced recovery of visual motion perception after extrastriate cortical damage in the adult cat, Cereb Cortex 14 (2004) 81-90.
[22] I.N. Pigarev, E.V. Levichkina, Distance modulated neuronal activity in the cortical visual areas of cats, Exp Brain Res 214 (2011) 105-111.
[23] I.N. Pigarev, E.I. Rodionova, Two visual areas located in the middle suprasylvian gyrus (cytoarchitectonic field 7) of the cat's cortex, Neuroscience 85 (1998) 717-732.
[24] L.C. Populin, T.C. Yin, Behavioral studies of sound localization in the cat, J Neurosci 18 (1998) 2147-2160.
[25] L.C. Populin, T.C. Yin, Bimodal interactions in the superior colliculus of the behaving cat, J Neurosci 22 (2002) 2826-2834.
[26] D.J. Tollin, L.C. Populin, J.M. Moore, J.L. Ruhland, T.C. Yin, Sound-localization performance in the cat: the effect of restraining the head, J Neurophysiol 93 (2005) 1223-1234.
[27] V.A. Korshunov, Miniature microdrive for extracellular recording of neuronal activity in freely moving animals, J Neurosci Methods 57 (1995) 77-80.
[28] M.D. McKown, J.C. Schadt, A modification of the Harper-McGinty microdrive for use in chronically prepared rabbits, J Neurosci Methods 153 (2006) 239-242.
[29] L.J. Velly, M.F. Rey, N.J. Bruder, F.A. Gouvitsos, T. Witjas, J.M. Regis, J.C. Peragut, F.M. Gouin, Differential dynamic of action on cortical and subcortical structures of anesthetic agents during induction of anesthesia, Anesthesiology 107 (2007) 202-212.
[30] A. Gevins, M.E. Smith, L. McEvoy, D. Yu, High-resolution EEG mapping of cortical activation related to working memory: effects of task difficulty, type of processing, and practice, Cereb Cortex 7 (1997) 374-385.
[31] L.T. Hsieh, A.D. Ekstrom, C. Ranganath, Neural oscillations associated with item and temporal order maintenance in working memory, J Neurosci 31 (2011) 10803-10810.
[32] L.T. Hsieh, C. Ranganath, Frontal midline theta oscillations during working memory maintenance and episodic encoding and retrieval, Neuroimage 85 Pt 2 (2014) 721-729.
[33] S. Liebe, G.M. Hoerzer, N.K. Logothetis, G. Rainer, Theta coupling between V4 and prefrontal cortex predicts visual short-term memory performance, Nat Neurosci 15 (2012) 456-462, S451-452.
[34] B.M. Roberts, L.T. Hsieh, C. Ranganath, Oscillatory activity during maintenance of spatial and temporal information in working memory, Neuropsychologia 51 (2013) 349-357.
[35] T. Ergenoglu, T. Demiralp, Z. Bayraktaroglu, M. Ergen, H. Beydagi, Y. Uresin, Alpha rhythm of the EEG modulates visual detection performance in humans, Brain Res Cogn Brain Res 20 (2004) 376-383.
[36] R.S. Schaefer, R.J. Vlek, P. Desain, Music perception and imagery in EEG: alpha band effects of task and stimulus, Int J Psychophysiol 82 (2011) 254-259.
[37] M.S. Worden, J.J. Foxe, N. Wang, G.V. Simpson, Anticipatory biasing of visuospatial attention indexed by retinotopically specific alpha-band electroencephalography increases over occipital cortex, J Neurosci 20 (2000) RC63.
[38] J.J. Foxe, A.C. Snyder, The Role of Alpha-Band Brain Oscillations as a Sensory Suppression Mechanism during Selective Attention, Front Psychol 2 (2011) 154.

[39] L. Michels, M. Moazami-Goudarzi, D. Jeanmonod, J. Sarnthein, EEG alpha distinguishes between cuneal and precuneal activation in working memory, Neuroimage 40 (2008) 1296-1310.
[40] P. Gombkoto, A. Berenyi, T. Nagypal, G. Benedek, G. Braunitzer, A. Nagy, Co-oscillation and synchronization between the posterior thalamus and the caudate nucleus during visual stimulation, Neuroscience 242 (2013) 21-27.
[41] R. Blake, M. Sloane, R. Fox, Further developments in binocular summation, Percept Psychophys 30 (1981) 266-276.
[42] A. di Summa, A. Polo, M. Tinazzi, G. Zanette, L. Bertolasi, L.G. Bongiovanni, A. Fiaschi, Binocular interaction in normal vision studied by pattern-reversal visual evoked potential (PR-VEPS), Ital J Neurol Sci 18 (1997) 81-86.
[43] B.A. Mitchell, K. Dougherty, J.A. Westerberg, B.M. Carlson, L. Daumail, A. Maier, M.A. Cox, Stimulating both eyes with matching stimuli enhances V1 responses, iScience 25 (2022) 104182.

Figure captions

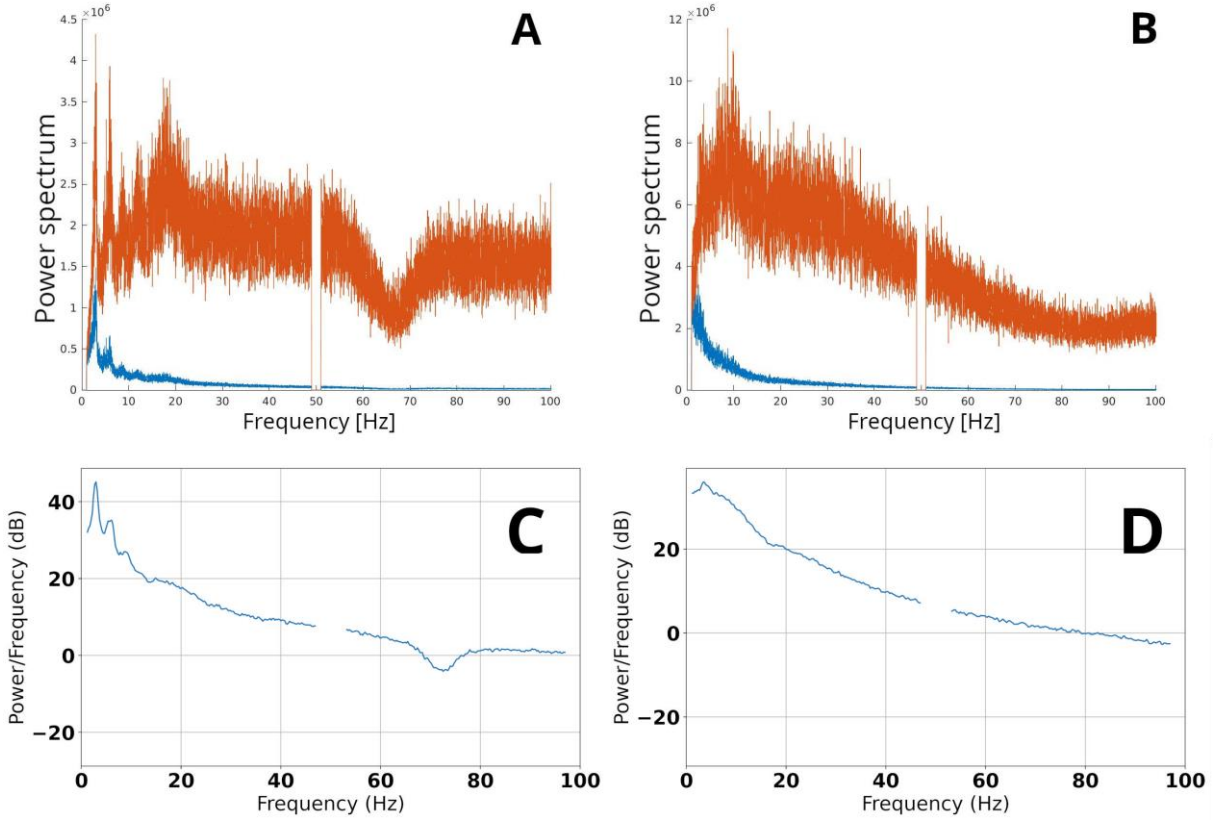

Figure 1 Spectral image of the LFP recordings

Part A shows the Fourier spectrum of a recorded signal (Cecilia589_ch4) from a behaving cat. Part B denotes the Fourier spectrum of a recorded signal (Igor067_ch11) from an anaesthetized cat. The blue colour shows the raw Fourier spectrum and the orange colour denotes the whitened one. Part C and Part D denote the spectral power of the same recorded signals calculated with the Welch function.

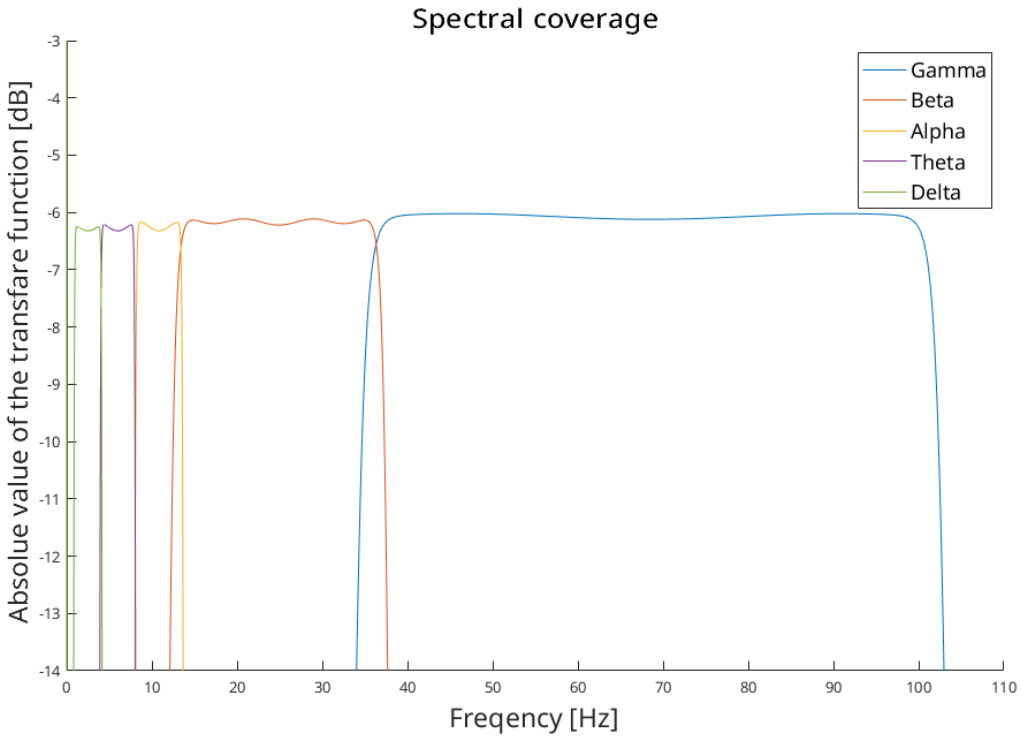

Figure 2 Spectral coverage of the applied band pass filters

The characteristics of the filters in each frequency band can be seen with different colors (green-delta, purple-theta, yellow-alpha, orange-beta, blue-gamma) section. Note the overlap between the frequency-based neighboring filters and their sharp filtering properties.

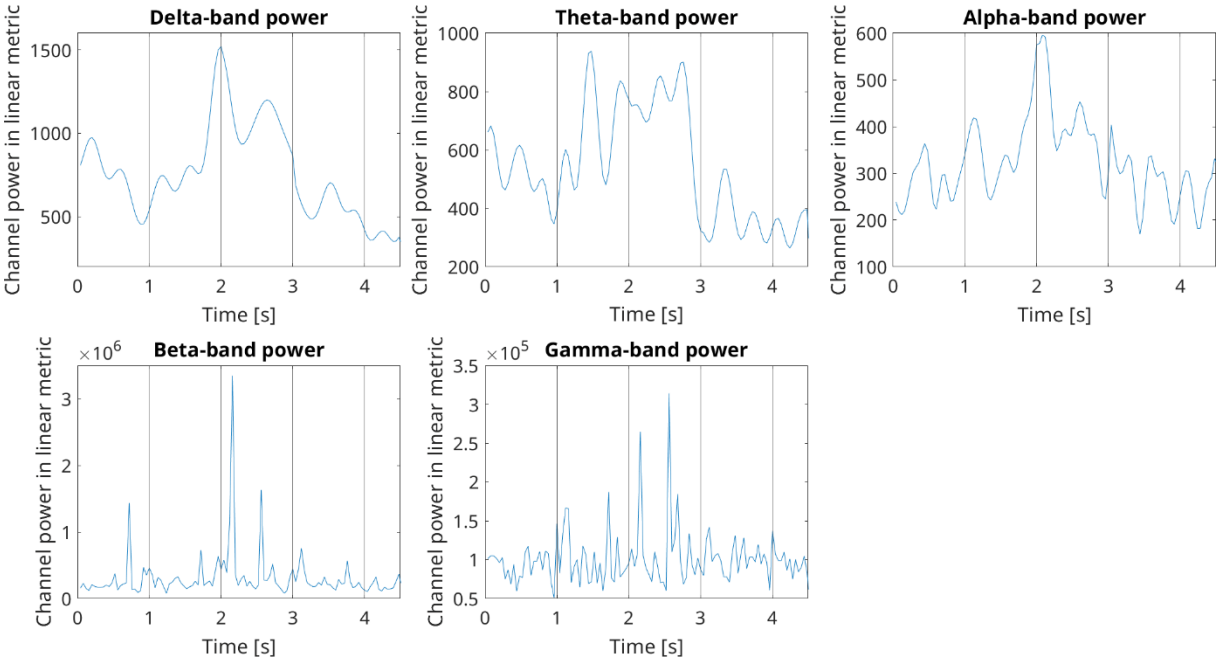

Figure 3 Visually evoked changes of the local field potentials in awake animal

Cumulated power of the wave bands (from delta to gamma) after applying the given spectral filter (see Figure 2) for each frequency band. The blue curve represents the mean activity for all trials. The vertical lines denote the borders between the different epochs of the visual paradigm (from left to right): background activity, fixation activity, response to static visual stimulus, response to dynamic visual stimulus and reward. The abscissa denotes the time relationship of the signals. The ordinate denotes the channel power in linear metrics.

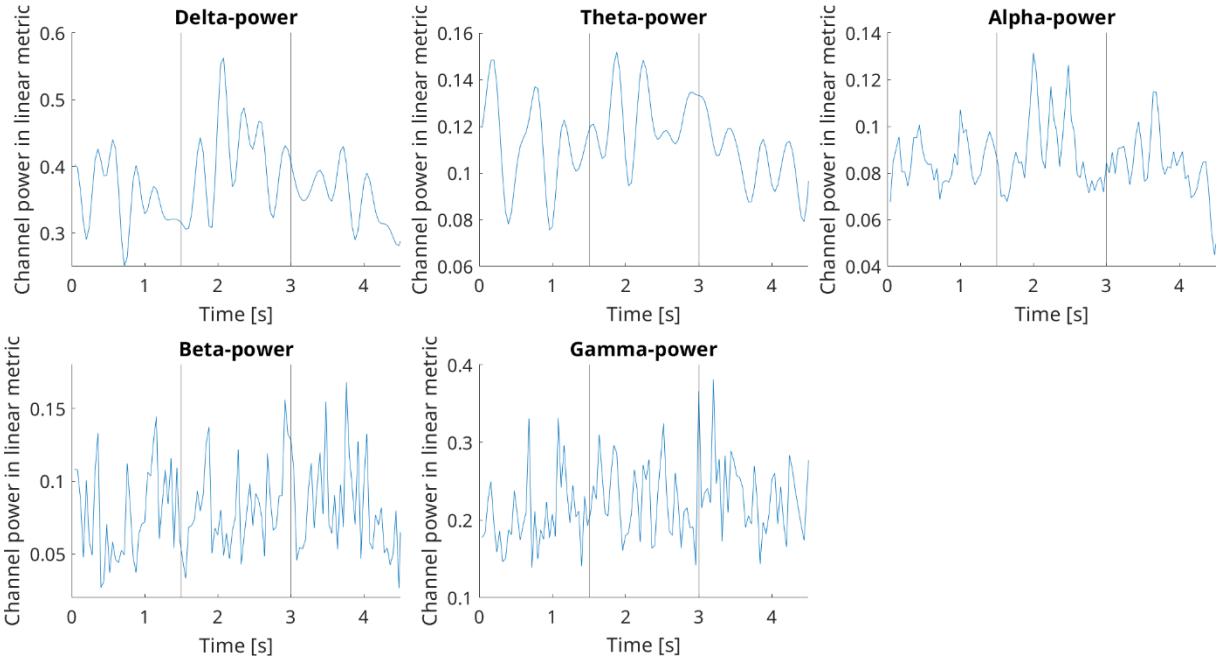

Figure 4 Visually evoked changes of the local field potentials in halothane anaesthetized cat

Cumulated power of the wave bands (from delta to gamma) after applying the given spectral filter for each frequency band. The blue curve represents the mean activity for all trials. The vertical lines denote the borders between the different epochs of the visual paradigm (from left to right): background activity, response to static visual stimulus and response to dynamic visual stimulus. The abscissa denotes the time relationship of the signals. The ordinate denotes the channel power in linear metrics.

Tables

Table 1*. Descriptive statistics of visually evoked LFPs during visual stimuli from awake, behaving, and anaesthetized animals*

	Awake *(N=226)*		Anesthetized *(N=960)*	
	N	%	N	%
Delta	80	35	168	17
Theta	98	43	178	19
Alpha	121	56	181	19
Beta	144	64	210	22
Gamma	53	23	220	23
All	204	90	609	63

In awake animals the percentage of LFPs that showed significant changes to visual stimulation in delta, theta, alpha and beta frequency band was higher than in the anesthetized animals.

Table 2. *Descriptive statistics of response activity during static and dynamic visual stimuli.*

	Static				Dynamic			
	Awake *(N=226)*		Anesthetized *(N=960)*		Awake *(N=226)*		Anesthetized *(N=960)*	
	N	%	N	%	N	%	N	%
Delta	68	30	178	19	61	27	218	23
Theta	58	26	282	29	89	39	183	19
Alpha	110	49	228	24	76	34	147	15
Beta	110	49	221	23	69	31	203	21
Gamma	72	32	225	23	46	20	215	22
All	187	83	602	63	172	76	611	64

Higher percentage of visually evoked LFP changes during static stimulation can be observed in the delta, alpha, beta, gamma frequency range in the behaving animals. This tendency can be observed in the theta, alpha, beta frequency bands during dynamic visual stimulation.